DIRECT RECOGNITION OF TUMORS BY REGULATORY T-CELLS WITH SUPPRESSION OF IMMUNE REJECTION

by
Matthew M. Moake

A dissertation submitted to Johns Hopkins University in conformity with the requirements for the degree of Doctor of Philosophy

Baltimore, Maryland
March 2014

Abstract

It is well established that the process of tumor progression is recognized by the immune system, and that cancer cells actively manipulate this system via production of inhibitory cytokines, antigenic loss, and alteration of immune-relevant cell surface molecules such as costimulatory ligands and Major Histocompatability Complex (MHC) II, which is required for CD4+ T-cell recognition. Regulatory T-cells (Tregs) plan an active part in the immune response to cancer. A growing body of literature suggests that Tregs demonstrate improved suppressive capacity when both Treg and effector T-cell (Teff) are specific for antigens within the same target cell, but the mechanisms behind this observation are as of yet unknown. In this study we hypothesized that the upregulation of MHCII by tumor cells allows for direct recognition by Tregs and provides a mechanism for antigen-specific suppression. Using a novel tumor model in which MHCII knockout mice were challenged with an MHCII-inducible, ovalbumin (OVA)-expressing B16 melanoma, we were able to demonstrate antigen-specific treatment with OVA-specific OTI CD8+ T-cells that was subsequently suppressed by OVA-specific OTII Tregs. Through bioluminescent imaging (BLI), histology, and *ex vivo* flow cytometry, we were able to demonstrate that our OTI cells proliferated, matured, trafficked to and accumulated within the tumor, and developed an effector phenotype consisting of IFNγ and TNFα cytokine production and efficient lysis of antigen-loaded targets. To expand upon our suppression findings, we developed a panel of OVA-expressing B16 tumors with variable expression levels of MHCII and evaluated their ability to induce Treg suppression. Unfortunately, we were unable to demonstrate suppression of tumor rejection or alteration in OTI phenotype by our Tregs, and

subsequently determined that, through an unknown mechanism, our OVA-expressing B16 tumors were unable to present OVA to OTII T-cells, thus nullifying our Treg studies. Although ultimately disappointing, the tumor model, B16 variants, and experimental framework generated here will serve as useful tools for the future analysis of direct antigen presentation by tumors.

Thesis Advisor: Dr. Hyam Levitsky

Second Reader: Dr. Ivan Borrello

Acknowledgements

I would like to thank all of those who have supported me during my nearly ten year journey in the Johns Hopkins University School of Medicine MD/PhD program. First, I would like to acknowledge my PhD advisor, Dr. Hyam Levitsky, for his never wavering role as advisor, mentor, cheerleader, and friend during the course of my dissertation work. I would also like to thank my thesis committee members Dr. Ivan Borrello, Dr. Avi Kupfer, Dr. Jonathan Powell, and Dr. Jonathan Schneck for their guidance and helpful suggestions during the course of my thesis.

This work would not have been accomplished without the help and support of my fellow lab members – Lu, Jie, Ashley, Joe, Chris L., Chris H., Kim, and many others. A special thanks to Michelle, our lab administrator and a good friend, for tolerating my innumerable rants and practical jokes. Thank you to all of my friends and colleagues of the CRBI fourth floor for your sharing of ideas, protocols, reagents, and the occasional cold drink. Thank you to the members of the CRBI Flow Cytometry, Cell Imaging, and Mouse Cores – Ada, Lee, Lillian, Dawn, and Sherrie – you provided advice, technical expertise, and hours of seemingly slave labor which were invaluable to this work. Thanks also to the NIH MSTP, CRI, and JHUSOM for funding this work and my time.

A special debt of gratitude goes to the JHUSOM MD/PhD Program –Sharon, Bob, Bernadine, and Martha – who supported me and had my back throughout my entire tenure, even in the rare occasion where I elected to speak my mind despite being advised otherwise. Thanks also to the CMM graduate program for their support and flexibility during my graduate years. Thank you to all of my clinical mentors for teaching me not only how to be a doctor, but how to be a caretaker of people. A special thank you to Dr.

John Flynn, who oversaw my clinical development for seven years and served as a model of a truly excellent physician and human being.

I am very grateful to all of my undergraduate research mentors – Dr. Randy Worobo, Dr. Marjorie Robert-Guroff, Dr. Curt Harris, and Dr. Eloy Rodriguez – for fostering my development as a scientist as well as a person. A special recognition to Randy, who besides mentoring me for almost four years also tirelessly harassed my stubborn self to go to the doctor for what was eventually diagnosed as lymphoma, was the best man at my wedding, and to this day is one of my closest friends.

Lastly, my deepest appreciation to all of my friends and family for your support and encouragement over the years. To my mother, who instilled in me at an early age the importance of education, has always given everything she had so that I may succeed, and has always believe that I would. To my father, who, despite starting our relationship a bit later in my life, is now a close and trusted friend. To my sister, with whom I faced numerous trials and tribulations growing up, the two of us always coming out on top. To my grandfather, my childhood role model and the man I hope to be some day, I wish you were here to see the person I have grown up to be. To my brothers, time and distance have kept us from getting to know each other as well as we should, which I would like to remedy. To my friends – the entering MD class of 2004, The Lion's Den, The Multiple Scorgasms, Night Moves, Shenanigans, Maryland Juniors, and many others – you have provided much needed enjoyment, amusement, and compassion during this long journey. Last but not least, to my wife, Rebecca. Your love, support, and tolerance of my shortcomings have allowed me to get where I am today, and are far more than any partner could ask.

Table of Contents

List of Figures

Chapter 1

Introduction

Regulatory T-cells (Tregs) play an important role in the control of immune responses, and in the setting of tumor immunity, this often results in the suppression of what might otherwise be a productive elimination of tumor cells. Tregs accomplish this suppression through a number of different mechanisms that often depend on the tissue, effector cell, target cell, and surrounding immune milieu. While this activity has classically been thought of as being antigen non-specific, a growing body of evidence suggests that Tregs function at greater capacity when both Treg and effector T-cell (Teff) share specificity of antigens within a common target cell. Tumors are not mere bystanders in this process, but are capable of undergoing a number of cellular alterations that can manipulate and help to avoid an otherwise productive immune response. These alterations include the production of inhibitory cytokines, antigenic loss/variation, and alteration of immune-relevant cell surface molecules such as Major Histocompatability Complex (MHC) I and II and costimulatory ligands. In this series of studies, we hypothesized that one such alteration, the upregulation of MHCII, could allow tumor cells the ability to directly present antigens to regulatory T-cells, and in doing so would provide a mechanism to allow for antigen-specific suppression.

In our first series of studies, we designed an *in vivo* model of immune-mediated tumor rejection that could subsequently be suppressed by Tregs. In order to accurately test our hypothesis, our model had to fulfill three requirements. First, we needed

recipient mice incapable of presenting MHCII antigens to our Tregs. Second, we needed a tumor cell line capable of inducible MHCII expression that expressed antigens appropriate for both CD8+ and CD4+ recognition. Finally, we needed appropriate antigen-specific CD8+ Teff and CD4+ Treg lines which recognized antigens within our tumor cell. To fulfill these requirements, we successfully created a tumor model within MHCII knockout (KO) recipient mice using the MHCII-inducible B16 melanoma line that expressed the model antigen ovalbumin (OVA), which bears antigenic epitopes recognized by the MHCI-dependent OTI CD8+ T-cell and the MHCII-dependent OTII CD4+ T-cell. We subsequently were able to show both treatment and suppression within MHCII KO mice using this model. As a means of expanding upon this model, we further developed and validated a series of OVA-containing B16 tumors with variable expression of MHCII that could serve as tools to tease out the intricacies of tumor-Treg direct presentation in later experiments.

The treatment model we designed utilized the adoptive transfer of naïve OVAI-specific OTI CD8+ cells that were subsequently capable of eliciting a treatment effect upon OVA-expressing B16 tumors. In order to elicit such an effect, our cells presumably had to undergo a number of alterations to convert them from naïve CD8+ cells to functional effector cells capable of enacting tumor clearance. These alterations included such processes as proliferation, maturation, trafficking, and execution of effector function. In our second study, we sought to better understand the physiology of our OTI CD8+ treatment system over the course of tumor progression. Using a number of *in vivo* and *ex vivo* techniques, we were able to accurately characterize the proliferation, trafficking and accumulation, cell surface molecule phenotype, and effector functionality

of our OTI CD8+ cells during this progression. With this characterization in hand, we hoped to evaluate the changes Tregs have upon this phenotype as a means of insight into the mechanisms used by Tregs to enact suppression.

Having established and characterized our treatment model, in our third series of studies we sought to evaluate the implications of direct antigen presentation by tumors to Tregs through examining the ability of our panel of variable MHCII-expressing B16.mOVA tumors to elicit Treg suppression. In examining this suppression, we further aimed to characterize the phenotypic and functional alterations imparted upon our OTI CD8+ cells by Tregs as a means of better understanding the suppressive mechanisms involved. Unfortunately, we were not unable to demonstrate suppression with our variable MHCII-expressing tumor variants, nor were we able to replicate the suppression seen with our original B16.mOVA tumor in our initial studies. We further did not demonstrate any alterations to our OTI CD8+ phenotype in the presence Tregs. In analyzing these two failed results, we determine that, through an unknown mechanism, our tumor cells were unable to present endogenously produced OVA antigen to our OTII T-cells. Thus, we were unable to make any conclusions regarding the implications of direct antigen presentation by tumors to Tregs.

While we were unable to accurately test our initial hypothesis due to the failed direct presentation of OVA antigen by tumor cells to OTII cells, this study is not without its merit. We succeeded in developing a novel tumor model system along with a series of OVA-expressing B16 tumors with variable MHCII expression patterns. Further, we were able to accurately characterize the phenotype and function of our OTI treatment cells during the course of tumor progression. The model system, reagents, and experimental

framework generated in this study will serve as valuable tools for future studies aimed at elucidating the ability of tumor cells to directly present class II antigens to regulatory T-cells.

Chapter 2

Background

2.1 Immune Tolerance and Regulatory T-Cells

The human body is composed of over 10^{13} cells (Bianconi et al, 2013) encased within the epithelial linings of the skin, gastrointestinal, urinary, reproductive, and respiratory tracts. Colonizing and frequently penetrating these barriers are innumerable microbial species. Many of these are beneficial if not necessary to their host, but a small number have the ability to cause infection and bring about significant pathology. It is the responsibility of the immune system to identify and respond to these pathogens in a timely and appropriate manner.

However, detection and clearance of infection does not take place in sequestration, but rather in the milieu of the host tissue. Distinguishing self from non-self, as well as harmful versus benign, requires an extremely high fidelity system. Further, many of the mechanisms used to limit and clear pathogenic invaders can be harmful to the host cells themselves, necessitating tight regulation of any appropriately triggered immune response. Insufficiency or over activity of any step in this process can result in its own pathology, highlighting the importance of processes involved in immune activation, homeostasis, and tolerance.

Within the immune system, tolerance implies a lack of response to a given antigen. This can arise in one of three separate but related mechanisms: central

tolerance, peripheral tolerance, and "clonal ignorance" (Van Parijs and Abbas, 1998). Central tolerance is established via clonal deletion, alternatively referred to as negative selection, of self-reactive T-cells during their maturation within the thymus (Kappler et al., 1987). Lymphocytes that pass this first round of editing make their way into the peripherally circulating pool where they are subject to peripheral tolerance, which can be brought about in several ways. These include antigenic seclusion, low T-cell receptor (TCR) avidity, anergy, and peripheral deletion (Arnold et al., 1993; Van Parijs and Abbas, 1998). These are passive, cell-intrinsic mechanisms that act in *cis* to prevent the unwanted activation of an individual T-cell bearing a given TCR. However, these mechanisms are not foolproof, and self-reactive T-cells do exist within the periphery and can on occasion be activated. Furthermore, even when responding to a foreign invader, reestablishment of homeostasis must follow a productive immune response. While again in this regard there are a number of mechanisms that act intrinsically to a given activated cell, such as death by neglect or activation induced apoptotic feedback loops (Van Parijs and Abbas, 1998) these mechanisms are not always sufficient. Therefore, a more 'active' mechanism of immune tolerance and suppression is necessary. This active mechanism occurs via T-cell dependent dominant control (Sakaguchi et al., 2001) at the hands of the regulatory T-cell (Treg).

Regulatory T-cells were first described in the early 1970s by Gershon and Kondo (Gershon & Kondo, 1970; Gershon & Kondo, 1971), and in the decades to follow have been shown to be involved in autoimmunity, tumor immunity, transplant tolerance (Kretschmer et al., 2006; Sakaguchi et al., 2001), allergy (Xystrakis et al., 2006), and infection (Belkaid, 2007; Rouse et al., 2006) including *Mycobacterium tuberculosis*

(Kursar et al., 2007), and *Leishmania major* (Anderson et al., 2007b). They represent 5-10% of the circulating CD4+ T-cell population (Zou, 2006) and are classically thought of as being thymically-derived CD4+ cells that are Foxp3+ CD25+, CD45Rb^{lo}, and express intermediate levels of ICOS, CTLA-4, GITR, and CD44 (Gavin et al., 2007).

Foxp3 is a member of the forkhead/winged-helix family of transcription factors. Foxp3 expression is considered to be the hallmark of murine Treg cells and indeed is required for their thymic development. Ectopic expression of the *FOXP3* gene within naïve CD4+ cells can recapitulate much of the same phenotype as shown by naturally arising Tregs (Fontenot et al., 2003; Hori et al., 2003). Mice lacking a functional *FOXP3* gene lack Tregs and develop the 'Scurfy' (sf) phenotype characterized by widespread autoimmunity, lymphocytic infiltration and hyperproliferation, and early onset death in affected mice (Brunkow et al., 2001). Mutation of this same gene within humans results in the IPEX syndrome (Immune dysregulation, Polyendocrinopathy, Enteropathy, X-linked syndrome), which is a recessive disorder of similar pathology to Scurfy and is usually lethal in infancy (Bennett et al., 2001; Wildin et al., 2001).

While the IPEX phenotype of humans closely resembles that of the Scurfin mouse, Foxp3 expression is not solely confined to regulatory T-cells in humans, and can be seen in both CD4+ and CD8+ cells upon activation (Morgan et al., 2005). Foxp3 expression is induced in *in vitro* activated human CD4+ CD25- T-cells. While this expression correlates with hyporesponsiveness to further stimulation and decreased cytokine production, it does not impart a dominant regulatory phenotype to these cells (Gavin et al., 2006; Wang et al., 2007). *In vitro* stimulation of human CD4+ CD25- T-cells in the presence of TGFß elicits strong Foxp3 expression but does not impart a

regulatory phenotype as it does in mice (Tran et al., 2007). These differences highlight not only discrepancies between mice and humans, but also open the door to the complexity of what defines the regulatory T-cell population as a whole.

2.2 Induced vs. Natural Regulatory T-Cells

A more in depth analysis of regulatory T-cells suggests a diverse population of cells with regulatory and suppressive activities. The classic thymically-derived CD4+ Foxp3+ Tregs represent what can be referred to as natural Treg (nTreg). These nTreg are not alone, however, and CD4+ Foxp3- T-cells can be converted in the periphery to Foxp3+ cells known as induced, adaptive, or converted Tregs (iTreg) (Curotto De Lafaille and Lafaille, 2009). Location of antigen presentation clearly affects Treg development, as nTregs are dependent upon thymic stromal expression of antigen while peripheral presentation results in iTreg development (Apostolou et al., 2002). This sometimes leads to the view that nTregs are responsible for tolerance to self while iTregs function to harness and control productive immune responses within the periphery. This dichotomy is vastly oversimplified, and iTregs have been shown to constitute a unique subdivision within the peripheral Treg pool that functions synergistically with nTregs (Haribhai et al., 2009; Zhou and Levitsky, 2007).

Further complicating the case of nTreg and iTreg are IL-10 producing T-regulatory 1 (Tr1) cells (Groux et al., 1997; Roncarolo et al., 2001) and TGFβ producing T-helper 3 cells (Th3), which are particularly prominent in the gut (Weiner, 2001). The high prevalence of gut-derived Treg lines highlights the fact that there clearly is a relationship between microbial infection/colonization and iTreg development (Curotto De

Lafaille and Lafaille, 2009). The 'hygiene hypothesis' proposes a link between the increased incidences of allergy in Western countries with decreased childhood infections resulting in reduced induction of polyclonal iTregs during infection that are capable of controlling future unwanted immune responses such as allergy (Belkaid, 2007; Maizels, 2005). DCs purified from small intestinal lamina propria show superior induction of iTregs relative to lymphoid organ-derived DC (Sun et al., 2007), and CD103+ DCs in mesenteric lymph nodes can induce Tregs from naïve T-cells in a manner that is dependent upon TGFß and retinoic acid (RA) (Coombes et al., 2007).

The differing sites of their generation are also reflected in the TCR repertoires of nTreg and iTreg. iTreg share the same repertoire as the entire naïve CD4+ pool, whereas nTreg are much more limited (Curotto De Lafaille and Lafaille, 2009), again likely reflecting the antigenic diversity encountered during their development. Besides TCR variability, nTreg and iTreg also express variable patterns of homing receptors (Haribhai et al., 2009), again suggesting a potential division of labor between the two populations.

Differences between nTregs and iTregs can be seen at the gene level as well. Gene profiling studies show that iTregs lack some of the genes associated with nTregs (Haribhai et al., 2009; Hill et al., 2007), and that *FOXP3* is not necessary for the initiation of iTreg development, but is essential to the their suppressive function (Haribhai et al., 2009). nTregs, *in vivo*-generated iTregs, and *in vitro*-generated iTregs show variability in the methylation patterns of an upstream region of the *FOXP3* gene TSDR (Treg cell-specific demethylated region) (Curotto De Lafaille and Lafaille, 2009). Recent studies suggest that there are likely higher-order controls over *FOXP3* in the development of Treg, and that TCR engagement, IL-2, and TGFß all have effects upon the Treg signature

(Hill et al., 2007). Foxp3 is suggested not to drive *de novo* Treg development but to amplify molecular changes, including promoting its own transcription, initiated by a Treg precursor and to solidify these cells towards a permanent Treg lineage (Gavin et al., 2007). In all, Tregs surmise an increasingly widening collection of T-cells with the capability to suppress varying arms of the immune system in a variety of different ways. The mechanisms they use to accomplish this suppression are as equally diverse as the populations themselves.

2.3 Mechanisms of Regulatory T-Cell Suppression

Regulatory T-cells are capable of suppressing effector cell function via a number of different pathways. The importance of each of these is much debated, and unlike absence of functional Foxp3 (Fontenot et al., 2003; Hori et al., 2003), loss of any single one of these mechanisms is not enough to completely abrogate overall Treg function (Vignali et al., 2008). Functional loss of many of these pathways is associated with different, often organ-specific deficits. Thus it would appear that these pathways act in a non-redundant fashion to maintain peripheral tolerance and immune homeostasis. Furthermore, identifying pathways necessary for generation and maintenance of the Treg pool versus those actively involved in suppressive activity is difficult and likely varies amongst the different Treg subsets. The first reports of Treg function suggested that Tregs must be activated via TCR engagement in order to suppress, and that suppression occurred via a contact-dependent, cytokine-independent inhibition of IL-2 production by effector cells (Thornton and Shevach, 1998). However, other reports have suggested that contact-mediated suppression is necessary for nTregs, whereas iTregs act via inhibitory

cytokines such as IL-10 and TGFß (Grossman et al., 2004a). While the data on the mechanisms of Treg-mediated suppressive function are highly varied and often conflicting, they are not necessarily mutually exclusive and in a number of setting may be due to differences in experimental setups, *in vivo* versus *in vitro* model systems, and human versus murine systems. Overall, these often conflicting data speak to the complexity of Treg-mediated immune suppression and tolerance.

The first mechanism regulatory T-cells use to inhibit effector function involves the production of inhibitory cytokines, most notably IL-10 and TGFβ, which are produced by Tregs upon TCR engagement (Nakamura et al., 2001). IL-10 is produced by a number of immune cells including those of the innate system as well as T-helper 1 (Th1) and Treg cells (Anderson et al., 2007b). The importance of Treg production of IL-10 is unclear. Several allergy & asthma models suggest that IL-10 production by nTregs and iTregs is important for disease control (Hawrylowicz and O'Garra, 2005). Further, IL-10 has been shown to be necessary for the function of Tregs in preventing colitis in adoptive transfer studies using SCID mice (Asseman et al., 1999), and IL-10 deficient mice develop autoimmune colitis but interestingly do not develop autoimmunity within other organs (Kühn et al., 1993). Conversely, IL-10 production by Th1 cells, and not Tregs, appears to be the primary source of IL-10 mediated suppression in chronic cutaneous leishmaniasis (Anderson et al., 2007), and IL-10 production by Tregs was not correlated with suppressed clearance of *M. tuberculosis* (Kursar et al., 2007).

TGFβ was one of the first recognized mechanisms of Treg-mediated suppression, and is also probably the most widely debated. As mentioned previously, TGFβ appears to be heavily involved in the generation of iTregs, and iTregs are enriched in genes

involved in the TGFß signaling pathway relative to nTregs (Haribhai et al., 2009). *In vitro* stimulation of human CD4+ CD25- T-cells in the presence of TGFβ elicits strong Foxp3 expression but does not impart a regulatory phenotype as it does in mice (Tran et al., 2007). Naïve murine CD4+ cells cultured in tumor cell-conditioned media develop an iTreg phenotype with suppressive capability. This conditioning is abrogated when anti-TGFβ antibody is included within the media (Liu et al., 2007). *In vitro* functional assays show mixed results. Most appear to agree that suppression is contact-dependent, but data addressing the importance of TGFβ is conflicting. Some studies have suggested that suppression can occur in the absence of TGFβ production by Tregs or TGFβ-responsiveness by Teff cells (Piccirillo et al., 2002), whereas other studies have suggested that Tregs utilize self-produced, membrane-bound TGFβ to exert their suppressive effects (Nakamura et al., 2001). These latter studies offer that perhaps the complicated biology of TGFβ production, and the multiple forms the molecule can be found in, likely complicates its analysis. *In vivo* models have shown that TGFß signaling is required for Treg-mediated control of pancreatic islet-reactive CD8+ cells in a type-I diabetes model (Green et al., 2003), and that administration of anti-TGFß antibody prevents suppression of autoimmune colitis in an adoptive transfer mouse model (Read et al., 2000). Finally, treatment of tumor-bearing mice with anti TGFß antibody results in increased tumor clearance and decreased conversion of iTregs in some models (Liu et al., 2007).

A third, recently identified suppressor cytokine produced by Tregs is IL-35. Tregs are thus far the only cells known to produce IL-35, and its ectopic expression confers a regulatory phenotype to naïve CD4+ cells. Furthermore, recombinant IL-35

suppresses proliferation *in vitro*, IL-35 KO mice were unable to suppress proliferation, and these same mice were unable to control homeostatic proliferation of adoptively transferred cells and resultant autoimmune inflammatory bowel disease *in vivo* (Collison et al., 2007).

The second mechanism utilized by Treg cells to mediate suppression involves the direct killing of effector cells via cytolytic pathways, most notably the granzyme/perforin systems akin to those used by CD8+ T-cells and NK cells. In humans, iTregs express high levels of granzyme B, but not granzyme A, and can mediate perforin-dependent cytolysis of allogeneic target cells in an MHC/TCR-independent fashion (Grossman et al., 2004b). Human nTregs, on the other hand, express high levels of granzyme A, with little granzyme B (Grossman et al., 2004a). Both populations are capable of mediating perforin-dependent cytolysis of autologous cells including T-cells and dendritic cells in a Fas/FasL independent manner (Grossman et al., 2004a). In mice, stimulation of iTregs results in the upregulation of granzyme B, but not granzyme A or perforin. Granzyme B KO mice show reduced *in vitro* iTreg suppression whereas perforin KO mice do not (Gondek et al., 2005). In another study, granzyme B deficient mice were shown to clear both allogeneic and syngeneic tumor challenges better than WT mice. Granzyme B was shown to be expressed at high levels in tumor-infiltrating Tregs but not in naïve Tregs, and adoptive transfer of WT, but not granzyme B or perforin KO Tregs led to decreased tumor clearance. Tumor-infiltrating Tregs are able to induce CD8+ and NK cell death in a granzyme B- and perforin-dependent manner (Cao et al., 2007). In some of these same mouse studies, iTregs were shown to cause dose-dependent apoptosis of Teff in a

polyclonal TCR-stimulated coculture. This effect was abrogated in the presence of anti-GITR stimulation, as was the upregulation of granzyme B (Gondek et al., 2005). Finally, besides the granzyme/perforin system, one study has demonstrated an antigen-specific CD4+ CD25+ cell line derived from a BalbC mouse that is able to kill B-cells bearing the appropriate antigen via the Fas/FasL pathway. This same cell line was unresponsive to cognate antigen stimulation, required exogenous IL-2, and mediated bystander suppression, consistent with a Treg phenotype (Janssens et al., 2003).

A third method that Tregs can utilize to suppress effector cells is through metabolic disruption of target cells. One mechanism therein involves the killing of Teff by Treg via cytokine-deprivation induced apoptosis (Pandiyan et al., 2007), the best studied of which involves IL-2. IL-2 is required for generation, peripheral maintenance, and acquisition of suppressor function by Tregs (Thornton et al., 2004). IL-2 is not necessary for the induction of Foxp3+ expression in developing T-cells, but is needed for the maintained expression of growth & metabolism genes, suggesting a role in the peripheral homeostasis and competitive fitness of Tregs (Fontenot et al., 2005a). Tregs do not produce IL-2, however, and must compete with Teff, which secrete it. Owing to this necessity, Tregs typically express CD25, also known as the high-affinity IL-2Rα, which when combined with CD122 (IL-2Rβ) and CD132 (IL-2Rγ) produces a heterotrimeric IL-2 receptor with a 100-fold increased affinity for IL-2 relative to the heterodimeric receptor expressed by conventional T-cells. This provides Tregs a significant competitive advantage over Teff and serves as a potential mechanism for suppression (von Boehmer, 2005; de la Rosa et al., 2004). Further supporting this concept, addition of anti-CD25 antibody blocks *in vitro* Treg suppression, as does anti-

IL-2 antibody. Both of these can be reversed with the addition of exogenous recombinant IL-2 (de la Rosa et al., 2004). Somewhat contrastingly, however, is the result that *in vitro* suppression can occur with cells from IL-2 KO and IL-2Rα KO mice (Fontenot et al., 2005a), providing further proof that Tregs utilize multiple mechanisms for suppression.

Another means of metabolic disruption utilized by Treg involves the manipulation of adenosine metabolism. Extracellular nucleotides and ATP are often released by damaged and dying cells and serve as natural proinflammatory mediators. Tregs selectively express both CD39 and CD73, which collectively metabolize these molecules into AMP and adenosine (Borsellino et al., 2007; Deaglio et al., 2007; Koie et al., 2006). AMP inhibits Th1 and Th2 cytokine expression and cell proliferation (Kobie et al., 2006) via interactions with the adenosine ASA receptor on Teff cells. CD39 KO mice show reduced *in vitro* suppressive capability and fail to block skin allograft rejection *in vivo* (Deaglio et al., 2007). Foxp3 has been shown to promote CD39 expression, and TCR stimulation increases CD39 catalytic activity. Interestingly, while virtually all murine Tregs express CD39, only a subset of human Tregs do. These CD39+ human Tregs are very sparse in the relapsing/remitting form of multiple sclerosis (Borsellino et al., 2007).

A separate but related form of adenosine-mediated suppression has been reported through cAMP signaling. cAMP is a common second messenger within innumerable cell signaling cascades. Within Teff cells, high levels of cAMP serve to inhibit IL-2 production, cell growth, and proliferation. Treg cells have a very high level of intracellular cAMP. Recent studies have shown that Tregs & Teff are able to form gap junctions through which this cAMP is able to be transferred. cAMP antagonists and gap junction inhibitors blocked this suppression (Bopp et al., 2007).

The mechanisms of cytokine inhibition, direct target cell killing, and metabolic disruption demonstrate the wide range of mechanisms Tregs can utilize to suppress Teff cell function. Tregs not only communicate with Teff, however, but many other cell types, most notably antigen presenting cells (APCs). These interactions provide another level of suppressive mechanisms whereby Tregs can eventually impact Teff function.

2.4 Interactions of Regulatory T-Cells and Dendritic Cells

Besides their direct interactions with target effector cells, Tregs also affect dendritic cells and other host antigen presenting cells (APCs). Through a variety of mechanisms, Treg have the ability to decrease the immune stimulatory capacity of these APCs, and in doing so suppress effector cell function. These same interactions affect the Treg cell as well, and quite often the reduction in Teff stimulatory capacity brought on by Tregs also increases the ability of the APC to stimulate Treg development.

The first mechanism through which Tregs can elicit suppressive function through DCs involves decreasing the costimulatory potential of these APCs. Upon acquiring antigen within their environment, peripheral DCs migrate to secondary lymphoid structures where they mature and present antigen in the context of MHC:TCR interactions, in the classic "signal 1." Production of an effector response requires this signal along with a stimulatory "signal 2," which is provided in the form of costimulatory molecules on the DC such as CD80 and CD86. T-cells bear ligands to these molecules in the form of CD28 and CTLA-4. Ligation of effector cell CD28 by DC CD80/86 results in activation of effector cells, whereas ligation by CTLA-4 results in downregulation of these costimulatory molecules (Oderup et al., 2006).

Tregs rapidly downregulate the expression of CD80 and CD86 by DC in *in vitro* cocultures in a contact-dependant mechanism (Cederbom et al., 2000), but do not decrease DC survival. Treatment with anti-CTLA-4 antibody abrogates this downregulation, and CD80 and CD86 expression are restored after removal of Tregs (Oderup et al., 2006). This ability to downregulate costimulatory molecules is highly context dependent, however. Immature BMDCs cocultured with Tregs show reduced expression of CD80, CD86, MHCII, CD40, and CD11c, and decreased stimulation of CD8 effector cells. However, coculture of Tregs with DCs previously matured with LPS, CpG, or anti-CD40 does not affect expression levels or stimulatory potential (Serra et al., 2003). In a related fashion, WT T-helper cells can assist in overcoming the suppressive effects of Tregs upon diabetogenic CD8 cells, whereas CD40L (CD154) KO T helper cells cannot, owing again to the maturation state of the DC in question (Serra et al., 2003).

A large proportion of Tregs constitutively expresses CTLA-4, and treatment with anti-CTLA-4 reverses protection from autoimmune gastritis by adoptively transferred Tregs (Read et al., 2000). Secretion of TGFβ by Tregs post-TCR engagement is increased by CTLA-4 costimulation (Nakamura et al., 2001). Anti-CTLA-4, but not anti-TGFβ or anti-IL-10 treatment abrogated anti-diabetogenic effects of adoptively transferred Treg (Serra et al., 2003). Further, pulmonary DCs show increased MHCII, CD80, and CD86 expression along with an increased ability to promote T-cell proliferation in the absence of Tregs in a mouse asthma model (Lewkowich et al., 2005). Human Tregs reduce DC stimulatory potential, lead to increased IL-10 production, and

decrease DC costimulatory molecules. Anti-TGFβ administration partially reversed these effects (Misra et al., 2004).

A second system used by Tregs to modulate suppressive function through DCs involves tryptophan catabolism through the enzyme indoleamine 2,3-dioxygenase (IDO), which is expressed by DCs. IDO/tryptophan catabolism has been shown to be involved in autoimmunity, tumor clearance, asthma, and pregnancy (Mellor and Munn, 2004). IDO leads to decreased tryptophan availability and the production of pro-apoptotic metabolites, which have T-cell suppressive effects. When stimulated by TCR engagement, Tregs are able to stimulate DC expression of IDO in two ways. The first involves a CTLA-4-dependent mechanism and requires CD80/86 expression along with cytokine production by DCs. The second mechanism is CTLA-4 independent, but cytokine-dependent and occurs in the presence of LPS. This second pathway occurs via the production of IFNγ by Tregs, which occurs in the presence of LPS and can stimulate IDO (Fallarino et al., 2003).

A third mechanism used by Tregs to steer DCs towards a suppressive state involves Lymphocyte Activation Gene 3 (LAG-3/CD223). LAG-3 is structurally similar to CD4 and interacts with MHCII on APCs with much higher affinity. It is expressed on activated CD4 & CD8 T-cells as well as Treg cells (Workman and Vignali, 2005). High levels of LAG-3 mRNA are seen in both nTregs & iTregs, but it is undetectable on the cell surface of nTregs immediately *ex vivo* (Huang et al., 2004), and is selectively upregulated by Tregs following activation. Ectopic expression of LAG-3 in naïve CD4+ (Huang et al., 2004) and even activated T-cells reduces their proliferation and confers a suppressive phenotype (Workman and Vignali, 2005). LAG-3 mediates both *in vivo* and

in vitro suppression. LAG-3 deficient Tregs show reduced suppression potential *in vitro,* which is also seen with administration of anti-LAG-3 antibody (Huang et al., 2004). LAG-3 deficient mice, or WT mice treated with anti-LAG-3 antibody, produce twice as many CD4 & CD8 as WT hosts, and LAG-3 deficient T-cells undergo increased homeostatic proliferation in lymphopenic recipients relative to WT cells (Workman and Vignali, 2005).

The mechanism involved in LAG-3 suppression appears to be two-fold, as the interaction of LAG-3 with MHCII induces changes both in DCs as well as in Tregs. LAG-3 engagement of MHCII on DCs inhibits DC maturation and immunostimulation via an ITAM-mediated signaling pathway that is both antigen- and contact-dependent. LAG-3 signaling is not required for this inhibition of DC maturation, as MHCII cross-linking produces similar results as LAG-3 engagement (Liang et al., 2008). In contrast, binding to MHCII and signaling through the cytoplasmic domain of LAG-3 is required for its effects upon the regulatory activity of Tregs (Workman and Vignali, 2005).

Yet another mechanism involved in the control of DC stimulatory capacity by Tregs involves extended contact by Treg with DCs. Two photon laser-scanning microscopy (TPLSM) has revealed that both Tregs and naïve T-cells indistinguishably interact directly with DCs in draining lymph nodes (DLN), but no direct Treg-Tnaive interactions were reported. Interaction of Tregs with DCs preceded the inhibition of Tnaive by DCs, with increasing numbers of Tregs leading to decreased Tnaive:DC swarms & clusters, and presumably reduced priming of Teffs. Both T-cell populations displayed similar lymph node homing to the paracortical T-cell zone in the absence of antigen, and to the T-cell:B-cell boundary in DLNs in the presence of antigen (Tang et

al., 2006). Further studies have shown that naïve T-cell motility is decreased and T-cell:DC interactions are longer in the absence of Treg (Tadokoro et al., 2006). One possible mediator of these effects is Neuropilin-1 (Nrp-1). Nrp-1 is expressed by most Tregs but not Tnaive and promotes prolonged interactions and more immune synapses with immature DCs, thus potentially giving Tregs an advantage in low antigen environments. Blocking antibody to Nrp-1 abrogates this extended Treg:DC interaction, and ectopic expression of Nrp-1 in Tnaive lengthens DC contact duration (Sarris et al., 2008).

Tregs have suppressive effects not only on DCs, but their progenitors, as well as other APC subsets. For instance, human Tregs can exert suppressive effects on monocytes/macrophages (Taams et al., 2005). Coculture of human Tregs with monocytes drives development of alternatively activated macrophages (AAM), which have a suppressive phenotype. Tregs make monocytes/macrophages less responsive to LPS, an effect attributable to IL-4, IL-10, and IL-13 (Tiemessen et al., 2007).

As mentioned, while Tregs can influence the stimulatory capacity of DCs, DCs themselves are crucial to the generation and function of Tregs. The maturation/activation state, DC subtype, DC costimulatory molecule expression, and surrounding cytokine milieu all have profound implications upon the generation of Tregs from Tnaive cells by DCs. Many of these changes in DCs are coordinated, such that the relative importance of each has yet to be fully elucidated. Further, given the wide range of DC subtypes, data from one model does not always correlate with others. Still some general themes are present.

DC maturation clearly affects Treg conversion from Tnaive. Pretreatment of DCs with LPS or anti-CD40 has been shown to decrease conversion of Tnaive into Tregs. This effect was found to be synergistic, and administration of anti-CD154 (CD40L) antibody conversely increased Treg conversion (Wang et al., 2008). Similar results were obtained when the Toll Like Receptor (TLR) poly(I:C) was used as a maturation signal (Yamazaki et al., 2008). These findings likely relate in part to alterations in costimulatory signals that result from DC maturation, as knockout of CD40, CD80, and CD86 within DCs has also been shown to increase conversion of Tregs relative to WT DCs. Further, signaling through other costimulatory/suppressor pathways such as CTLA-4, PD-L1, and GITR have also been shown to affect Treg conversion by DCs (Wang et al., 2008).

Besides maturation status, different DC populations appear to have greater innate propensity for Treg conversion than others. The ability of CD103+ DCs in mesenteric lymph nodes to induce Tregs in the presence of TGFß and retinoic acid (RA) has already been mentioned (Coombes et al., 2007). Further, *in vivo* antigen delivery to splenic CD8+ DC but not CD8- DC has been shown to preferentially convert Tnaive to Tregs. These same studies also showed a significant role for TGFβ, as CD8+ DCs were able to produce endogenous TGFβ and TGFβ binding protein, which were not produced by CD8- DCs, and addition of TGFβ blocking antibodies abrogated the enhanced Treg conversion seen in CD8+ DCs. Interestingly, CD8- DCs were shown to express the TGFβ receptor, and addition of exogenous TGFβ to CD8- DCs allowed for improved Treg conversion (Yamazaki et al., 2008). Similarly, CD8+ DCs have shown increased *in vitro* conversion in the presence of TGFβ relative to CD8- DC (Wang et al., 2008). In

related work, it has been shown that DC deficiency of alpha-V-beta-8 ($\alpha V\beta 8$) integrin, which is involved in conversion of TGFß into its active state, results in reduced Treg conversion *in vitro* in a TGFß-dependent manner. Mice with DCs lacking this integrin develop autoimmune colitis with reduced colonic Tregs (Travis et al., 2007).

These studies indicate not only baseline differences in Treg conversion potential among differing DC populations, but also highlight some of the functional differences between these populations that likely account for their differing Treg converting potential, amongst which cytokine profiles are of high importance. Besides the implications of TGFβ, DC production of IL-6 and IL-10 have also shown importance. IL-6 is secreted by matured DCs, and IL-6 knockout DCs show an increased Treg conversion relative to WT (Wang et al., 2008). Tregs have been shown to induce APCs to secrete IL-10. In turn, IL-10 knockout APCs result in reduced suppressive capability of Tregs, as does addition of anti-IL-10 (Kryczek et al., 2006). Cytokines in the surrounding milieu also affect DC-Treg interaction. Both the Th1 and Th2 cytokines IFNγ and IL-4, respectively, have been shown to inhibit *in vitro* conversion of Tregs, an effect that was reversed with addition of appropriate blocking antibodies (Wang et al., 2008).

In all, these studies highlight the importance of the DC-Treg interaction and the many mechanisms by which the two cell populations bidirectionally affect one another's function. The bulk of these mechanisms are focused on secondary and tertiary signals within this immune crosstalk. The importance of the MHC-TCR interaction, the so-called "signal 1," has yet to be addressed. This signal is itself at the heart of the adaptive

immune response, and is of significant importance when examining the specificity of Treg function.

2.5 Specificity of Regulatory T-Cell Function

The question of Treg specificity is one of significant debate. Classically, Tregs have been thought to undergo antigen-specific generation and activation, but once activated, to function non-specifically. This dogma originates from early work by Thornton & Shevach (Thornton and Shevach, 2000) who used a series of *in vitro* coculture experiments to characterize the antigenic requirements of Tregs. They found that Tregs required TCR stimulation, either through cognate antigen-MHC interaction or anti-CD3, to become activated, but once activated, mediated suppression in a cytokine-independent, contact-dependent, APC-independent, antigen-non-specific fashion. Activated Tregs could suppress Teffs from different TCR specificities, even when those T-cells were of different MHC background or were anti-CD3 stimulated. Similarly, evidence for Treg specificity *in vivo* in models of autoimmunity, transplant, cancer, and infection clearly demonstrates that Tregs bear antigen specificity as it pertains to their generation and activation, but is less clear when examining functional specificity.

Many groups have now been able to isolate tumor-associated antigen (TAA) specific Tregs from human samples. Nishikawa et al (Nishikawa et al., 2005a) found that NY-ESO-1-specific CD4+ Th1 cells could be induced from PBMCs of both normal donors as well as patients with NY-ESO-1 positive melanoma. However, except in patients that were seropositive for NY-ESO-1, these populations could only be detected following depletion of CD4+ CD25+ Tregs, suggesting suppression of Th1 cells in the

assay. Further separation of these populations into naïve (CD45RA) and effector/memory(CD45RO) cells revealed that NY-ESO-1-specific Th1 induced from normal donors and seronegative patients came from naïve CD4+ cells, whereas those from seropositive patients came from both populations. These Th1 from memory populations were found to be more resistant to Treg suppression.

Wang et al (Wang et al., 2004) isolated a Treg clone from a pool of TILS from a melanoma patient with specificity for the cancer-testis antigen LAGE1. The clone was CD4+ CD25+ GITR+ CTLA4+ Foxp3+ and when ligand-activated could suppress anti-CD3 stimulated polyclonal Teff response in a contact-dependent manner. Vence et al (Vence et al., 2007) recently isolated a panel of TAA-specific Tregs from the peripheral blood of melanoma patients, but not from healthy donors. They found specificities to a variety of tumor antigens including gp100, TRP1, NY-ESO-1, & survivin. These Tregs proliferated in culture when provided with appropriate antigenic peptide, secreted IL-10, expressed high levels of Foxp3, and were able to suppress autologous T-cells in a contact-dependent manner.

In another study, Van der Burg et al (van der Burg et al., 2007) identified increased frequencies of Tregs within the tumor and corresponding DLNs of cervical cancer patients and isolated a panel of CD4+ Tregs with specificity for the HPV oncoproteins E6 & E7 from these tissues. These Tregs did not display a singular cell marker & cytokine secretory profile, but rather were variable in these regards. However, all clones were able to suppress the proliferation and cytokine secretion of responder T-cells when placed into *in vitro* coculture, including responder T-cells with specificities for alloantigen, HIV-1 antigens, and HA antigens.

Jandus et al (Jandus et al., 2009) recently identified a population of DQ6/Melan-A_{25-36} multimer+ CD4+ cells within a series of melanoma patients that were involved in a peptide vaccine trial using Melan-$A_{26-35\ (A27L)}$ peptide vaccine aimed at boosting antigen-specific CD8+ responses. They found these multimer+ cells in a high percentage of melanoma patients' peripheral blood, but only sparingly in healthy controls. In several cases where tumor-infiltrated lymph nodes were available, they found increased multimer-positive cells relative to the peripheral blood. Within these multimer+ cells, a high percentage (19-74%) were found to be Foxp3+. These multimer+ cells failed to proliferate *in vitro* prior to vaccination, even after CD25-depletion or addition of CpG, CD40L, IL-2, IL-6, IL-15, or IL-7. Over the course of peptide vaccination, the overall numbers of multimer+ cells stayed fairly consistent, however the percentage of multimer+ Foxp3+ cells decreased dramatically (0-21%). In post-vaccine samples where Foxp3+ cells were <10%, proliferative capacity was restored. Further, not only did these cells now proliferate, they also secreted Th1 cytokines. To determine the source of these pre- versus post-vaccine multimer+ cells, the authors sequenced the TCR Vβ region along with the CDR3 of several different patient samples. They found restricted Vβ usage post-vaccine with no overlap of CDR3 sequences pre- and post-vaccine, indicating the *de novo* expansion of antigen-specific, multimer+ cells.

Recently, Bonertz et al (Bonertz et al., 2009) described a system in which they were able to identify a number of TAA-specific Teffector/memory cells as well as Treg cells within the peripheral blood of 170 colorectal cancer patients. DCs were pulsed with a panel of synthetic long peptides representing 11 known tumor antigens (EGFR, Muc-1 signal sequence, Muc-1 tandem repeat, Her-2/neu, p53, telomerase, survivin, heparanase

1, heparanase 2, & CEA) or non-TAA controls and then incubated with patient T-cells to identify Teff via IFNγ ELISPOT. They also repeated this same procedure using T-cells that had been depleted of CD4+ CD25+ T-cells (Tregs) and similarly evaluated for IFNγ ELISPOT. TAA-specific Tregs were identified by incubating these same peptide-pulsed DCs with MACS-enriched CD4+ CD25+ T-cells, and then subsequently evaluating this Treg pool for the ability to suppress the proliferation of anti-CD3 stimulated polyclonal Teff. They were able to identify a highly individualistic pattern of TAA-specific Teff and Treg cells within the peripheral blood of these patients that did not exist in control patients. Depletion of Treg cells increased the IFNγ signature only for a certain set of these TAAs, but not others. Interestingly, they found that these TAAs were the same ones that also produced TAA-specific Tregs.

Finally, recent work in a model of mucosal allergy response has shown an expansion of CD4+ CD25+ CD127- Foxp3+ Tregs with specificity to fungal antigens from *Aspergillus fumigatus* and *Candida albicans*. In addition to the expanded number of Tregs, patients who suffer from the allergic disease allergic bronchopulmonary aspergillosis (ABPA) demonstrated an increased frequency of fungus-specific Th2 cells, suggesting a failed suppression of these cells by Tregs in symptomatic individuals (Bacher et al., 2013).

These human studies have definitively shown the presence of antigen-specific Tregs, but have as of yet been unable to demonstrate functional specificity, and if anything have demonstrated antigen non-specific function. A number of mouse models have similarly shown the presence of antigen-specific Tregs. In one such study, vaccination with a panel of SEREX-identified self-antigens derived from a chemically-

induced mouse sarcoma induced CD4+ CD25+ Foxp3+ Tregs that were capable of peptide-dependent *in vitro* suppression that was contact-dependent, cytokine-independent, and abrogated with anti-GITR antibody. This suppressive capability waned over 8 weeks post-vaccination but was regained upon *in vitro* cognate peptide stimulation (Nishikawa et al., 2005b). This study, however, like the human studies, failed to assess the ability of Tregs to function in an antigen-specific manner. The best studies examining this concept have come from mouse models of transplant tolerance and autoimmunity.

Hori et al (Hori et al., 2002) examined the developmental and functional requirements for CD4+ CD25+ Tregs in mice bearing an anti-myelin basic protein (MBP) transgenic TCR. When this TCR is crossed onto the RAG-/- background, mice spontaneously develop Experimental Autoimmune Encephalitis (EAE), a disease similar to multiple sclerosis. Mice on a RAG+/+ background do not develop EAE. Transfer of total CD4+ cells from a RAG+ MBP mouse into a RAG-/- recipient does not lead to EAE, but transfer from a RAG- MBP mouse, or transfer of CD25-depleted CD4+ from a RAG+ MBP mouse does lead to EAE. They found that RAG- MBP mice lack CD4+ CD25+ Treg, while RAG+ MBP mice do not. Transfer of CD25+ CD4+ cells from either a RAG+ WT mouse or a RAG+ MBP mouse protected RAG- recipients from EAE induced by adoptive transfer of RAG- MBP CD4+ cells. Interestingly, transfer of CD4+ CD25+ MBP-depleted cells from RAG+ MBP donors did not prevent recipient EAE. Analysis of TCRα & TCRβ usage revealed that non-transgenic CD25+ CD4+ cells from RAG+ MBP+ animals displayed oligoclonal TCR usage, suggesting perhaps that their failure to protect from EAE was due to a reduced TCR repertoire.

In a second model, Tarbell et al (Tarbell et al., 2004) utilized DCs from NOD mice to *ex vivo* expand BDC2.5 TCR transgenic T-cells, which see a single pancreatic islet autoantigen, into CD4+ CD25+ Tregs. These expanded Tregs demonstrated more potent suppression *in vitro* than their non-expanded counterparts. *In vivo*, as few as 5000 expanded antigen-specific Tregs were able to suppress insulitis (Type-1 DM) that results from the transfer of polyclonal Teff cells into NOD.Scid mice, whereas 10E5 polyclonal Tregs from NOD mice could not. Furthermore, these Tregs could suppress insulitis even when administered 14 days following transfer of diabetogenic T-cells.

Samy et al (Samy et al., 2005) analyzed the role of polyclonal Tregs in Autoimmune Ovarian Disease (AOD), which occurs in day 3 thymectomized (d3tx) mice. They found that the ovarian DLN was the site of the T-cell activation that leads to AOD, and that polyclonal Tregs could suppress this activation in the draining ovarian lymph node. They also found similar suppression of the organ-specific draining lymph nodes in mouse models of dacroadenitis and autoimmune prostatitis. While polyclonal Tregs capable of suppressing AOD where found throughout the body, they were enriched within the draining ovarian lymph node. Depletion of adoptively transferred Tregs resulted in reversal of protection and severe AOD. Finally, they found that polyclonal Tregs from female mice were superior to Tregs from male mice at protecting from AOD when Treg contact with ovarian antigen was delayed by removal of the ovary prior to adoptive transfer and then later transplant of an ovary back into the recipient. This female > male response was not present, however, when the ovarian antigens were present at the time of Treg adoptive transfer.

Yu et al (Yu et al., 2005) examined the ability of proteolipid protein-1 (PLP-1) antigen-specific Tregs from TCR transgenic 5B6 mice to suppress EAE induced by a variety of antigen-specific Teff cells. They found that they could expand PLP-1 Tregs from 5B6 mice using *in vivo* delivery of an Ig-PLP-1 fusion protein in an adjuvant-free setting. These Tregs, when adoptively transferred, were able to suppress EAE in RAG-/- recipients brought about by adoptive transfer of pathogenic 5B6 Teff cells. This effect was reversed upon administration of anti-IL-10 antibody. These 5B6 Tregs were also able to suppress EAE when transferred into WT mice that had been vaccinated against PLP-1 peptide or CNS homogenate along with adjuvant. When injected into (C57B6 x SJL/J) F1 mice (which are MHCII $I\text{-}A^b$ x $I\text{-}A^s$) 5B6 Treg (which see $I\text{-}A^s$) were able to protect mice from EAE when vaccinated with PLP-1 peptide ($I\text{-}A^s$ restricted), but not when vaccinated against myelin oligodendrocyte glycoprotein (MOG) ($I\text{-}A^b$ restricted) or myelin basic protein (MBP) ($I\text{-}A^s$ restricted). However, when the 5B6 Treg were pre-activated with PLP1 peptide *in vitro*, they were able to suppress EAE in mice vaccinated with MOG peptide. Also, administration of Ig-PLP-1, Ig-PLP-2, and Ig-MBP3, but not control Ig post induction of EAE with CNS homogenate vaccination all reversed EAE in SJL/J mice. Depletion of Tregs with anti-CD25 prior to EAE induction reversed this protection from EAE. Finally, 5B6 Tregs were able to ameliorate EAE in SJL/J mice vaccinated with CNS homogenate and PLP-2 peptide, but not MBP peptide (both peptides are $I\text{-}A^s$ restricted), suggesting intra-molecular (PLP-2), but not inter-molecular (MBP) suppressive functions.

Sánchez-Fueyo et al (Sánchez-Fueyo et al., 2006) developed a transplant model of alloantigen specificity utilizing a transgenic mouse (ABM) with a TCR highly specific

for the class II molecule I-A^{bm12}, which is expressed on a variant strain of the B6 mouse known as B6.C-$H2^{bm12}$/KhEg (bm12). The I-A^{bm12} differs from the parental B6 I-A^{b} by only 3 amino acids, and yet this difference results in bm12 skin allograft rejection by WT B6 mice. The authors identified a Treg population within the AMB TCR-transgenic T-cell pool. These ABM Tregs were anergic to stimulation with bm12 splenocytes and were capable of suppressing ABM Teff proliferation *in vitro*, whereas WT B6 Tregs were not. Further, the ABM Tregs were capable of mediating bystander suppression of Teffs bearing a different TCR. *In vivo* ABM Tregs were able to prevent bm12 skin graft rejection by adoptively transferred AMB Teff at a 1:1 ratio in a nude B6 model. WT B6 Treg were able to provide some protection, but only when used in much higher Treg:Teff (3:1) ratios. ABM Tregs were also able to prevent rejection of bm12 skin grafts by WT B6 polyclonal Teff in these same B6 nude recipients. AMB Treg were not able to protect BalbC skin grafts, even when used in high Treg:Teff ratios. However, ABM Treg, when transferred at a high Treg:Teff (4:1) ratio, were able to protect (Balbc x bm12) F1 skin grafts from rejection by WT B6 polyclonal Teff, demonstrating 'linked suppression.'

Collectively, these mouse studies demonstrate antigen-specific activation of Tregs with improved functional capacity when antigen specificity is maintained. Further, through concepts such as linked suppression, the necessity for the Treg's antigen to be present on the protected cell for suppression to take place, strongly suggests at least an element of functional antigenic specificity. It does not, however, definitively show that Tregs function in an antigen-specific manner *in vivo*.

To answer this question definitively, Zhou & Levitsky (Zhou & Levitsky, unpublished data) devised an elegant series of experiments utilizing a mixed tumor model

within the BalbC A20 mouse lymphoma system. In that model, mice were challenged subcutaneously with a 1:1 mixture of A20 tumor bearing the model antigen influenza hemagluttinin (HA) and the bioluminescent luciferase (luci) enzyme (A20.HA.luci) along with a second A20 tumor bearing the model antigen chicken egg ovalbumin (OVA) (A20.OVA). Tumor-bearing mice were then treated with *in vitro* polarized Th1 cells from transgenic 6.5 αβ TCR mice, which recognize HA peptide 100-120 presented by I-E^d (Kirberg et al., 1994), with the addition of increasing amounts of one of two sets of *in vitro* generated Tregs. These Tregs were either derived from the same 6.5 TCR mouse as the Th1 cells and thus bore the same antigenic specificity, or were from the transgenic DO11 αβ TCR mice, which recognize OVA peptide 323-339 presented by I-A^d (Murphy et al., 1990) and therefore bore a different antigenic specificity. Then, through bioluminescent imaging they were able to directly monitor growth of the A20.HA.luci tumor, and via caliper measurements were able to measure total tumor mass. As shown in Figure 2.1, they were able to demonstrate the antigen-specific suppression of 6.5 Th1 cells by the 6.5 Treg with no suppression by the DO11 Treg. The 6.5 Tregs were then validated to be non-suppressive to a DO11 Th1 response in the reverse 'criss-cross' experiment as shown. They further were able to explant these tumors at the end of the treatment course and through *in vitro* proliferation assays using 6.5 and DO11 responder cells verified that the HA and OVA antigens were appropriately present or absent based upon the tumor curves. These experiments very clearly demonstrate that Tregs are capable of antigen-specific suppression in the setting of a heterogeneous mixed-tumor model, but left open the question as to the mechanism through which this functional specificity was achieved.

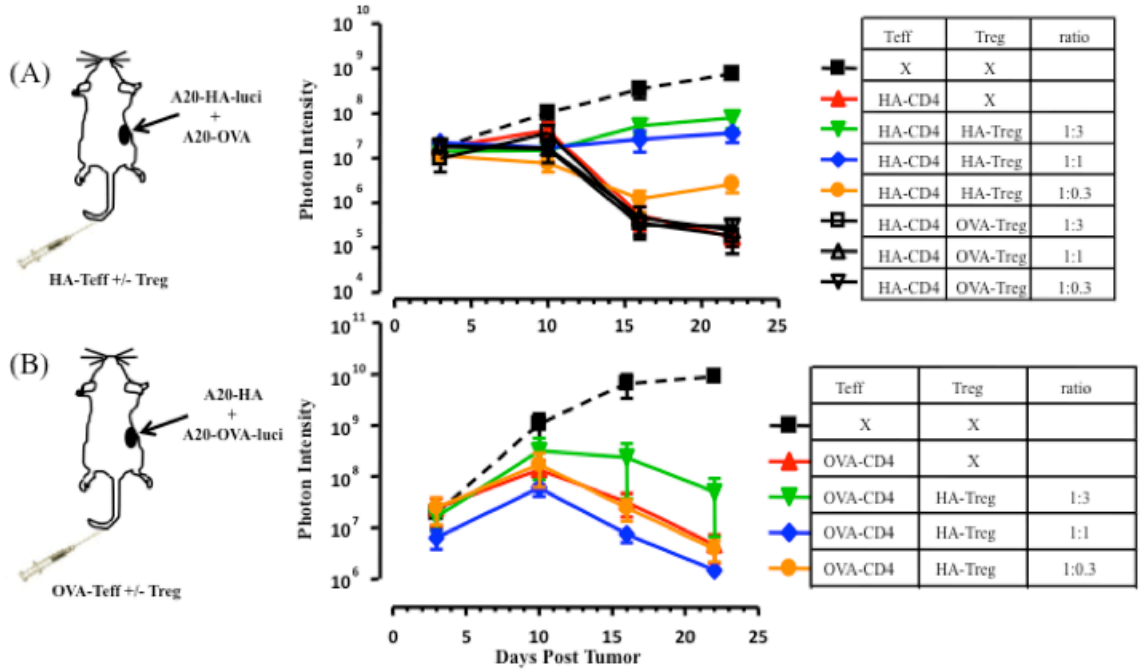

Figure 2.1 Tregs demonstrate antigen-specific suppression of Th1-mediated tumor rejection *in vivo*.

Recipient mice were injected with a 1:1 mix of either A20.HA.luci and A20.OVA (A) or A20.OVA.luci and A20.HA (B). Mice were then treated with Teffs and Tregs as indicated and tumor size monitored with bioluminescence and caliper measurements. Shown here is bioluminescent imaging data measuring luci-bearing tumor size. (A) 6.5 Treg, but not DO11 Treg, are able to suppress the rejection of A20.HA.luci tumor cells by 6.5 Th1 cells. (B) These same 6.5 Tregs do not suppress the rejection of A20.OVA.luci tumors by DO11 Th1 cells.

2.6 Regulatory T-Cells and Cancer

It has long been recognized that the immune system plays an important role in the development and progression of cancer. The idea that the immune system sees and suppresses a continuous onslaught of cancerous precursors was first suggested by Ehrlich in 1909 (Ehrlich, 1909). This idea was further expanded upon and the formal "cancer immunosurveillance" model proposed by Burnett and Thomas in the late 1950s (Burnett, 1957; Thomas, 1959). Since that time, a large volume of work has gone into clarifying the exact roles that the immune system plays during the process of tumorigenesis, immune editing, and tumor immune escape (reviewed in Dunn et al., 2002; Dunn et al., 2004).

Tregs were first proposed to have a negative effect on tumor immunotherapy back in 1975 (Fujimoto et al., 1975). A large body of data supporting the idea that Tregs have a negative impact upon cancer progression comes from mouse models wherein a number of studies have shown that the depletion of Tregs or reduction in their suppressive capability improves immune-mediated tumor clearance (reviewed in Zou, 2006). This has been accomplished in several ways. Administration of antibody against CD25, the high-affinity IL2 receptor subunit expressed on Tregs and Teffs, has been shown to effectively deplete Tregs and lead to reduced tumor growth (Onizuka et al., 1999; Shimizu et al., 1999). Tregs have also been shown to be preferentially depleted with administration of cyclophosphamide. While also a primary chemotherapeutic agent, this drug has been shown to deplete Tregs at much lower doses than are required for its direct anti-tumor activity, and administration of low-dose cyclophosphamide has been shown to promote immune-mediated rejection in a number of models (Rollinghoff et al., 1977;

Glaser, 1979; Turk et al., 2004), including a cyclophosphamide-resistant leukemia model (Awwad & North, 1989).

Blocking of Treg function has also been shown to promote improved tumor outcomes. Antibody targeted against glucocorticoid-induced tumor-necrosis factor receptor related protein (GITR), a molecule expressed by Tregs and involved in their suppressive function, has been found to reduce the suppressive capacity of Tregs *in vitro* (Shimizu et al., 2002) and was subsequently shown to result in protection from melanoma challenge (Turk et al., 2004) and in rejection of established sarcoma (Ko et al., 2005). Finally, administration of blocking antibodies to cytotoxic T-lymphocyte associated antigen 4 (CTLA-4), another marker expressed by Tregs and involved in their suppressive function, resulted in rejection of established melanoma tumors with protection against subsequent challenge (Leach et al., 1996).

Along with the aforementioned studies that suggest the removal of Tregs or dampening of their function results in improved tumor outcomes, studies have also investigated the ability of adoptively transferred Tregs to suppress otherwise potent anti-tumor immune responses. Multiple studies in mouse melanoma models have shown that the co-transfer of CD4+ CD25+ T-cells, i.e. Tregs, but not CD4+ CD25-, i.e. T naïve, can abolish the anti-tumor effect of tumor-antigen specific cytotoxic CD8+ T-cells, thus suggesting an active role of Tregs in the suppression of immune-mediated tumor rejection (Turk et al., 2004; Antony et al., 2005; Chen et al., 2005).

In human studies, evidence supporting the idea that Tregs negatively affect tumor immune clearance and prognosis begins with correlative data from cancer patients. Increased frequencies of Tregs in patients with lung and ovarian cancer were first

described by Woo and colleagues (Woo et al., 2001) and have since been seen in peripheral blood of patients with a wide range of tumors including breast, ovarian, lung, leukemia, esophageal, hepatocellular, gastric, melanoma, colorectal, lymphoma, and pancreatic (reviewed in Zou, 2006). Many of these same studies were able to demonstrate *in vitro* suppressive capability of patient Tregs to tumor-associated antigens.

Beyond their often increased frequency within peripheral blood, Treg numbers have also been shown to be altered within tumor, peritumoral tissue, and draining lymphatic tissue. In malignant melanoma samples, Tregs have been shown to selectively accumulate within tumor tissue as opposed to surrounding tissue or peripheral blood (Ahmadzadeh et al., 2008). In ovarian cancer, increased numbers of tumor-infiltrating Tregs have been correlated with a decreased survival. These same Tregs, as well as Tregs from tumor ascites, were shown to inhibit Her-2/neu TAA-specific CD8+ cytotoxicity both *in vitro* and *in vivo* (Curiel et al., 2004). Increased numbers of Tregs within lymphoid infiltrates surrounding the tumor, but not within the tumor body, are associated with poor prognosis in breast cancer (Gobert et al., 2009), and Tregs from similar lymphoid infiltrates have been associated with an active, proliferating $ICOS^{hi}$ Ki67+ phenotype that co-localized with mature DC-LAMP+ and pDC+ cells which are both involved in Treg proliferation and survival (Menetrier-Caux et al., 2009).

More recently, strategies based upon Treg depletion via CD25+ similar to those employed in mouse models have made an impact within human studies of ovary, breast, lung (Barnett et al., 2005), renal cell (Dannull et al., 2005), and melanoma (Attia et al., 2005). Also, administration of low-dose cyclophosphamide in cancer patients has also shown the ability to improve immune responses (Berd & Mastrangelo, 1988). Further,

administration of anti-CTLA-4 antibodies have recently been shown to produce tumor regression in patients with both metastatic melanoma and ovarian cancer (Phan et al., 2003; Hodi et al., 2003), and have now been FDA approved for treatment of metastatic melanoma, providing further translational evidence that Tregs in fact play an important role in the evasion of immune-mediated tumor clearance. Overall it is now clear that active suppression by Tregs is one of the main methods by which tumors evade immune clearance (Dunn et al., 2002; Dunn et al., 2004; Zhou, 2006).

2.7 Tumor Immune Manipulation

It is now clear that functional Tregs can be found within a variety of different tumors and are often associated with an overall poor prognosis. The role that the tumors themselves play in this process is an evolving one, but evidence increasingly suggests that tumors are not bystanders in this process, but rather are actively involved in the recruitment, conversion, and functional manipulation of Tregs and Teffs within the tumor microenvironment.

Tregs located within tumors are the result of both trafficking of previously generated thymically-derived nTregs as well as conversion from circulating Tnaive cells into iTreg, and in fact iTreg and nTreg have been shown to contribute independently to tumor-specific immune tolerance (Zhou and Levitsky, 2007). As many tumor antigens are self antigens (Khong & Restifo, 2002), a substantial proportion of the circulating nTreg pool likely bears specificity for antigens with the tumor microenvironment. Tregs have been shown to traffic based upon a number of different signals. One such signaling system involves the chemokine CCL22, also known as macrophage-derived chemokine

(MDC), which binds to the CCR4 receptor on T-cells. DCs and macrophages have both been shown to produce CCL22 which rapidly binds to CCR4 on activated T-cells, including Tregs, with much greater affinity than naïve T-cells (Wu et al., 2001). Recently, Curiel and colleagues (Curiel et al., 2004) demonstrated that CCL22 is effectively produced by both tumor resident macrophages as well as tumor cells themselves. Further, they found that administration of anti-CCL22 antibody reduced tumor-infiltrating Tregs, implicating that CCL22 signaling plays a major role in Treg recruitment into tumors.

Besides recruitment of pre-existing nTregs, tumors are highly capable of the conversion of iTregs from Tnaive cells. Antigen-specific T-cell anergy has been shown to occur early in the course of tumor progression (Stavely-O'Carroll et al., 1998) and to be dependent upon host APC processing of antigen (cross-tolerance) rather than direct tumor-T-cell interaction (Cuenca et al., 2003; Sotomayor et al., 2001). The tumor microenvironment produces a number of signals, including VEGF, IL-10, and TGFβ, leading to suppression of DC maturation and immature/dysfunctional DCs (Gabrilovich, 2004; Zou, 2005). These DCs in turn further secrete TGFβ and IL-10, and are capable of inducing conversion and proliferation of Tregs in the tumor (Jonuleit et al., 2000; Ghiringelli et al., 2005; Seo et al., 2001; Chen et al., 2003; Fantini et al., 2004).

While tumors create a microenvironment that promotes Treg influx and conversion, they also manipulate T-cell function through a number of different mechanisms. A growing number of immune cell-surface proteins with important roles in the regulation of cell-mediated immunity have been found on tumor cells. Notable within

these are the negative coregulatory molecules PD-L1 and galectin-9, as well as the antigen-presenting molecules MHCI and MHCII.

Programmed death ligand-1 (PD-L1), also known as B7-H1, binds to the programmed death-1 (PD-1) molecule, which is expressed by a number of immune cell subsets including T, B, and myeloid derived cells. PD-1 expression is considered a marker of immune exhaustion, and T-cells expressing this molecule are typically dysfunctional in their proliferative and effector capacities (Blackburn et al., 2009; Wherry et al., 2007; Day et al., 2006). High levels of PD-1 expression on these same cells is associated with an immunosuppressive environment that is favorable to tumor growth in a number of models (Ahmadzadeh et al., 2009; Sfanos et al., 2009).

PD-1 binds to one of two receptors; PD-L1 and PD-L2. PD-L2 is exclusively expressed by APCs, whereas PD-L1 expression has a much broader tissue distribution including liver, lung, spleen, and marrow (Blank & Mackensen, 2007; Latchman et al., 2001; Freeman et al., 2000). PD-L1 expression has also been found on a number of different tumors (Loos et al., 2008; Zhang et al., 2009), and its expression within tumor cells is increased following exposure to IFNγ, an important Th1 cytokine (Zhang et al., 2009; Zhou et al., 2010). PD-L1 expression by tumor cells has been associated with a poor prognosis in a number cancers, including melanoma, pancreatic, lung, stomach, colon, breast, renal, cervical, and leukemia (Blank et al., 2007; Loos et al., 2008; Gao et al., 2009; Thompson et al., 2004; Geng et al., 2008; Karim et al., 2009).

Ligation of PD-1 by PD-L1 can lead to effector cell exhaustion, suppression of cytokine production, and apoptosis (Day et al., 2006; Ahmadzadeh et al., 2009; Isogawa et al., 2005; Dong et al., 2002), and thus the expression of PD-L1 by tumors potentially

allows a direct suppressive mechanism between tumor and Teff. Interestingly, co-infiltration of tumors by Tregs and PD-1+ Teffs has been described in high-risk breast cancer patients (Ghebeh et al., 2007) as well as in the tumor-laden livers of AML-bearing mice (Zhou et al., 2009a). This suggests that perhaps PD-1/PD-L1 may also play a role in the suppressive capacity of Tregs. Recent studies by Zhou and colleagues (Zhou et al., 2010) have in fact shown that the ability of Tregs to suppress Teff *in vitro* is dramatically reduced when the PD-1/PD-L1 pathway is altered via either knockout or blocking antibodies. They were further able to show that blocking this same pathway *in vivo* enhances the efficacy of adoptive cell therapy; an effect that was made even more robust when specific Treg depletion was incorporated. Similarly, combination blockage of PD-1 and CTLA-4 has recently been shown by multiple groups to impair Treg function and improve tumor outcomes (Duraiswamy et al., 2013; Curran et al., 2010). Multiple other studies have also shown that blocking the PD-1/PD-L1 axis improves adoptive immunotherapy (Strone et al., 2003; Okudaira et al., 2009; Thompson et al., 2005). Thus it would appear that the PD-1/PD-L1 pathway is an important one for tumor immunity, and manipulation of this pathway by tumors can serve as a potential means for tumor immune manipulation and escape via alterations of both Teff and Treg functions.

A second negative regulatory pathway tumors can make use of involves the inhibitory effects of galectins upon the immune system. Galectins are glycan-binding proteins with affinity for N-acetyllactosamine sequences on cell surface glycoconjugates (Camby et al., 2006). Glycan binding can mediate intracellular signaling which results in downstream effects upon multiple cellular processes including cell survival and apoptosis (Taams et al., 2006). Galectins have been found in tumor and tumor-associated stroma in

multiple tumor types including melanoma, glioma, breast, and gastric tumors and their expression levels have shown correlation with aggressiveness of tumor growth and metastasis (Liu & Rabinovich, 2005). Galectin-1 has been shown to be secreted by melanoma cells and have immunosuppressive effects upon Th1 responses (Rubenstein et al., 2004).

Another particularly interesting galectin is galectin-9. Galectin 9 has been shown to serve as a ligand for T-cell immunoglobulin and mucin domain 3 (TIM-3), a molecule expressed by lymphocytes, DCs, and monocytes (Zhu et al., 2005; Anderson et al, 2007a). Binding of galectin-9 to TIM-3 results in Th1 cell death (Zhu et al., 2005), and TIM-3 blockade has been shown to increase the frequency of IFNγ-secreting T-cells (Sabatos et al., 2003). Combination of TIM-3 blockade with either PD-1 or CTLA-4 blockade has also been investigated and found to have increased anti-tumor affect compared to single agent blockade (Ngiow et al., 2011). Interestingly, recent work by Sakuishi and colleagues (Sakuishi et al., 2013) has demonstrated that intratumoral Tregs show a high degree of TIM-3 positivity, and intratumoral TIM-3+ Tregs had greater suppressive capability than their TIM-3 negative counterparts. They further found that combined blockade using TIM-3 and PD-1 resulted in improved tumor clearance as well as multiple alterations in Treg phenotype including downregulation of key genes involved in Treg suppression including perforin, IL-10, PD-1, and LAG-3. Finally, they found a synergistic effect on tumor clearance when TIM-3 blockade was couple to Treg-specific depletion using Foxp3-DTR mice. In all, their data suggest once again that the TIM3 pathway is another potent negative inhibitory pathway with implications upon tumor, Tregs, and Teffs.

B and T lymphocyte attenuator (BTLA), a CD28 family member, is another inhibitory molecule involved in negative regulation and is expressed by multiple immune effector cells (Watanabe et al., 2003). It binds to the herpes virus entry mediator (HVEM) molecule, which is expressed by a wide range of immune cells (Murphy & Murphy, 2010), but can also be found in tumors including melanoma cells (Derre et al., 2010). Blockade of the BTLA/HVEM pathway has been shown to augment TIL expansion and function (Fourcade et al., 2012), and serves as yet another example of a negative costimulatory pathway that tumor cells can utilize to alter immune response.

Besides the recruitment of Tregs and the utilization of negative costimulatory pathways, tumor cells also make use of multiple alterations in antigen presentation molecules. The most classic example of this finding occurs with the loss of MHCI expression. MHCI presents antigens to CD8+ T-cells, making them prone for CTL recognition. Loss, downregulation, or alteration of MHCI coding sequences are all mechanisms by which tumors can evade CD8+ T-cell recognition. (Rivoltini et al., 2002; Hicklin et al., 1999; Bicknell et al., 1994; Natali et al., 1989). MHCI loss is considered to be the most common strategy used by tumors to avoid T-cell-mediated rejection (Drake et al., 2006; Marincola et al., 2006), with some studies showing MHCI loss in 50% of human tumor samples (Rees & Mian, 1999). MHCI loss comes with a cost, making cells susceptible to NK-mediated killing due to lack of MHCI negative signaling to NK-cell killer inhibitory receptors (KIRs). Besides the absence of MHCI negative signaling, NK cells also require activating signaling via molecules such as MICA and MICB, which are expressed on a number of tumors. Loss of these molecules by tumors, therefore,

potentially allows MHCI-negative cells to avoid killing by NK cells (Rees & Mian 1999; Lanier 2005; Groh et al., 2002).

In contrast to the loss of expression seen for MHCI, many tumor cells have been found to upregulate expression of MHCII genes. MHCII is an αβ-heterodimeric transmembrane glycoprotein capable of presenting antigenic peptides to cognate T-cell receptors (TCRs) of CD4+ T-cells, and in humans is composed primarily of the HLA-DR, -DQ, and –DP molecules (Benacerraf, 1981; Janeway et al., 1988). MHCII expression is tissue specific, with constitutive expression in many antigen presenting cells and inducible expression in many cell types including tumors (Goodwin et al., 2001). Both human and mouse melanomas provide an excellent example of this phenomenon. Melanocytes are naturally devoid of MHCII molecules, but melanomas on the other hand often express such molecules, especially HLA-DR (Aoudjit et al., 2004; Holzmann et al., 1987; Ruiter et al., 1991; Bernsen et al., 2003). This expression can be either inducible or constitutive, with inducible expression frequently elicited by exposure to inflammatory cytokines, most notably IFNγ (Deffrennes et al., 2001). Increasing frequency of MHCII expression is seen through the transformation of benign nevi to dysplastic nevi to primary melanoma to malignant melanoma (Ruiter et al., 1984), and melanomas constitutively expressing HLA-DR demonstrate increased metastasis and poor prognosis (Holzmann et al., 1987; Ruiter et al., 1991; Zaloudik et al., 1988) with similar findings also found for HLA-DQ and HLA-DP (Ostmeier et al., 2001).

MHCII expression is dependent upon the transcription factor class II transactivator (CIITA), which is the master switch for MHCII expression (Deffrennes et al., 2001; Goodwin et al., 2001). CIITA is essential for transcriptional activation of all

MHCII genes and has a helper function in MHCI gene expression (Holling et al., 2006; LeibundGut-Landmann et al., 2004). Constitutive expression of CIITA results from activation of the upstream promoter III element, which is classically used by B-lymphocytes. IFNγ-inducible expression, on the other hand, is from promoter IV, which is known to be an IFNγ-responsive sequence (Deffrennes et al., 2001; van der Stoep et al., 2007; Goodwin et al., 2001). Exactly how CIITA becomes activated in cancers is not fully understood. It is now evident that CIITA expression is highly influenced by epigenetic modifications (Holling et al., 2006), which are well known to be a hallmark of cancer (Esteller, 2003). Further, there has been recent demonstration of mitogen-activated protein kinase (MAPK) pathways as regulators of CIITA transcription in melanoma, with particular identification of an AP-1 responsive site in the CIITA promoter III region (Martins et al., 2007).

The expression of MHCII in tumors is somewhat paradoxical, since it allows direct presentation to CD4 cells by tumor-expressed MHC:peptide complexes (Zarour et al., 2002; Zeng et al., 2001), which one might think would make tumors more prone to immune-mediated clearance. This is in fact not the case, however, as evidenced by the aforementioned correlation between melanoma progression and increasing MHCII expression frequency. Explanations for this phenomenon are varied and inconclusive. Classically, it has been hypothesized that expression of MHCII with a lack of costimulatory molecules on tumor cells results in a "signal 1" without "signal 2" with resultant induction of T-cell anergy (Rosenberg 2001; Rivoiltini et al., 2002; Rabinovich et al., 2007). More recently, improved understanding of negative costimulatory pathways such as PD-1/PD-L1 and their utilization by tumor cells has provided another possible

explanation that reinforces and goes beyond the simple lack of costimulation, and given their shared IFNγ-inducible features is particularly intriguing (Zhang et al., 2009; Zhou et al., 2010).

Somewhat akin to the actions of the PD-1/PD-L1 pathway is the interaction of MHCII with lymphocyte activation gene 3 (LAG-3). LAG-3 is a negative regulator of activated T-cells with close relationship to the CD4 molecule itself (Huard et al., 1994; Hannier et al., 1998). Both LAG-3 and CD4 bind to MHCII, but LAG-3 binds with much higher affinity (Workman et al., 2002; Huard et al., 1995). LAG-3 has previously been shown to regulate activated T-cell expansion (Workman et al., 2004). LAG-3 has been further shown to negatively regulate T-cell homeostasis via Treg dependent and independent mechanisms (Workman & Vignali, 2005). Recently it has been shown that LAG-3 and PD-1 work synergistically and their combined blockade results in improved tumor clearance (Woo et al., 2012). Thus, through interactions with LAG-3, MHCII may be able to not only serve as a supplier of "signal 1," but may also allow negative costimulatory signaling.

2.8 Experimental Motivation

A growing body of evidence suggests the potential for functional specificity in regulatory T-cells, and the data of Zhou and Levitsky (Figure 2.1; unpublished) demonstrating the antigen-specific suppression of immune-mediated rejection in the A20 lymphoma model strongly supports this idea. Their findings further raise a number of questions regarding the mechanisms by which Tregs enact their suppressive effects. Their model utilized a heterogeneous tumor in which all relevant antigens were present in

the tumor microenvironment and available to tissue- and draining lymph node-resident APCs. The fact that they saw antigen-specific suppression would seem to suggest that these APCs were somehow being bypassed and were not involved in the suppressive mechanism used. Direct presentation by the tumor to the Tregs would, therefore, serve as a reasonable explanation for the specificity they demonstrated. One caveat to that interpretation, however, is the fact that the A20 tumor line used is itself a functional APC bearing high levels of MHCII and costimulatory molecules (Sotomayor et al., 2001). Thus, arguing that direct tumor antigen presentation is responsible as opposed to presentation by a third party APC is a bit like splitting hairs, with application only to lymphoid malignancies.

The idea becomes strengthened and implications broadened when taking into account the large volume of data demonstrating the upregulation of MHCII on solid tumors, most notably melanomas. While a number of explanations for this upregulation have been postulated it certainly stands to be considered that the upregulation of MHCII by tumors during the course of their progression may in fact be beneficial to tumor cells through direct recognition by CD4+ T-cells. This seems particularly plausible given the tendency for MHCII expression to increase in the setting of inflammatory cytokines such as IFNγ (Deffrennes et al., 2001). Such inflammatory cytokines likely represent preceding tumor recognition and an already ongoing immune response. Induction of MHCII in this setting could allow for direct presentation to Tregs in an attempt by the tumor to elicit suppression; a sort of immunologic 'Hail Mary.' In support of this idea, Wang and colleagues (Wang et al., 2005) have isolated and characterized a Treg clone (TIL164) from a melanoma TIL pool, which recognizes a previously undescribed gene

ARCTI (Ag recognized by Treg cells 1). This clone was able to suppress proliferation and IL-2 secretion of melanoma-reactive T-cells. Interestingly, they found that tumor cells themselves, but not B-cells loaded with tumor lysate, were able to activate TIL164. This is potentially explained with findings from Tsuji and colleagues (Tsuji et al., 2012) who recently identified a novel HSP90-dependent antigen presentation pathway that exists within MHCII+ melanoma cells and allows for direct presentation of endogenous tumor antigen to CD4+ cells.

Taken as a whole, it seems reasonable to hypothesize that the upregulation of MHCII by tumor cells, potentially coupled with novel antigen processing pathways, could allow for direct presentation of tumor-derived antigens to Tregs with resultant antigen-specific suppression of immune-mediated tumor rejection. The following experiments were undertaken to investigate this hypothesis.

Chapter 3

Development of the B16 Variant Model

3.1 Introduction

In order to test our hypothesis, we first had to establish a model of an antigen-specific immune-mediated tumor rejection that could subsequently be suppressed by Tregs. While a number of such models have been previously described (Chen et al., 2005; Antony et al., 2005; Turk et al., 2004) and even used in our laboratory, the goal of our studies necessitated development of a new model. To begin with, we desired to have an *in vivo* mouse model wherein tumor cells could potentially be the only MHCII+ cell capable of presenting antigen to Tregs. While this could potentially be accomplished with bone marrow chimeras, the simplest solution was the use of an MHCII knockout (KO) mouse. Of the many commonly used mouse strains, the C57BL/6 mouse expresses only one MHCII allele (I-A^b), and an MHCII knockout mouse for that strain has previously been described (Madsen et al., 1999), making the C57BL/6 strain an ideal host for our experiments.

Second, our hypothesis was dependent on the upregulation of MHCII by tumor cells, and thus required a tumor line that did not express MHCII at baseline but could upregulate MHCII when exposed to inflammatory cytokines such as IFNγ. The B16-F10 tumor line is a C57BL/6 background melanoma that has previously been described to

demonstrate IFNγ-inducible expression of MHCII (Xie et al., 2010; Quezada et al., 2010) and was a commonly used line within our own laboratory. Further, B16-F10 expresses a number of well-known tumor antigens and has been extensively studied in adoptive cell therapy (ACT) models (Overwijk et al., 1998; Muranski et al., 2008; Overwijk & Restifo, 2001), making it well suited for our studies.

Finally, in order to establish a model of antigen-specific immune-mediated tumor rejection with suppression by Tregs, we had to have definable antigens within our tumor that could be targeted by both effector and regulatory T-cells. Given that our target tumor was to be MHCII negative at baseline, a treatment based upon CD8+ effector cells was sought. Several such models have been utilized in the B16-F10 tumor, including targeting of the self-antigen gp100 using CD8+ cells from the TCR transgenic Pmel mouse (Overwijk et al., 1998) and targeting of the model antigen ovalbumin (OVA) using CD8+ cells from the TCR transgenic OTI mouse (Hogquist et al., 1994; Dobrzanski et al., 1999; 2000; 2001). This latter method was of particular interest for several reasons. First, our laboratory had extensive experience with the OVA antigen including prior work with OVA in the B16-F10 system. Further, besides MHCI recognition of antigen from the OVA protein by the OTI TCR transgenic mouse, MHCII recognition of antigen from the OVA protein by the OTII TCR transgenic mouse has also been well described (Barnden et al., 1998), making the OVA antigen and its recognition by the MHCI-dependent OTI and MHCII-dependent OTII TCR transgenic mice an ideal target.

In this first study, we set out to design a model wherein C57BL/6 WT and MHCII knockout mice would be challenged with B16 tumor cells bearing the OVA antigen and

treated with OVA-specific OTI CD8+ cells with subsequent suppression of this treatment using OVA-specific OTII Treg cells. After evaluating several different iterations of this concept, we successfully identified a subcutaneous tumor challenge model using the B16.mOVA tumor line that showed an appropriate treatment response to adoptive transfer of OTI CD8+ cells. We were also able to demonstrate an apparent suppression of this response with addition of OTII Tregs in the MHCII knockout mouse, suggesting a role for direct antigen presentation of tumors to Tregs. Further, given the suppression demonstrated using our MHCII-inducible tumor, we developed and characterized MHCII-constitutive and non-inducible variants of the B16.mOVA tumor line as tools to allow future experiments to explore further the suppression seen in this study.

3.2 Materials and Methods

3.2.1 Mice

Mice six to eight weeks old were used for all experiments, with matching of donor/recipient gender whenever possible. All mice were housed and bred in the Johns Hopkins University Cancer Research Building I mouse facility using standard procedures, and all experiments involving the use of mice were performed in accordance with protocols approved by the Animal Care and Use Committee of the Johns Hopkins University School of Medicine.

C57BL/6 WT (C57BL/6NCr) and C57BL/6 45.1+/+ (B6-LY5.2/Cr) mice homozygous for the CD45.1/Ly5.2 congenic marker were purchased from the NCI (Frederick, MD). C57BL/6 Thy1.1+/+ (B6.PL-Thy1^{a}/CyJ) mice homozygous for the

Thy1.1/CD90.1 congenic marker, C57BL/6 I-A^b-/- (B6.129S2-$H2^{dlAB1\text{-}Ea}$/J) mice bearing a homozygous deletion within the *MHCII* gene locus (Madsen et al., 1999), C57BL/6 RAG1-/- (B6.129S7-$Rag1^{tm1Mom}$/J) mice bearing a homozygous deletion of the *Rag1* gene, and C57BL/6 OTII+/+ (B6.Cg-Tg(TcraTcrb)425Cbn/J) mice bearing homozygous insertion of the OTII αβ TCR specific for chicken ovalbumin peptide 323-339 (OVAII - ISQAVHAAHAEINEAGR) presented by the MHCII molecule I-A^b (Barnden et al., 1998) were purchased from Jackson Laboratory (Bar Harbor, ME). C57BL/6 RAG1-/- OTI+/+ (B6.129S7-$Rag1^{tm1Mom}$Tg(TcraTcrb)1100Mjb) mice bearing homozygous knockout of the *Rag1* gene along with homozygous insertion of the OTI αβ TCR specific for chicken ovalbumin peptide 257-264 (OVAI - SIINFEKL) presented by the MHCI molecule H-$2K^b$ (Hogquist et al., 1994) and C57BL/6 RAG1-/- OTII+/+ (B6.129S7-$Rag1^{tm1Mom}$Tg(TcraTcrb)425Cbn) mice bearing homozygous knockout of the *Rag1* gene along with homozygous insertion of the OTII αβ TCR specific for OVAII were purchased from Taconic (Germantown, NY). C57BL/6 Foxp3-GFP+/+ and +/y mice were a generous gift from Dr. Alexander Rudensky (Fontenot et al., 2005b).

C57BL/6 OTII+/+ Thy1.1+/+ mice were created by crossing C57BL/6 OTII+/+ with C57BL/6 Thy1.1+/+ to create OTII+/- Thy1.1+/- F1 progeny. These F1 progeny were then intercrossed and F2 progeny typed according to the presence of Thy1.1, absence of Thy1.2, and increase in CD4:CD8 ratio as seen in CD4 transgenic mice to suggest OTII+/? Thy1.1+/+ status. Since this CD4:CD8 skewing cannot differentiate between OTII+/- and OTII+/+, F2 offspring were then testcrossed to C57BL/6 WT mice and progeny again typed for CD4, CD8, Thy1.1, and Thy1.2. F2 parents were considered to be OTII+/+ only if all pups showed CD4:CD8 skewing with a minimum of 8 pups

typed. Once successfully generated, male and female OTII+/+ Thy.1.1+/+ mice were maintained as an independent colony.

C57BL/6 OTII+/- Thy1.1+/- Foxp3+/y mice were generated by crossing C57BL/6 OTII+/+ Thy1.1+/+ male mice with a C57BL/6 Foxp3-GFP+/+ female. Resultant female progeny were OTII+/- Thy1.1+/- Foxp3-GFP+/- and were not utilized due to decreased frequency of Foxp3 expression resulting from random X-inactivation in Foxp3-GFP heterozygotes. Male progeny on the other hand were Foxp3-GFP hemizygotes (+/y) and thus all Foxp3+ cells expressed the transgenic Foxp3-GFP and were subsequently used as Treg donors.

C57BL/6 RAG1+/- OTI+/- CD45.1+/- mice were generated by crossing C57BL/6 RAG1-/- OTI+/+ mice with C57BL/6 45.1+/+ mice to create heterozygote F1 progeny that were used as donors in experiments.

3.2.2 Tumor Cell Lines and Culture

All tumor cell lines were grown in 'CTL' media comprised of RPMI 1640 supplemented with 10% fetal bovine serum (FBS), penicillin-streptomycin (100 IU/ml & 100 ug/ml), L-glutamine (2 mM), HEPES buffer (5 mM), and 2-mercaptoethanol (100 uM) at 37°C in a humidified 5% CO_2 incubator. Addition of G418 (1000 ug/ml) was used for selection/maintenance of mOVA expression, and hygromycin (200 ug/ml) was used for selection/maintenance of C2TA expression. For *in vitro* induction of MHCI & MHCII, cells were cultured in 100 U/ml IFNγ (Peprotech; Rocky Hill, NJ) for three days.

The B16-F10 cell line is a melanoma derived from the C57BL/6 background. It has undetectable baseline MHCI and MHCII expression, both of which can be induced by

exposure to IFNγ. The B16-F10-D cell line is a variant of this same B16-F10 tumor that similarly has undetectable baseline MHCI and MHCII, but through unknown mechanisms has lost the ability upregulate MHCII in the presence of IFNγ. Both of these tumor lines were contained within longstanding laboratory stocks. B16.mOVA is a derivative of the B16-F10 line, which has been engineered to express a membrane-bound version of chicken ovalbumin (OVA) via stable transfection with pcDNA3.1(+)/mOVA under G418 selection as previously described (Preynat-Seauve et al., 2007) and was a gift from Dr. Bertrand Huard along with the parental pcDNA3.1(+)/mOVA construct.

B16-F10-D.mOVA was created by stably transfecting the parental B16-F10-D line with the same pcDNA3.1(+)/mOVA construct used to create the B16.mOVA line. Briefly, 2E6 B16-F10-D cells were transfected with 2 ug of pcDNA3.1(+)/mOVA plasmid DNA using Amaxa nucleofection solution V under program P-020 (Lonza; Allendale, NJ) and plated into non-selective CTL media. 48 hours post transfection G418 selection media was added and cells allowed to grow for approximately two weeks. Following this selection window, cells were seeded into flat-bottom, 96-well culture plates (Corning; Tewksbury, MA) at limiting dilution and cultures continued for another two weeks until single cell-clones could be identified in 1/3 or less of dilution wells. These single-cell clones were harvested and evaluated for OVA content via B3Z assay. OVA-positive clones were then challenged subcutaneously into C57BL/6 WT and I-A^b KO mouse recipients to verify tumor growth. A single OVA-expressing clone capable of growing in both WT and I-A^b KO mice was utilized for all subsequent experiments.

B16.mOVA.C2TA was created by stably transfecting the parental B16.mOVA line with the plasmid construct pcDNA3.1/Hygro/CIITA. This construct contained a full-

length human *CIITA* gene, previously cloned from pcDNA1-amp-tagCIITA, which was kindly provided by Dr. Suzanne Ostrand-Rosenberg (Tai et al., 1999), within a hygromycin selectable vector. B16mOVA cells were nucleofected with this construct and stably selected with G418 and hygromycin. Following initial selection, bulk stable transfectants were single-cell sorted on a BD FACSAria™ (BD Biosciences; San Jose, CA) for high levels of I-A^b expression and single-cell plated into 96-well flat-bottom plates (Corning; Tewksbury, MA). Single-cell clones were subsequently analyzed for OVA content with B3Z assay, CIITA expression via I-A^b expression in flow cytometry, and challenged into C57BL/6 WT and I-A^b KO mouse recipients to verify tumor growth as above. A single OVA-expressing, I-A^b positive clone capable of growing in both WT and I-A^b KO mice was utilized for all subsequent experiments.

3.2.3 B3Z Assay

The B3Z cell line is a CD8+ T-cell hybridoma expressing a TCR specific for OVA peptide 257-264 (OVAI – SIINFEKL) presented by the MHCI molecule H-$2K^b$. The cells further carry a beta-galactosidase (lacZ) construct under the control of the IL-2 promoter (Shastri & Gonzalez, 1993). Upon TCR engagement and activation, these cells express beta-galactosidase, which is capable of producing a quantifiable colorimetric readout using Chlorphenolred-β-D-galactopyranoside (CPRG) (Millipore; Billerica, MA) in B3Z lysates. B3Z hybridoma cells were seeded at 5E4 cells/well in 200 ul CTL media in a 96-well round-bottom plate (Corning; Tewksbury, MA) along with varying ratios of tumor (starting at 1:1 and diluting down) and incubated for 18 hours in a humidified 37°C 5% CO_2 incubator. Addition of 5 ug/ml OVAI peptide (Genscript; Piscataway, NJ) was

used as a positive control. After 18 hours, 150 ul media was removed and replaced with 50 ul PBS and 100 ul CPRG lysis solution containing 0.5 mM CPRG and 0.5% NP40 detergent in PBS. Cells were incubated in this solution for 5 or 24 hours in a humidified 37°C 5% CO_2 incubator, and then light absorbance at 595 nm was determined on a Powerwave X340 spectrophotometer (Bio-Tek Instruments; Winooski, VT).

3.2.4 OTI Tc1 Culture

Generation of OTI Tc1 cells was based upon a method modified from Dobrzanski and colleagues (Dobrzanski et al., 1999). C57BL/6 RAG1+/- OTI+/- 45.1+/- splenocytes were harvested into single cell suspension by crushing through a 100 um cell strainer (BD Biosciences; San Jose, CA) followed by subsequent red blood cell (RBC) lysis using ammonium-chloride-potassium lysis buffer (ACK) (Gibco; Carlsbad, CA). RBC-free splenocytes were then peptide loaded by incubating 10E6 cells/ml in warmed CTL media containing 2 ug/ml OVA I peptide (Genscript; Piscataway, NJ) in culture flasks for 2 hours in a humidified 37°C 5% CO_2 incubator. Cells were then washed twice and counted. Peptide-loaded splenocytes were then seeded at 1E6 cells/ml in 30 ml 'Tc1 media' consisting of CTL containing 20 U/ml human IL-2 (NCI Clinical Repository; Rockville, MD), 2 ng/ml IL-12 (Peprotech; Rocky Hill, NJ), and 2 ug/ml anti-IL-4 antibody (NCI Clinical Repository; Rockville, MD) and cultured upright in a T162 flask (Corning; Tewksbury, MA) for two days in a humidified 37°C 5% CO_2 incubator. On day two, 30 ml of warmed Tc1 media was added and flasks laid flat for another day of culture. On day 3, an additional 40 ml of warmed Tc1 media was again added and the cells cultured for another day. Cells were harvested on day 4 and subjected to dead cell

removal using two rounds of ficoll-paque (GE Life Sciences; Piscataway, NJ) separation. Following dead cell removal, cells were stored at 4°C in CTL media until ready for use. Cell purity was analyzed by FACS analysis for CD8 and CD45.1 and was consistently greater than 95% CD8+. Prior to adoptive transfer, cells were washed 3 times in ice-cold PBS, counted, and diluted as needed.

3.2.5 OTI Tc0 Isolation

C57BL/6 OTI+ splenocytes were harvested into single cell suspension by crushing through a 100 um cell strainer (BD Biosciences; San Jose, CA) followed by subsequent red blood cell (RBC) lysis using ammonium-chloride-potassium lysis buffer (ACK) (Gibco; Carlsbad, CA). RBC-free splenocytes were then enumerated and washed with ice-cold PBS. CD8+ cells were then purified using negative selection with MACS CD8a+ T-cell Isolation Kit I or II according to manufacturer instruction using MACS LS separation columns (Miltenyi; Auburn, CA). Following purification, cells were stored at 4°C in CTL media until ready for use. Cell purity was analyzed by FACS analysis for CD8, CD4, and Thy1.2 and was consistently greater than 95% CD8+ Thy1.2+ CD4-. Prior to adoptive transfer, cells were washed 3 times in ice-cold PBS, counted, and diluted as needed.

3.2.6 Regulatory T-Cell Culture

Regulatory T-cells were generated using two different culture methods which each produced equivalent *in vitro* suppressive ability (data not shown). In the first method, C57BL/6 RAG-/-OTII+/+ splenocytes were harvested into single cell suspension

by crushing through a 100 um cell strainer (BD Biosciences; San Jose, CA) followed by subsequent red blood cell (RBC) lysis using ammonium-chloride-potassium lysis buffer (ACK) (Gibco; Carlsbad, CA). RBC-free splenocytes were then enumerated and washed with ice-cold PBS. CD4+ cells were then purified using positive selection with MACS CD4 (L3T4) Microbeads according to manufacturer instruction using MACS LS separation columns (Miltenyi; Auburn, CA). Following purification, cells were stored at 4°C in CTL media in preparation for culture and cell purity was analyzed by FACS analysis for CD4 and Thy1.2 and was typically around 75% CD4+ Thy1.2+. 10 cm tissue culture plates (Corning; Tewksbury, MA) were coated for 2 hours at room temperature with 10 ml PBS containing 2 ug/ml of non-azide, low-endotoxin anti-CD28 (clone 37.51) and anti-CD3 (clone 145-2C11) antibodies (BD Biosciences; San Jose, CA) and subsequently washed twice with 10 ml PBS. Purified CD4+ cells were then seeded into antibody-coated plates at 1E6 CD4+ cells/ml in 10 ml 'Treg media' consisting of CTL containing 5 ng/ml hTGFβ (R&D Systems; Minneapolis, MN), 500 U/ml hIL-2 (NCI Clinical Repository; Rockville, MD), and 100 nM Retinoic Acid (Sigma; St. Louis, MO). Cells were then cultured for 2 days in a humidified 37°C 5% CO_2 incubator. On day 2, 30 ml additional pre-warmed Treg media was added and the culture continued for a total of 6 or 7 days. Cells were harvested, washed in ice-cold PBS, counted, and stored at 4°C in CTL media until ready for use. Cells were analyzed for purity using FACS analysis for Foxp3, CD4, and CD25. Purity usually exceeded 75% Foxp3+ CD4+ CD25+. Prior to adoptive transfer, cells were washed 3 times in ice-cold PBS, counted, and diluted as needed.

In the second method of Treg culture, C57BL/6 OTII+/- Thy1.1+/- Foxp3-GFP+/y splenocytes were harvested into single cell suspension and subjected to RBC lysis as above. RBC-free splenocytes were then enumerated and seeded at 1E6 splenocytes/ml in 50 ml Treg media into at T162 flask (Corning; Tewksbury, MA). 2 ug/ml OVAII peptide (Genscript; Piscataway, NJ) was added to each flask and the cells cultured upright for 4 days. On day 4, an additional 50 ml of pre-warmed Treg media was added, and the flasks were laid down for an additional day of culture. On day 5, an additional 20 ml of pre-warmed CTL media containing 500 U/ml hIL-2 was added and the cells cultured a final day. On day 6 cells were harvested, washed with ice-cold PBS, and FACS sorted for CD4+ Foxp3-GFP+ on a BD FACSAria™ (BD Biosciences; San Jose, CA) to a final purity of >98%. Following sorting, cells were stored in CTL at 4°C until ready for use. Prior to adoptive transfer, cells were washed 3 times in ice-cold PBS, counted, and diluted as needed.

3.2.7 IV Tumor Challenge Model

A fresh vial of tumor cells was thawed for each challenge experiment and grown for approximately 7 days with harvest at approximately 70% confluency to ensure exponential growth. For challenge, cells were harvested from adherent culture flasks using 0.25% trypsin-EDTA (Gibco; Carlsbad, CA) and washed in ice-cold CTL media. Cells were washed 3 times in ice-cold PBS, counted, and diluted to 5E5 cells/ml in ice-cold PBS. Mice were then challenged with 1E5 tumor cells via tail vein injection of 200 ul tumor suspension on day 0. On day 7 mice were adoptively transferred via tail vein injection with OTI Tc0 or Tc1 cells with or without OTII Tregs. For evaluation of lung

metastases, mice were sacrificed on day 21. Lungs were harvested and washed in PBS followed by fixation in Fekete's Solution (70% ETOH/ 3.7% Paraformaldehyde/0.75 M Glacial Acetic Acid) (Sigma; St. Louis, MO) for at least 24 hours. Left lung surface metastases were then enumerated using a Leica EZ4 dissecting microscope (Leica Microsystems; Wetzlar, Germany). For survival studies, mice were evaluated daily beginning at day 21 and sacrificed at the first sign of suffering. All mice were autopsied to confirm presence of lung metastatic burden as a reasonable cause of death/illness.

3.2.8 Subcutaneous Tumor Challenge Model

A fresh vial of tumor cells was thawed for each challenge experiment and grown for approximately 7 days with harvest at approximately 70% confluency to ensure exponential growth. For challenge, cells were harvested from adherent culture flasks using 0.25% trypsin-EDTA (Gibco; Carlsbad, CA) and washed in ice-cold CTL media. Cells were washed 3 times in ice-cold PBS, counted, and diluted to 1E6 cells/ml in ice-cold PBS. Mice were then challenged subcutaneously with 1E5 tumor cells in the previously shaved right flank on day 0. On day 6, mice were transferred to fresh clean caging and provided with water containing trimethoprim/sulfamethoxazole (Sulfatrim; dosed for 95 mg/kg/24hr; obtained from the Johns Hopkins Hospital pharmacy) in preparation for irradiation. On day 7, mice were irradiated at 500 Rads whole body irradiation and then adoptively transferred via tail vein injection with OTI Tc0 or Tc1 with or without OTII Tregs. Tumor size was then determined with cross-sectional caliper measurement once or twice weekly. Mice were sacrificed at the first sign of suffering or for timed explant sampling as indicated.

3.2.9 Antibodies and Flow Cytometry

I-A^b-FITC (clone AF6-120.1), I-E^k-FITC (clone 14-4-4S), H-2K^b-FITC (clone AF6-88.5), H-2D^d-FITC (clone 34-2-12), CD25-PE (clone PC61), CD4-APC (clone RM4-5), CD8-PE (clone 53-6.7), Thy1.1-PerCP (clone OX-7), and Thy1.2-FITC (clone 30-H12) were purchased from BD Biosciences (San Jose, CA). PD-L1-BrilliantViolet™421 (clone 10F.9G2) was purchased from BioLegend (San Diego, CA). Foxp3-FITC (clone FJK-16s) was purchased from eBioscience (San Diego, CA). All antibodies were titrated for optimal staining intensity vs. background signal for 1E6 cells/reaction. All isotype control antibodies were from the same manufacturer and used at the same concentration as their associated test antibody.

For all extracellular antibody staining, 1E6 cells were washed with FACS buffer containing 1X Hanks Balanced Salt Solution (HBSS), 10 mM HEPES buffer, 2% FBS, and 0.1% sodium azide and stained with appropriate antibody for 15 minutes at room temperature in the dark followed by two washings with FACS buffer. No more than 5 antibodies were stained at a single time. Cellular fixation/permeabilization was performed using the Foxp3 Staining Buffer Set (eBioscience; San Diego, CA) according to manufacturer instructions with fixation performed for 45 minutes at 4°C in the dark. Subsequent intracellular staining was performed for 30 minutes at 4°C in the dark with washes using the staining buffer set. For multi-step staining sequences, the following sequence was always followed: extracellular antibody, fixation/permeabiliation, intracellular stain. Following staining, cells were stored in FACS buffer at 4°C in the dark and were analyzed within 24 hours of staining.

Flow cytometry was performed on the BD FACSCaliber™, FACSAria™, or LSRII™ with data acquisition using CellQuest Pro™ or FACSDiva™ (BD Biosciences; San Jose, CA). Data analysis was further performed with FACSDiva™ as well as FlowJo (Tree Star Inc.; Ashland, OR).

3.2.10 Histology

Mice were sacrificed and tumors harvested into ice-cold CTL media. Tissues were then blotted to remove excess CTL and transferred to Intermediate Tissue-Tek CryoMolds (Sakura Finetek; Torrance, CA) containing a small layer of Optimal Cutting Temperature (OCT) media (Sakura Finetek; Torrance, CA) and subsequently covered with OCT media. Tissue chambers were then flash-frozen in a beaker of liquid nitrogen-cooled isopentane (Sigma; St. Louis, MO). Once fully frozen, samples were transferred on dry ice to an -80°C freezer for storage prior to cryosectioning. Tissue was subsequently cryosectioned at 5 um sections onto "Plus" slides, fixed in ice-cold acetone for 10 minutes, and air dried for 30 minutes by the Johns Hopkins Histology Core. Following sectioning and fixation, slides were stored in a -80°C freezer until stained.

Primary antibodies used for staining included: I-A^b-biotin (clone AF6-120.1; Ms IgG2a), H-$2K^b$-FITC (clone AF6-88.5; Ms IgG2a) (BD Biosciences; San Jose, CA), and Rat anti-CD274 (PD-L1) (clone MIH6; Rat IgG2a) (Abcam; Cambridge, MA). All isotype controls were used at the same concentration and were from the same supplier as the test antibody. Fluorescein/Oregon Green® Rabbit IgG Antibody (Invitrogen; Camarillo, CA) was used as a secondary antibody to increase primary antibody-FITC signal. Goat anti-Rabbit AlexaFluor®488, Goat anti-Rat AlexaFluor®647 (Invitrogen;

Camarillo, CA), and Stretavidin-Cy3 (Sigma; St. Louis, MO) were used for tertiary staining.

For staining, slides were allowed to warm to room temperature for 5 minutes in a laminar flow hood and then tissue demarcated with an ImmunEdge Pen (Vector Labs; Burlingame, CA) prior to rehydration with PBS for 10 minutes at room temperature. All subsequent staining and blocking steps were performed in a light-protected, humidified chamber with three PBS washes between steps. Samples were first treated with 1-2 drops Molecular Probes Endogenous Biotin Blocking Kit (Invitrogen; Camarillo, CA) solutions A and B for 30 minutes each at room temperature. They were then covered with 100 ul isotype-control blocking antibodies at 10 ug/ml in Blocking Buffer (2% IgG-free BSA and 5% normal mouse serum (Jackson Immunoresearch; West Grove, PA) in PBS) for 1 hour at room temperature. This blocking solution was then shaken off without PBS wash and replaced with primary antibodies at 10 ug/ml in Blocking Buffer and incubated overnight at 4°C. Slides were then incubated with 100 ul of 2 ug/ml secondary antibody in PBS/2%BSA for 1 hour at room temperature, washed, and incubated with 100 ul of tertiary antibodies diluted 1:100 in PBS/2%BSA for 1 hour at room temperature. Nuclei were then counterstained with Hoechst 33342 (Invitrogen; Camarillo, CA) diluted 1:50,000 in PBS for 15 minutes at room temperature. Following PBS wash, slides were fixed and mounted using a single drop of Aqua Poly/Mount (Polysciences; Warrington, PA) and cover slips placed and immobilized with nail polish. Slides were then stored face-up in light-protected slide boxes at 4°C until imaging.

Imaging was performed using a Nikon E800 fluorescent microscope using standard DAPI, FITC, Cy3, and Cy5 filter sets. Image acquisition and analysis was performed using Nikon Elements Software (Nikon Metrology; Brighton, MI).

3.3 Results

3.3.1 Treatment and Suppression in the IV Challenge Model

The first tumor model evaluated was a B16 pulmonary metastasis model. B57BL/6 WT mice were challenged on day 0 with 1E5 B16.mOVA and treated on day 7 with increasing amounts of Tc1-polarized OTI CD8+ cells. Mice were subsequently sacrificed on day 21 to evaluate tumor burden within the lungs. As shown in Figure 3.1, OTI Tc1 demonstrated a dramatic and dose-dependent treatment effect upon lung metastasis at the day 21 time point, with treatments of 3E6 or greater OTI Tc1 resulting in nearly complete tumor eradication.

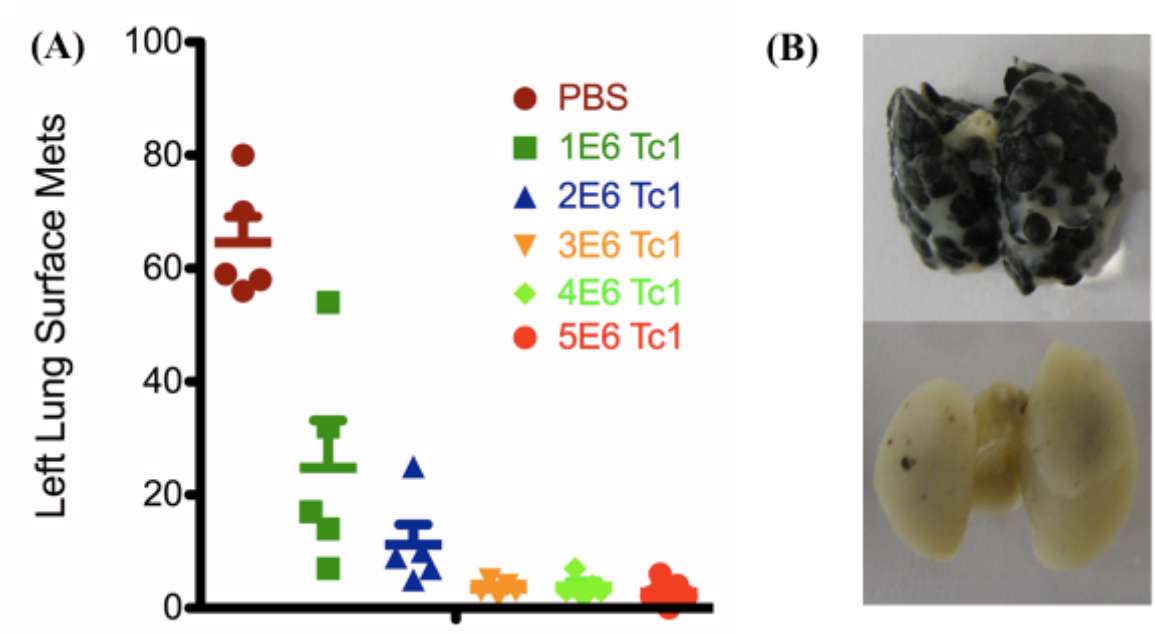

Figure 3.1 OTI Tc1 decrease B16.mOVA lung metastases in a dose-dependent fashion in WT mice.

C57BL/6 WT mice IV challenged with 1E5 B16.mOVA on day 0 and treated on day 7 with indicated doses of OTI Tc1 cells were sacrificed on day 21 and lungs harvested for evaluation. (A) Left lung surface metastases were enumerated as a means of evaluating overall tumor burden. Data from each mouse in a single study is presented, with bars indicating Mean and Standard Deviation in each group of 5 mice. (B) Representative images of lungs from mice treated with PBS (upper) or 5E6 OTI Tc1 cells (lower).

Based upon the impressive response seen at day 21, we next investigated the duration of this treatment effect by following mice in a survival study. WT mice were challenged and treated as in the previous study, but instead of sacrificing at day 21 were followed daily with sacrifice and autopsy performed at the first signs of suffering. As shown in Figure 3.2, despite the apparent magnitude of response seen at the single day 21 time point, treatment benefit was not long lived, with mean survival being 28 days for untreated mice and a maximum of 49 days for the 5E6 treated group; a mere three weeks survival benefit. Several explanations for this lack of treatment durability were considered, including loss of OVA from tumor cells and effector cell exhaustion. The first of these, OVA antigen loss, was evaluated by seeding tumor explants into *in vitro* proliferation assays using naïve OTI responder splenocytes. These studies indicated that antigen loss had not occurred, as explant samples by and large maintained the ability to stimulate naïve OTI splenocytes (data not shown). Effector cell exhaustion was not evaluated.

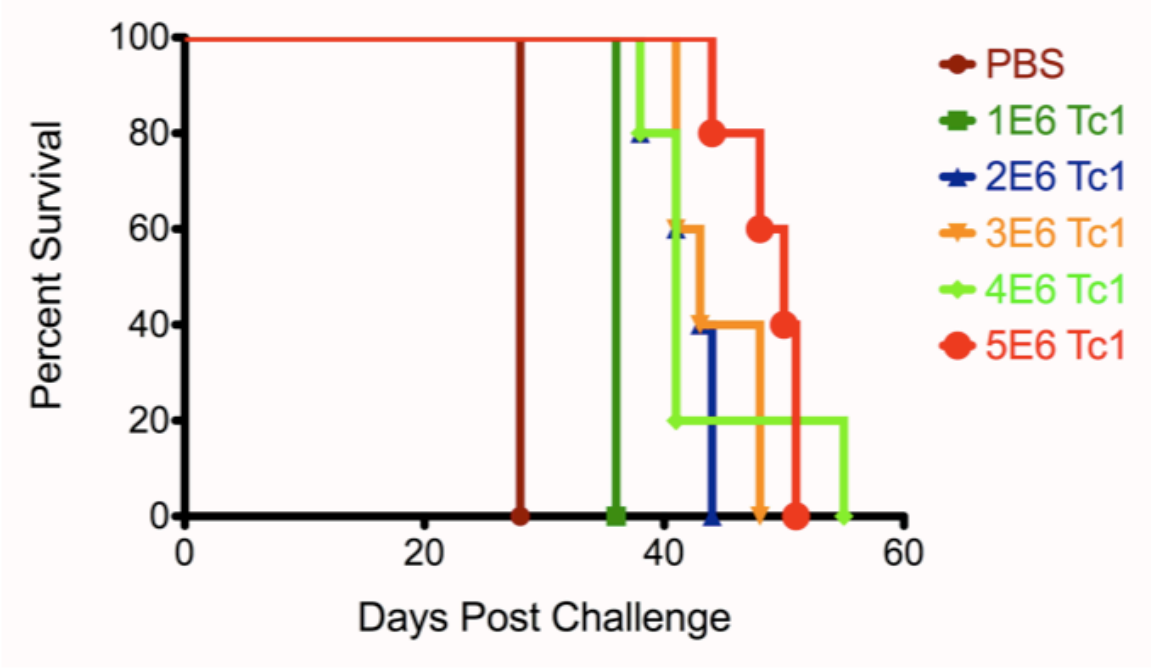

Figure 3.2 Survival of WT mice in the B16.mOVA lung metastasis model.

C57BL/6 WT mice IV challenged with 1E5 B16.mOVA on day 0 and treated on day 7 with indicated doses of OTI Tc1 cells were followed and sacrificed with confirmatory autopsy at the first sign of illness. Kaplan-Meier survival curves are shown, with median survival for the groups being as follows: PBS – 28 days; 1E6 – 36; 2E6 – 42; 3E6 – 42; 4E6 – 40; 5E6 – 49. 5 mice were used per group.

Despite the fact that the treatment effect seen for Tc1 was not permanent, the response seen at day 21 was striking enough to warrant evaluating the effect that addition of Tregs would have to the observed treatment response. As before, WT mice were IV challenged with B16.mOVA on day 0 and subsequently treated on day 7. Based upon the results from our prior studies, a dose of 2.5E6 Tc1 was given since this dose fell at the edge of complete treatment vs. tumor breakthrough and was thought to be an appropriate dose to evaluate Treg suppression. OTI Tc1 treatment was performed with or without the simultaneous administration of 10E6 OTII Tregs. This dose of Tregs represented a 4:1 Treg:Tc1 ratio, which our experience in other models had shown to be an appropriate high-end starting ratio. As shown in Figure 3.3, the addition of OTII Tregs had no effect upon the treatment effect seen for OTI Tc1 at day 21.

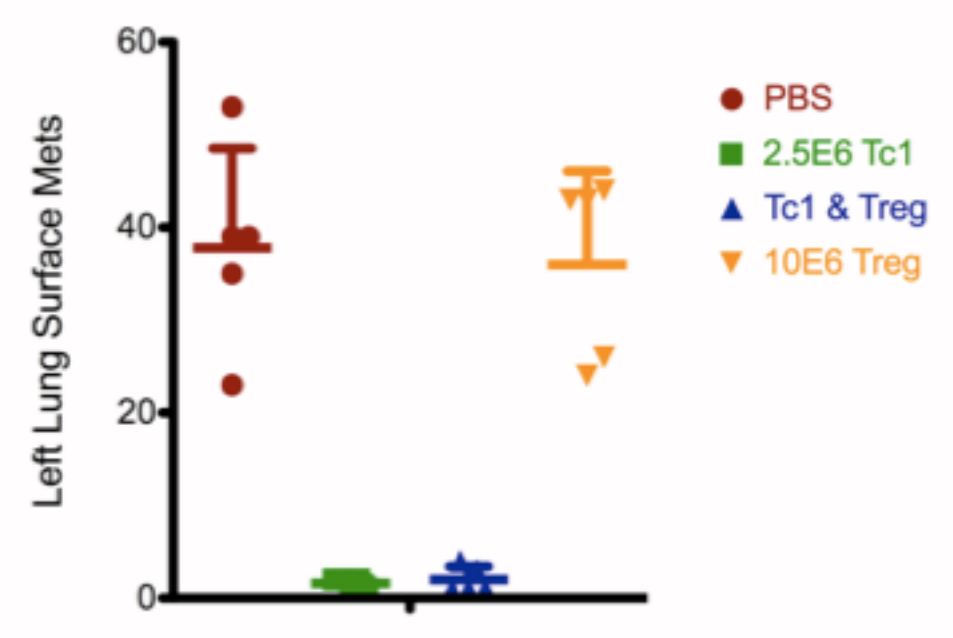

Figure 3.3 OTII Tregs do not suppress OTI Tc1 in the lung metastasis model. C57BL/6 WT mice IV challenged with 1E5 B16.mOVA on day 0 and treated on day 7 with indicated doses of OTI Tc1 and/or 10E6 OTII Tregs were sacrificed on day 21 and lungs harvested for evaluation. Left lung surface metastases were enumerated as a means of evaluating overall tumor burden. Data from each mouse in a single study is presented, with bars indicating Mean and Standard Deviation in each group of 5 mice.

The failure of OTII Tregs to suppress the OTI Tc1 could be explained by a number of possibilities. First, the ratio used here was 4 Treg to 1 Teff, which in prior studies using primarily CD4 Teffs had been shown to be sufficient in cases where suppression was achievable. However, this was our first experience with attempting to suppress a CD8+ response in this fashion, and given the differences in tumor model, treatment modality, antigen, and TCR donor mice, the assumption of this dosing ratio being adequate may not have been accurate. That being said, the fact that no suppression was seen at all made this seem less likely, as inadequate numbers should have at least shown some effect. Further, given the technical difficulty of generating Tregs, the number used here was at the upper limit of achievable *in vitro* production, and thus increasing the Treg dose was not a feasible option for further evaluation.

Besides a possible inadequate dosing of Tregs, we also considered the possibility that the OTI Tc1 cells may have been terminally polarized in a manner that would be beyond the suppressive capabilities of our Tregs. In our early phase studies to evaluate these cells as a treatment modality, we had found them to be highly potent at eliciting antigen-dependent target cytotoxicity, with high-level expression of IFNγ and granzyme (data not shown). Perhaps the effector function of our Tc1 was too overwhelming to be suppressed by our Tregs, and another less polarized treatment modality would be more appropriate.

Potentially compounding this effect was the route we had chosen for our tumor challenge. The IV tumor challenge model used here successfully seeded melanoma cells primarily within the capillary beds of the lung. As our treatment cells and Tregs were adoptively transferred in the same IV fashion, they would have had nearly immediate

access to the tumor upon transfer. This immediate access of Teff to target may have bypassed certain suppressive mechanisms, or simply cut short the timing needed for Tregs to interact appropriately with tumor, Teff, and/or host APC machinery in order to enact suppression. An alternative route of challenge that would allow more limited tumor access and require greater T-cell trafficking might allow our Tregs more time and perhaps a broader range of mechanisms to enact suppression.

3.3.2 Treatment and Suppression in the Subcutaneous Challenge Model

To address several of the considerations raised in the IV challenge model, we next sought to evaluate treatment using a subcutaneous tumor challenge model. The hope here being that by transferring the tumor burden from the immediately hematogenously-accessible site afforded with the IV challenge to a site not immediately accessibly to an IV-injected effector cell, we would broaden the mechanistic scope and timing available for suppression. Further, we also sought to evaluate an alternative treatment option, since there were concerns that our Tc1 cells may not have been amenable to Treg suppression. We thus chose to evaluate the use of naïve OTI CD8+ cells which we subsequently referred to as 'Tc0' cells, with the multiple steps required for naïve cells to proliferate, traffic, and develop effector phenotype providing ample opportunities for Treg suppression.

To this end, C57BL/6 WT and MCHII knockout (KO) mice (I-A^b-/-) were challenged subcutaneously with 1E5 B16.mOVA tumor cells on day 0 and subsequently treated with 500 Rads non-myeloablative whole-body irradiation followed by adoptive transfer of 2.5E6 OTI Tc1 or Tc0 cells to compare the two formats. A third group of WT

mice was challenge with the parental B16-F10 tumor line and similarly treated to serve as a control for treatment antigen-dependence. Mice were subsequently followed with weekly measurement of tumor size. As shown in Figure 3.4, Tc1 and Tc0 were able to provide significant treatment effect in both WT and MHCII KO mice challenged with B16.mOVA, but as expected failed to provide such an effect in WT mice challenge with non-OVA bearing parental B16-F10. Tc0 were equivalent if not slightly superior to Tc1 in their treatment effect at equal dosing, and thus a subsequent experiment, shown in Figure 3.4(D) was performed to titrate the treatment dosing of OTI Tc0. This titration experiment suggested that the 2.5E6 dosing was in fact appropriate for OTI Tc0.

Based upon these results, we decided to next evaluate the addition of OTII Tregs to the subcutaneous challenge model with treatment by OTI Tc0. C57BL/6 WT and MHCII KO mice were similarly challenged, treated, and followed as before, with addition of 7.5E6 OTII Treg given along with Tc0 treatment, representing a 3:1 Treg:Tc0 ratio. As shown in Figure 3.5, addition of OTII Tregs resulted in what appeared to be suppression of OTI Tc1 in MHCII KO mice but not in WT mice.

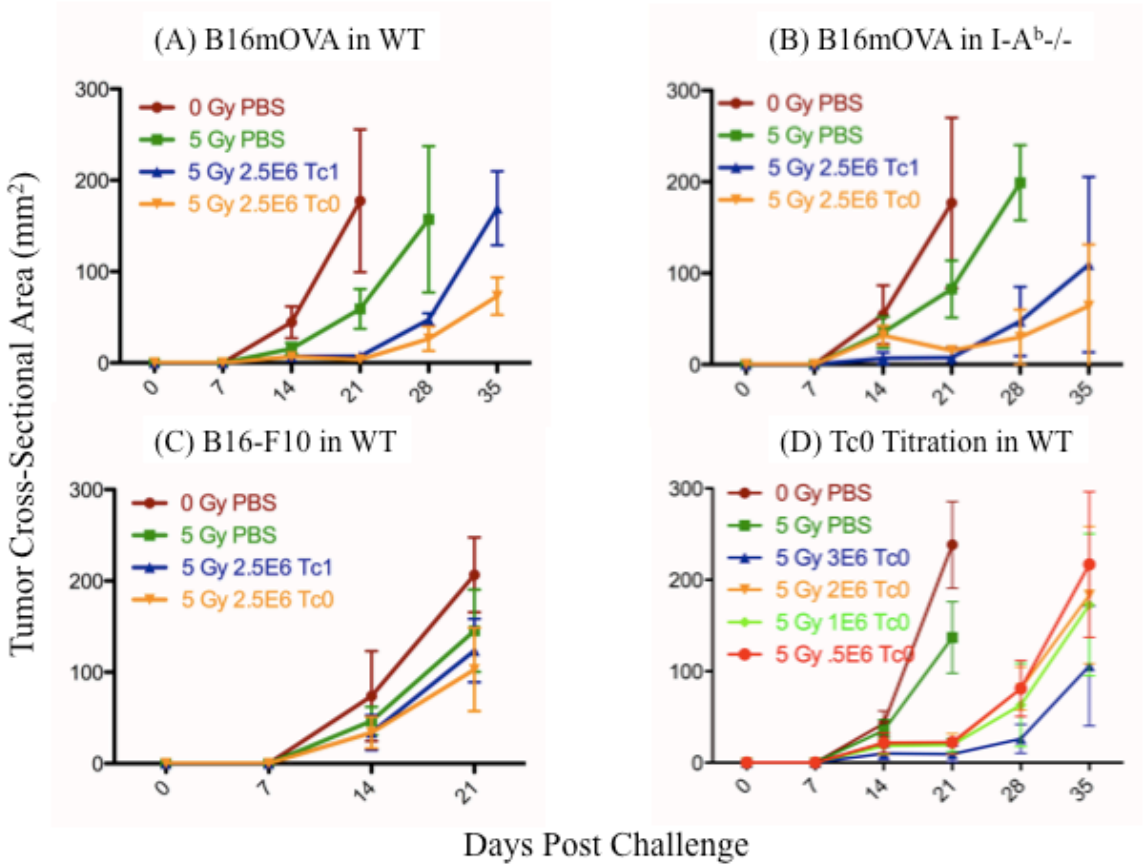

Figure 3.4 OTI Tc1 and Tc0 treat subcutaneous B16.mOVA in an antigen-dependent fashion in both WT and MHCII KO mice.

C57BL/6 WT and MHCII KO mice were subcutaneously challenged with 1E5 B16.mOVA or parental B16-F10 on day 0 and treated on day 7 with 500 Rads non-myeloablative whole body irradiation followed by indicated doses of OTI Tc1 or Tc0 cells. Tumor size was then monitored weekly using caliper measurements of tumor cross-sectional area. Mean +/- Standard Deviation for each group of 5 mice is shown. (A) Treatment of B16mOVA in WT mice. (B) Treatment of B16mOVA in MHCII KO mice. (C) Treatment of B16-F10 in WT mice. (D) Tc0 treatment titration in B16mOVA-bearing WT mice.

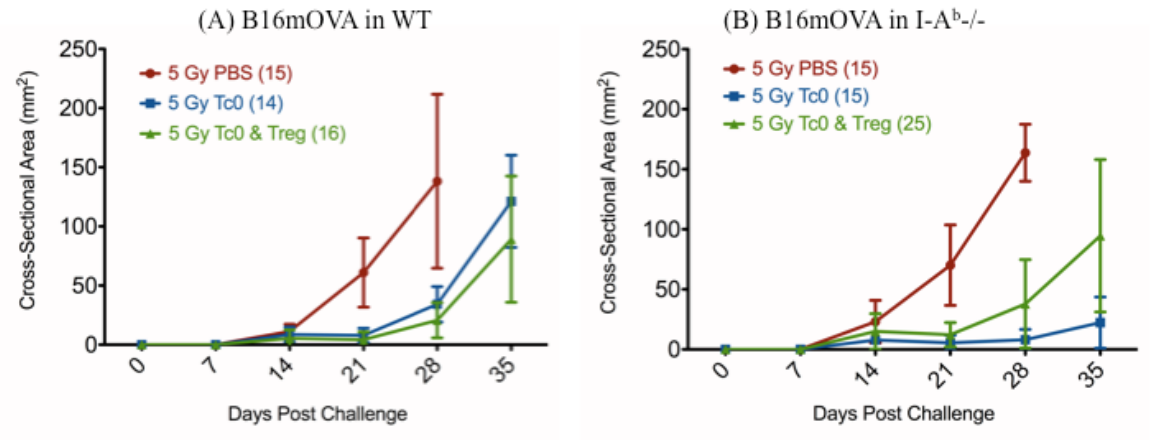

Figure 3.5 OTII Treg suppress OTI Tc0 in MHCII KO but not WT recipients.

(A) C57BL/6 WT and (B) MHCII KO mice were subcutaneously challenged with 1E5 B16.mOVA on day 0 and treated on day 7 with 500 Rads non-myeloablative whole body irradiation followed by 2.5E6 OTI Tc0 cells with or without co-administration of 7.5E6 OTII Tregs. Tumor size was then monitored weekly using caliper measurements of tumor cross-sectional area. Mean +/- Standard Deviation for combined data from three independent experiments is shown, with numbers in parentheses indicating the total number of mice per group.

The findings in Figure 3.5 were encouraging but also somewhat difficult to interpret, and were consistent within three independent experiments (as shown pooled in the figure). While there was some overlap between the curves, there appeared to be a real suppressive effect of OTII Tregs upon Tc0 in the MHCII KO mice, which was not observed in the WT mice. Upon closer examination, it was evident that the difference between the two groups of mice was not in the Treg curves, which were quite similar, but in the Tc0 only curves. MHCII mice treated with Tc0 showed a prolonged treatment effect compared to WT mice when comparing the 28 and 35 day time points. This allowed for separation of the Treg group from the Tc0 only group in the MHCII KO mice but not in the WT mice. One possible explanation for this finding was that the WT recipient mice bear CD4 cells, particularly Tregs, which are not present in the MHCII KO mice. Our treatment strategy had utilized whole-body irradiation to help eliminate endogenous immune cells in the recipients, but we had selected a non-myeloablative dose and thus recovery of these cells would eventually occur. Recovery of endogenous polyclonal Tregs in the WT mice could potentially allow for suppression of our Tc0 cells. In contrast, MHCII KO mice do not bear CD4 cells, so no endogenous Treg population would be present to suppress our Tc0 upon bone marrow recovery. A better understanding of the immune response in our model was needed in order to truly evaluate this possibility, which would be the focus of future studies.

3.3.3 Development and Characterization of B16 Variants

Although difficult to interpret, the findings in Figure 3.5 were certainly encouraging, as there did appear to be suppression in the MHCII KO mice. This

suppression was not complete, however, and displayed a lag relative to untreated mice. However, if suppression was dependent upon tumor MHCII expression as we had hypothesized, then a model where MHCII was expressed only after inflammation, as was thought to be the case for our B16.mOVA tumor, would be expected to display a lag such as the one seen in our results. Presumably, if the tumor were to constitutively express MHCII this lag would not occur. In order to evaluate this concept further, we needed to broaden our tumor repertoire with the construction of B16.mOVA tumors with variable expression patterns of MHCII. Specifically, to couple with our MHCII-inducible line, we desired to create OVA-expressing B16 melanoma lines wherein MHCII was constitutively expressed and a second where MHCII could not be expressed.

To accomplish this goal, two new cell lines had to be created and validated. First, we took our B16.mOVA line and stably transfected it with the human *CIITA* gene, which is the master regulator of MHCII expression, to create the MHCII-constitutive line B16.mOVA.CIITA. In parallel, we took the B16-F10-D line, a B16-F10 derivative that has lost the ability to upregulate MHCII, and stably transfected it with the *mOVA* gene construct to create the MHCII-non-inducible line B16-F10-D.mOVA. After selection, limiting dilution cloning, and validation of *in vivo* growth for both lines (data not shown) we set out to verify antigen content and MHC expression profiles of our B16.mOVA variants *in vitro* and *in vivo*.

To begin with, we first assessed the *in vitro* expression of MHCI and MHCII in the presence and absence of exposure to IFNγ. Tumor cells were cultured for 72 hours with and without 100 U/ml IFNγ and then evaluated for cell surface MHCI and MHCII expression via flow cytometry. As shown in Figure 3.6, we were successful in creating

B16 melanoma lines with non-inducible, inducible, and constitutive expression of MHCII *in vitro*. Inducible expression of MHCI was also seen in all three lines, with the B16.mOVA.CIITA line showing detectable baseline MHCI expression unlike the other two lines.

Based upon the MHCI and MHCII expression seen in our tumor variants, we also investigated the expression pattern of PD-L1, a negative costimulatory molecule known to be expressed on some tumors with upregulation in the presence of IFNγ. B16 variants were cultured as before with and without IFNγ and analyzed for cell surface PD-L1 expression via flow cytometry. As shown in Figure 3.7, PD-L1 expression was present at low levels in the absence of IFNγ and demonstrated marked upregulation in the presence of IFNγ.

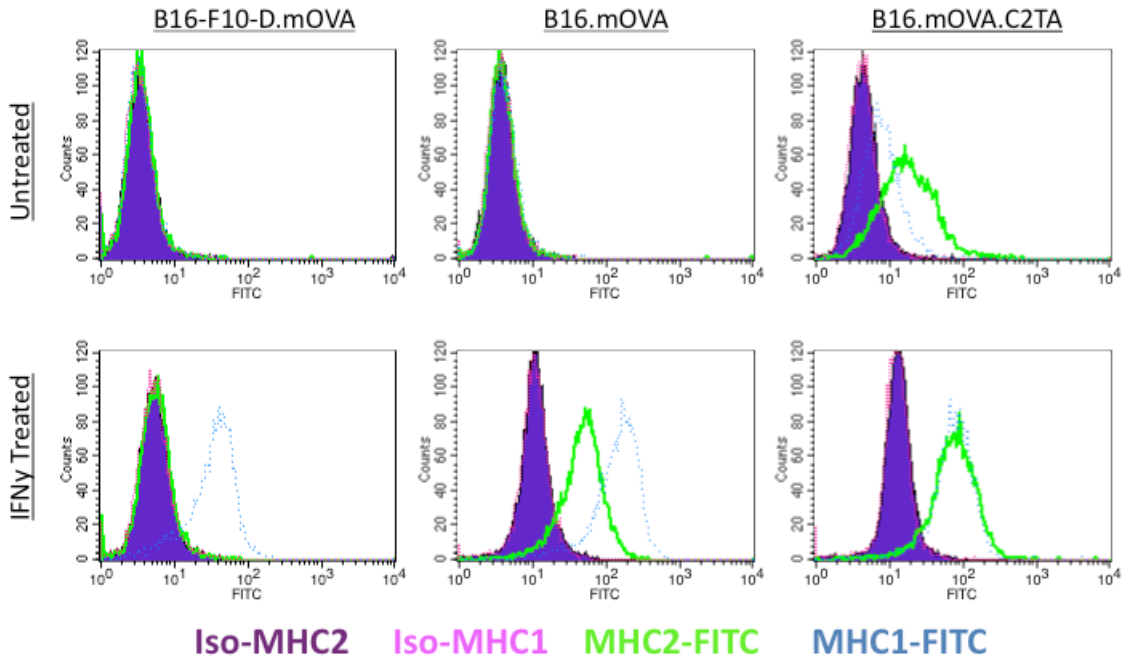

Figure 3.6 *In vitro* MHCI and MHCII expression of B16.mOVA variants in the presence and absence of IFNγ.

B16-F10-D.mOVA, B16.mOVA, and B16.mOVA.CIITA tumor lines were cultured for 72 hours with and without 100 U/ml IFNγ and then evaluated for cell-surface expression of MHCI (H-2K^{b}) and MHCII (I-A^{b}) via flow cytometry.

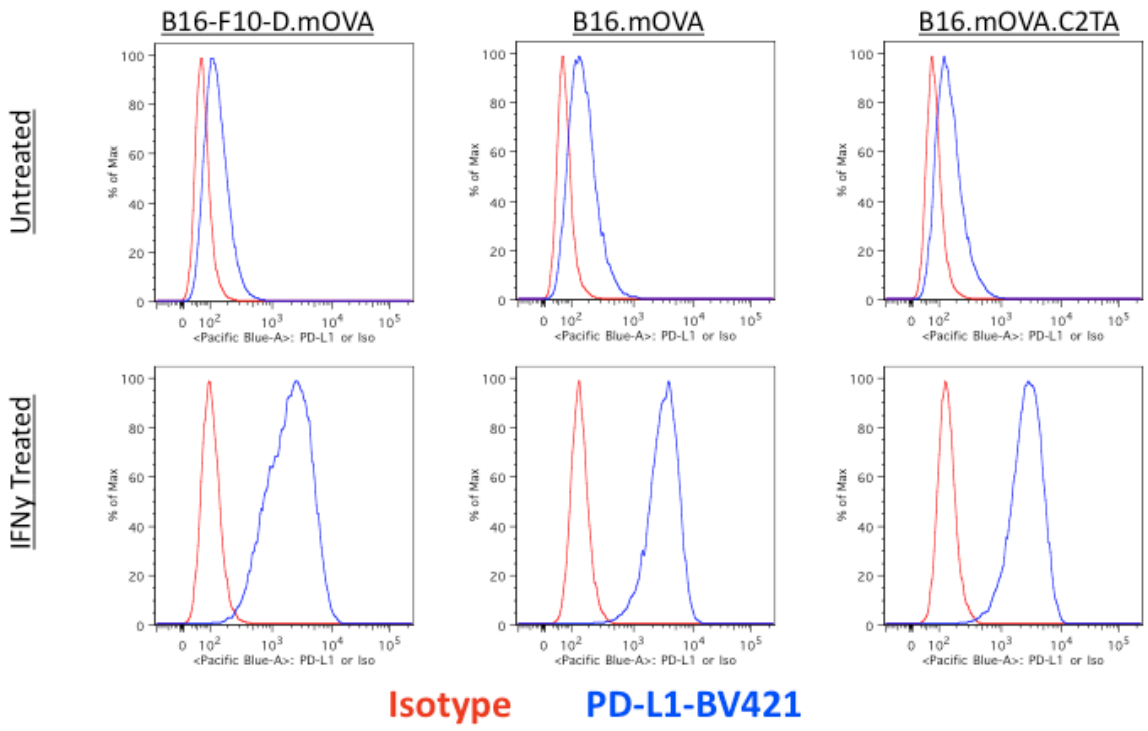

Figure 3.7 *In vitro* PD-L1 expression of B16.mOVA variants in the presence and absence of IFNγ.

B16-F10-D.mOVA, B16.mOVA, and B16.mOVA.CIITA tumor lines were cultured for 72 hours with and without 100 U/ml IFNγ and then evaluated for cell-surface expression of PD-L1 via flow cytometry.

We next verified the OVA antigen content of our lines using *in vitro* recognition with the OVA-specific hybridoma B3Z. B16.mOVA variants and non-OVA containing parental lines were cultured as before with and without IFNγ and then placed into overnight coculture with B3Z cells. Cultures were then lysed and incubated with the colorimetric CPRG substrate to assess for the presence of β-galactosidase (β-gal), which in the B3Z line is under the control of the IL-2 promoter and is expressed only upon antigen-specific stimulation. As seen in Figure 3.8, OVA-containing B16 variants exposed to IFNγ were capable of stimulating B3Z cells as seen with readout at both 5 and 24 hours. In contrast, non OVA-expressing parental variants exposed to IFNγ did not stimulate B3Z cells. Interestingly, B16.mOVA variants not exposed to IFNγ were unable to stimulate B3Z cells, which in conjunction with the data from Figure 3.6 suggests that the baseline MHCI expression of these cells was too low to adequately present OVA to the B3Z hybridoma.

With the *in vitro* OVA content and expression of MHCI, MHCII, and PD-L1 determined, we next sought to verify that these same changes occurred *in vivo*. To accomplish this, C57BL/6 WT and MHCII KO mice were challenged with 1E5 B16.mOVA tumor variants on day 0 and treated on day 7 with 500 Rads non-myeloablative whole body irradiation followed by adoptive transfer of 2.5E6 OTI Tc0 or PBS as performed previously. Mice were then sacrificed one week after treatment and tumor masses harvested and processed for histologic evaluation of MHCI, MHCII, and PD-L1 expression. As can be seen in Figure 3.9, exposure of B16.mOVA variants to OTI Tc0 *in vivo* resulted in MHCI, MHCII, and PD-L1 expression patterns that closely resembled those seen with *in vitro* exposure to IFNγ.

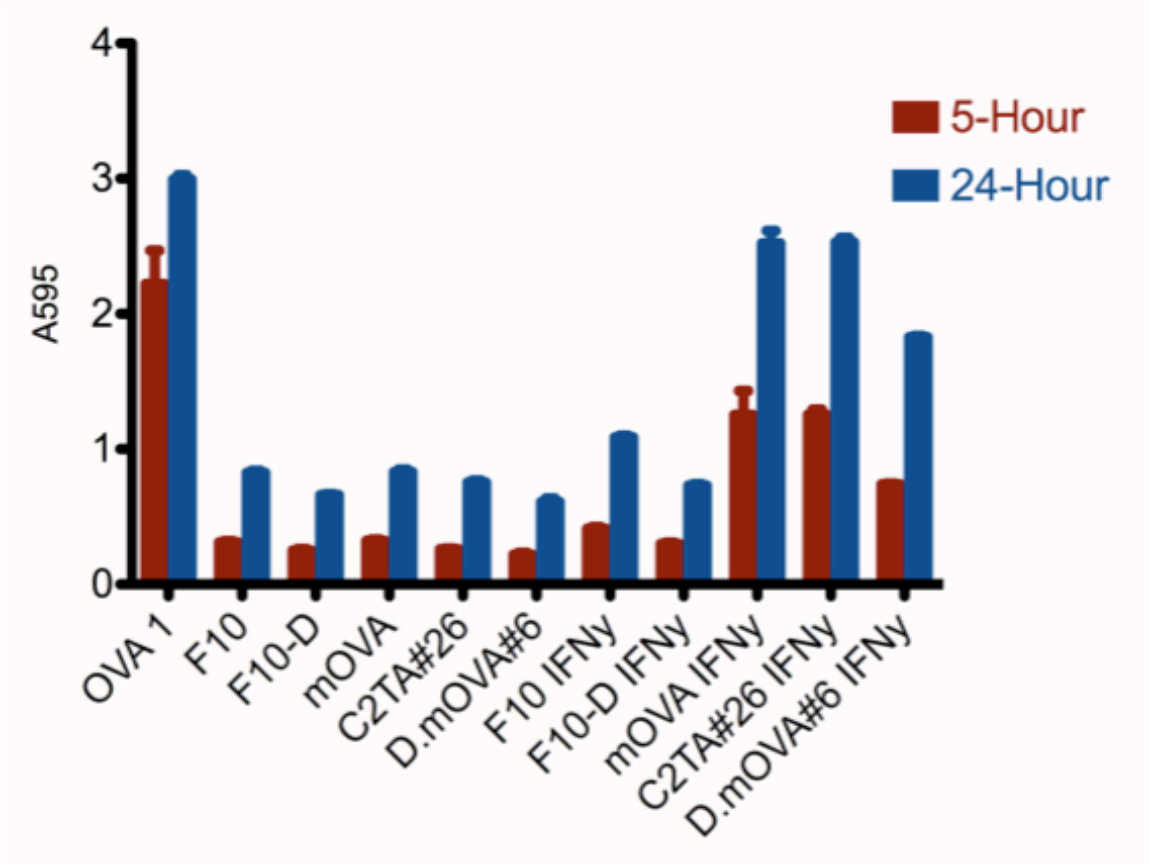

Figure 3.8 OVA-containing B16 variants stimulate the OVA-specific B3Z hybridoma *in vitro*.

OVA-containing B16 tumor lines B16-F10-D.mOVA, B16.mOVA, and B16.mOVA.CIITA, along with non OVA-containing parental lines B16-F10 and B16-F10-D, were cultured for 72 hours with and without 100 U/ml IFNγ and then cocultured overnight with the B3Z hybridoma. Cultures were lysed and β-gal activity detected by incubation for 5 or 24 hours with the colorimetric substrate CPRG followed by measurement of light absorption at 595 nm. Mean +/- Standard Deviation for 3 replicate wells is shown for each sample, with 5 ug/ml OVAI peptide used as a positive control.

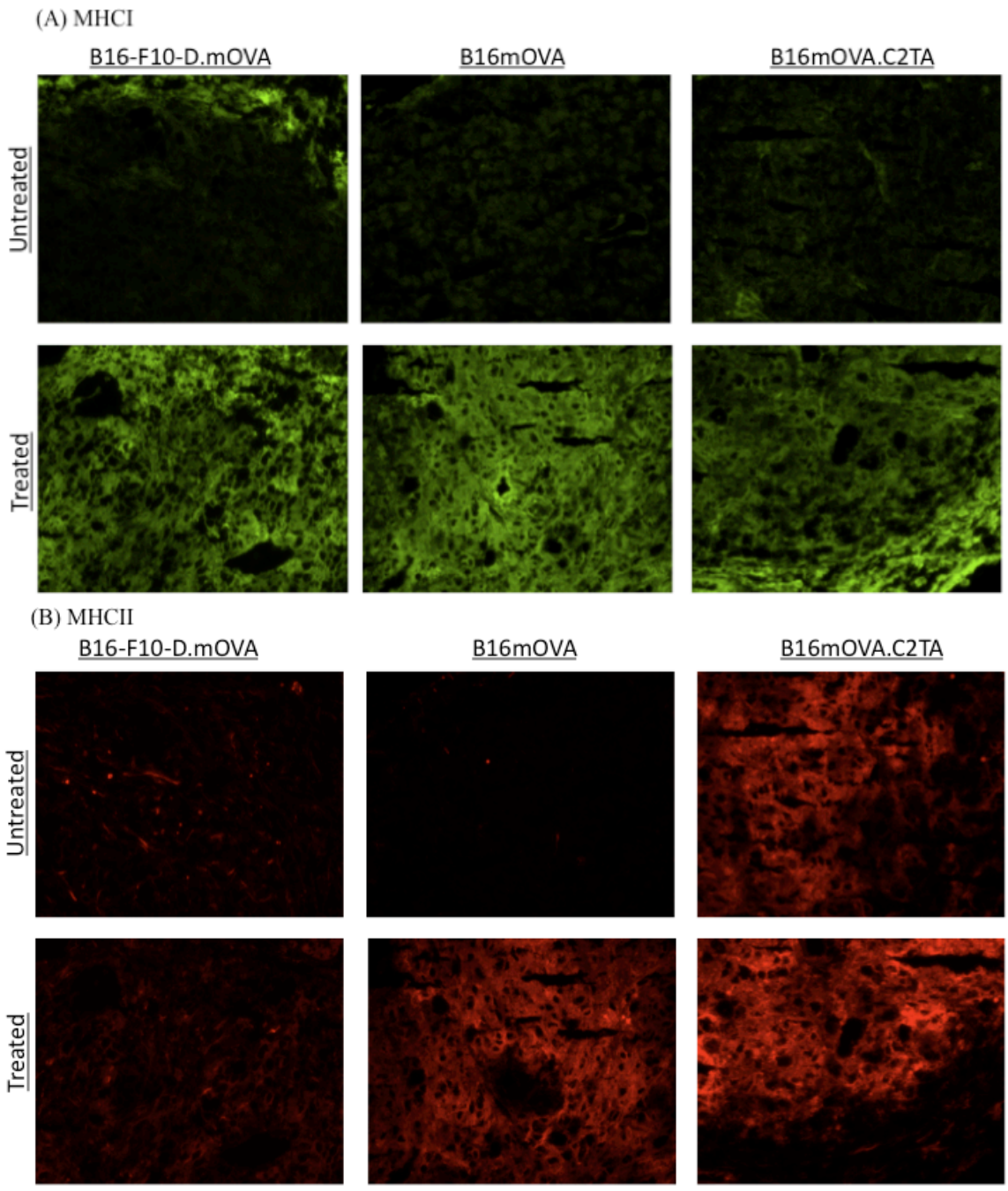
(A) MHCI
B16-F10-D.mOVA
B16mOVA
B16mOVA.C2TA
Untreated
Treated
(B) MHCII
B16-F10-D.mOVA
B16mOVA
B16mOVA.C2TA
Untreated
Treated

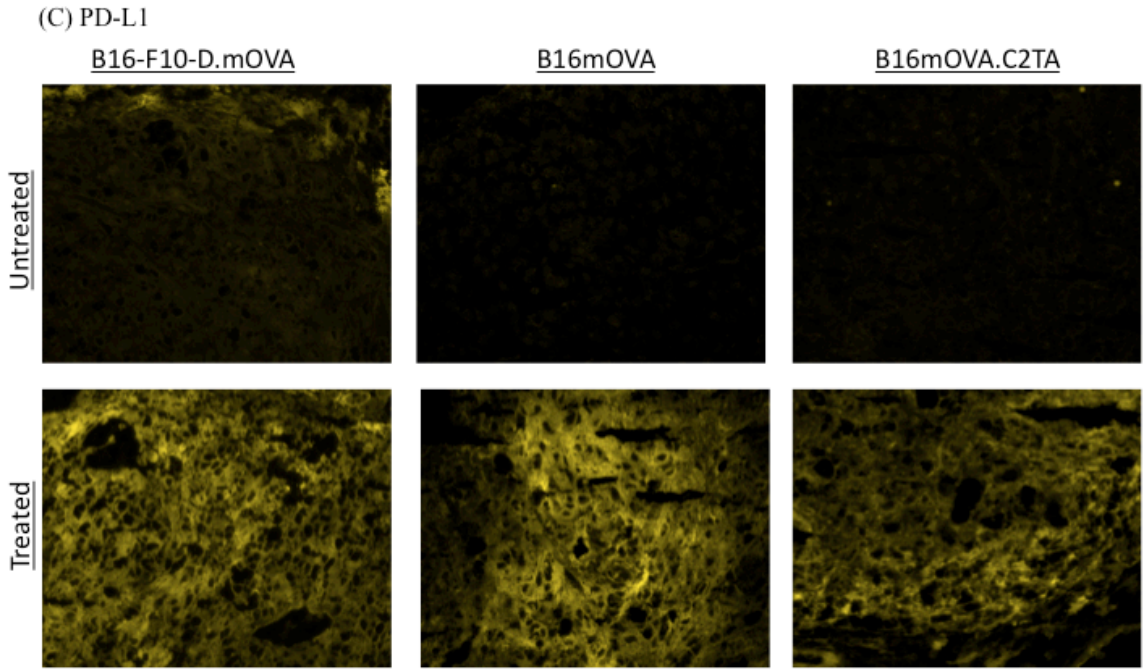

Figure 3.9 *In vivo* expression of MHCI, MHCII, and PD-L1 in B16.mOVA variants upon exposure to OTI Tc0.

C57BL/6 WT and MHCII KO mice were challenged with 1E5 B16.mOVA tumor variants on day 0 and treated on day 7 with 500 Rads non-myeloablative whole body irradiation followed by adoptive transfer of 2.5E6 OTI Tc0 or PBS. Mice were sacrificed one week after treatment (day 14) and tumor masses harvested and processed for histologic evaluation of (A) MHCI (H-2K^{b}), (B) MHCII (I-A^{b}), and (C) PD-L1 expression. Shown here are representative images from I-A^{b}-/- recipients. 3 mice were used per group.

Specifically, all three tumors upregulated MHCI and PD-L1 upon OTI Tc0 treatment, and both B16.mOVA and B16.mOVA.CIITA, but not B16-F10-D.mOVA, demonstrated expression of MHCII, with B16.mOVA.CIITA also demonstrating MHCII expression in untreated tumors as expected. As displayed in Figure 3.10, combination of these markers clearly demonstrated the restriction of MHCII expression to the tumor mass in MHCII KO mice, with overlying host epidermis demonstrating MHCI expression but not MHCII expression. Collectively, these data demonstrate the B16.mOVA variants created here express OVA, are recognized by OTI Tc0, and demonstrate the desired variability in MHCII expression we sought to create.

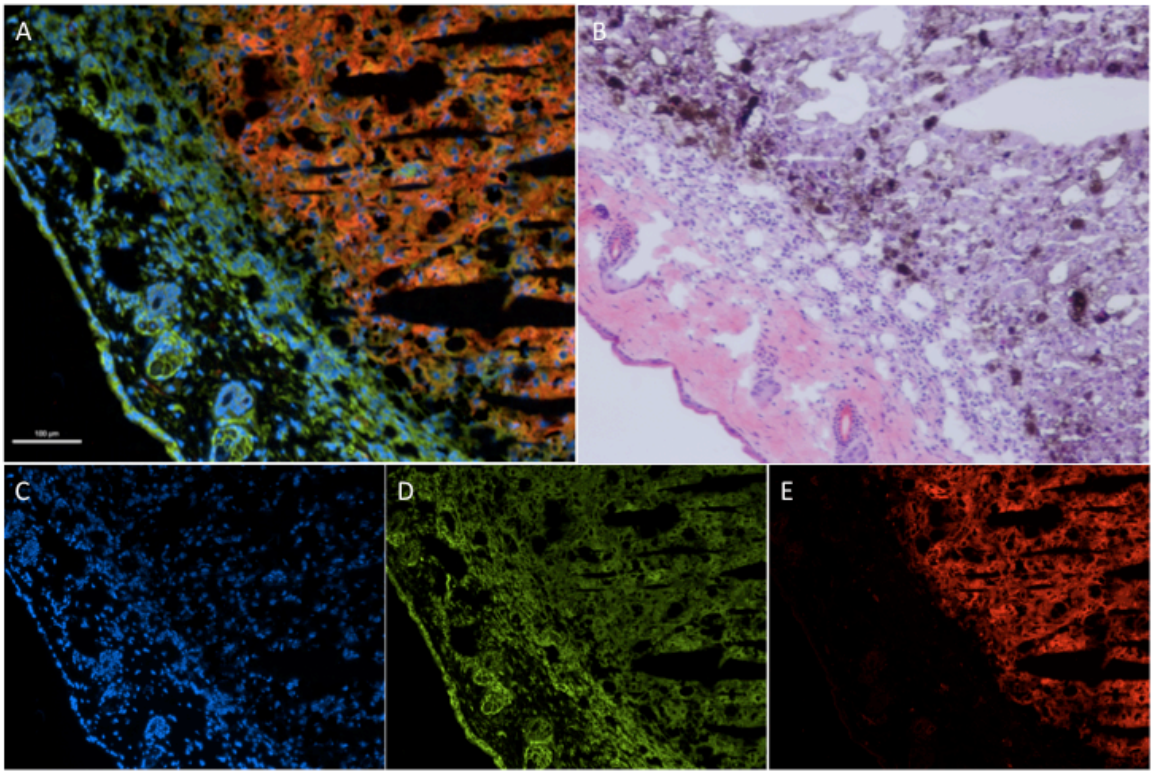

Figure 3.10 MHCII clearly demarcates the tumor in OTI Tc0 treated MHCII KO mice.

C57BL/6 WT and MHCII KO mice were challenged with 1E5 B16.mOVA tumor variants on day 0 and treated on day 7 with 500 Rads non-myeloablative whole body irradiation followed by adoptive transfer of 2.5E6 OTI Tc0 or PBS. Mice were sacrificed one week after treatment and tumor masses harvested and processed for histologic evaluation. Displayed here are a Merge (A) of DAPI nuclear stain (C), MHCI (H-2K^{b}) (D), and MHCII (I-A^{b}) (E), as well as an H&E stain (B) demonstrating necrotic tumor mass with overlying epidermis. Representative images from I-A^{b}-/- recipients are shown. 3 mice were used per group.

3.4 Discussion

The B16-F10 tumor line was generated in the 1970s by Fidler and colleagues (Fidler et al., 1976; Fidler & Bucana, 1977) and since has been widely disseminated. As such, it has experienced a great deal of drift and tumors from different sources are known to demonstrate a wide degree of variability in growth kinetics, metastatic potential, and treatment capability (Overwijk & Restifo, 2001). In this first study, we therefore first sought to establish an appropriate treatment model with our B16.mOVA tumor line. Particular emphasis was placed upon defining a minimum treatment dose for tumor response, as prior experience within our laboratory had demonstrated that Treg suppression requires a careful balance of tumor burden, effector cell number, and Treg cell number, with Tregs failing to demonstrate suppression when Teff are in extreme excess.

Our initial attempts utilized a lung metastasis model with treatment by OTI Tc1 previously described by Dobrzanski and colleagues (Dobrzanski et al., 1999; 2000; 2001). We were able to successfully generate *in vitro* polarized OTI cells that produced IFNγ and granzyme and lysed OVA-bearing target cells *in vitro* (data not shown). When utilized for *in vivo* treatment, these cells were able to show tumor killing (Figure 3.1), but when compared to the dosing used in the experiments by Dobrzanski and colleagues, we needed much higher doses of Tc1 cells to accomplish tumor treatment. Furthermore, their studies were able to demonstrate long-term tumor-free survival with treatment by OTI Tc1, whereas in our study this treatment effect was short lived (Figure 3.2), providing a maximum increased survival of only three weeks. The cause for these

differences is unknown at this time. Differences in our tumor could account for these differences. As noted above, the B16-F10 line as a whole has become highly variable since its generation over 30 years ago. Further, our derivative line B16.mOVA was fairly recently derived (Preynat-Seauve et al., 2007) and the OVA construct, its cellular location, and its antigenic processing could all have varied between the two models. While we were able to verify that tumor explants in our mice had not lost OVA expression (data not shown), we did not further characterize these explants. We also considered it a strong possibility that our Tc1 cells were either exhausted or even perhaps dying within recipient mice. In fact, multiple recent studies have indicated that *in vitro* acquisition of effector phenotype results in inferior antitumor response *in vivo,* owing largely to impaired proliferative and survival capacities of effector cells (Gattinoni et al., 2005b; 2006; Klebanoff et al., 2005). At the time, our studies were not designed to evaluate this possibility, however, and thus that question remains unanswered.

Although not ideal, the treatment benefit afforded by our Tc1 cells in the lung metastasis model was thought to be large enough to allow detection of a Treg suppressive effect, and thus Tregs were evaluated in this model. We initially aimed to use as few treatment cells as possible with as many Tregs as possible to give the best chance of seeing suppression. Unfortunately, as shown in Figure 3.3, even at a 4:1 Treg:Tc1 ratio we were unable to see suppression in our model. As previously discussed, we considered a number of causes for this failure, including inadequate Treg numbers, inappropriate Teffector phenotype, and poor tumor location. Amongst these options, Treg numbers could not be increased, as we were at the technical limit of *in vitro* production in our system.

Regarding the phenotype of our effector cells, our Tc1 polarization had been based upon the aforementioned studies by Dobrzanski and colleagues, which had been successful at treating B16-OVA lung metastases, but had not evaluated the interactions of Tregs with these cells. It seemed entirely possible that these Tc1 cells may have been so heavily polarized that they were 'insuppressible.' Given this concern, along with concerns regarding the long-term treatment failure the Tc1 cells demonstrated, we decided to evaluate a different effector cell method. A study by Chen and colleagues (Chen et al., 2005) had demonstrated the ability of naïve HA-specific CD8 cells to proliferate, traffic, polarize, and kill antigen-bearing tumor cells *in vivo*. They further demonstrated the ability of antigen-specific Tregs to suppress this CD8-mediated effect. The concept of using naïve CD8 cells as effectors was appealing, as we envisioned that their use could potentially solve both the long-term treatment failure as well as the failure of suppression seen in our Tc1 model. As such we attempted to treat our B16.mOVA line with naïve OTI CD8+, which we termed 'Tc0.'

In parallel with this switch, we also changed the route of tumor challenge used in our studies. Besides inadequate Treg numbers and inappropriate effector cell phenotype, we also thought that the location of our tumor might make it difficult for suppression to take place, although we could find no studies that had investigated the idea previously. By using IV tumor challenge we were seeding lung capillaries with tumor. These same capillary beds would be the first ones encountered by our treatment cells, and they would do so prior to exposure to any lymphoid organs such as spleen or lymph nodes. It seemed reasonable to think that this direct access of highly polarized effector cells to tumor would potentially bypass a number of regulatory mechanisms used for suppression. This

shortcoming would presumably be less of an issue for Tc0 cells, since as naïve cells they would need host lymphatic tissue to become polarized. Use of a subcutaneous model would further allow multiple time point measurement and generation of growth curves as opposed to the single data points generated in the lung metastasis model.

In switching to the subcutaneous treatment model, we also incorporated the use of non-myeloablative whole body irradiation of our mice prior to the administration of treatment cells. This was done largely on the basis of multiple studies (Gattinoni et al., 2005a; Dudley et al., 2008), including our own preliminary data in this model (not shown), which demonstrated an enhanced treatment efficacy when irradiation was incorporated to adoptive cell therapies. A number of explanations for this effect have been proposed, including decreased host immune cell competition, increased availability of cytokines, and liberation of tumor antigens, but none have been fully proven to be the cause for the treatment benefit seen. Despite the lack of full mechanistic understanding, the treatment benefit of irradiation is well established and was successfully utilized here.

Thus, we converted our model to one where tumor cells were challenged subcutaneously and treated with OTI Tc0 cells. As demonstrated in Figure 3.4, this model allowed for antigen-specific treatment of B16.mOVA in both WT and MHCII KO mice in a manner that was comparable if not superior to Tc1 cells. Addition of Tregs to this model, as shown in Figure 3.5, resulted in what appeared to be suppression in the MHCII KO hosts but not WT hosts. Upon further examining this data, we were stuck with two general observations.

The first of these was that, while the Treg curves between the WT and MHCII KO groups were similar, the treatment effect seen in WT mice was less robust than that in

MHCII KO mice. This decreased treatment intensity reduced the window available for Treg suppression making interpretation within the WT recipients more difficult. While a number of explanations could be provided for this observation, the obvious one that occurred to us was the presence of endogenous Tregs in WT mice but not in MHCII KO mice. While we had utilized lymphocyte-depleting radiation prior to our adoptive transfer, this depletion is not perfect, and further the host bone marrow was still intact and would resume immune cell production. Recovery of endogenous polyclonal Tregs in WT mice could potentially allow for suppression of our Tc0 cells. In contrast, MHCII KO mice do not possess CD4 cells, and therefore recovery of their bone marrow would not produce endogenous Tregs that could suppress our OTI. To investigate this theory further, we first needed a better characterization of the OTI cells in our model, which subsequent studies would later seek to achieve.

The second observation we were struck by in Figure 3.5 was the lag in suppression that occurred in the MHCII KO mice. In our hypothesis, the recognition of tumor cells by effector cells would result in exposure to inflammatory cytokines that could induce upregulation of MHCII on the tumors, thereby allowing them to directly present antigens to Tregs. This would presumably result in a lag of suppression during the interval where tumors were being seen and killed by effector cells but had not yet upregulated MHCII. Thus, our findings with an MHCII-inducible tumor fit very well with the model we had proposed. To further extend and support this idea, we hypothesized that the constitutive expression of MHCII by our tumor would result in a reduction, or perhaps elimination, in this suppressive lag, and conversely a decrease or

complete inability to up-regulate MHCII would result in a decreased to absent suppressive potential.

To answer this question, we had to create B16 tumor variants with constitutive and non-inducible MHCII expression. To accomplish the first of these, we inserted the *CIITA* gene into our B16.mOVA line to create B16.mOVA.CIITA. CIITA is essential for transcriptional activation of all MHCII genes and has a helper function in MHCI gene expression (Holling et al., 2006), and we envisioned its forced expression within our tumor cell would result in constitutive MHCII expression. To accomplish the second of these, we utilized a B16 variant, B16-F10-D, which had been shown years earlier by the lab to not up-regulate MHCII in the presence of IFNγ (data not shown). To this cell we added the same mOVA antigen expressed by our MHCII-inducible B16-F10 line to create B16-F10-D.mOVA. Once created, we successfully showed that all three of our B16 variants expressed OVA (Figure 3.8) and demonstrated the desired pattern of MHCI and MHCII expression in the presence and absence of IFNγ *in vitro* (Figure 3.6). We further were able to demonstrate that these *in vitro* findings were recapitulated upon effector cell exposure (and presumably IFNγ exposure) *in vivo* (Figures 3.9 and 3.10). Finally, along with the expression patterns of MHCI and MHCII, we were able to demonstrate that our B16 variants upregulated the expression of the negative co-stimulatory molecule PD-L1 in the presence of IFNγ both *in vitro* (Figure 3.7) and *in vivo* (Figure 3.9). This expression of PD-L1 by tumors and upregulation by IFNγ has been well documented (Zhang et al., 2009; Zhou et al., 2010) and shown to have important implications upon tumor outcome and Treg function within tumors (Ghebeh et al., 2007; Zhou et al., 2009a; Zhou et al., 2010).

In conclusion, in this first study we were able to develop a novel subcutaneous B16 tumor challenge system in which OVA-expressing B16 cells were treated by a combination of non-myeloablative whole body irradiation and adoptive transfer of OTI Tc0 cells in both WT and MHCII KO recipients. Although not perfect, we were further able to demonstrate a suppressive effect of OTII Tregs upon this treatment in our MHCII KO recipients. To allow for further elucidation of this effect, we successfully generated and validated both *in vitro* and *in vivo* two new OVA-expressing B16 tumor lines with constitutive and non-inducible MHCII expression to go along with our initial MHCII-inducible B16.mOVA line. Future studies will aim to better understand the treatment model generated here by evaluating the phenotype of our Tc0 cells over the course of tumor progression, evaluate the effect of Tregs upon this Tc0 phenotype, and finally to determine the effects that variable tumor MHCII expression has upon the suppressive capabilities of Tregs in this model.

Chapter 4

Characterization of the OTI Treatment System

4.1 Introduction

In our first study, we were able to establish a model of antigen-specific immune-mediated tumor rejection of B16.mOVA by OTI CD8+ that could subsequently be suppressed by OTII Tregs in MHCII KO mice. To better understand the physiology of this model, we next set out to characterize the phenotype of our OTI Tc0 (naïve) CD8+ cells as they elicited the treatment effect seen. Through accurately defining our CD8+ populations and effector cell phenotype, we hoped to eventually evaluate the changes Tregs have upon this phenotype as a means of insight into the mechanisms used by Tregs to enact suppression.

CD8+ T-cells exist as a series of distinct functional subpopulations comprised of antigen-inexperienced naïve (T_N) cells and antigen-experienced effector (T_E), effector memory (T_{EM}), and central memory (T_{CM}) cells. After encountering antigen, T-cells undergo proliferation and differentiation based upon a number of signals from the surrounding immune environment including TCRs, cytokines, and costimulatory molecules (Sallusto et al, 2004; Wherry et al., 2003). The largest pool of cells generated are T_E cells, the majority of which are short lived and die as their effector function eliminates antigen. A smaller pool of T_{CM} and T_{EM} cells is also generated which can

respond to repeated exposure to antigen by proliferating and differentiating into T_E cells. These T_E cells are once again typically short lived but can also revert back to memory cells (Wherry et al., 2003; Fearon et al., 2001).

Each of these subpopulations differs in its phenotype, including tissue trafficking, accumulation, function, and long-term persistence potential (Sallusto et al., 2004), all of which influence their ability to enact long-standing immunity. Once example of phenotypic variability within CD8+ cells involves cell surface expression of the adhesion molecule CD62L. T_{CM} cells are classically considered to be CD62L+, allowing them to migrate into secondary lymphatic tissue such as lymph nodes where they are capable of rapidly proliferating when exposed to antigen. In contrast, T_{EM} cells lack CD62L expression, enabling them to migrate away from lymph nodes into peripheral tissues where they can enact effector function (Butcher & Pickler, 1996). T_E cells, also known as cytotoxic T-cells (Tc or CTL), also lack CD62L and can be further divided into type 1 (Tc1) and type 2 (Tc2), both of which are capable of killing through the granzyme/perforin pathway. Tc1 cells produce IL-2, IFNγ, and TNFα, whereas Tc2 cells typically produce IL-4, IL-5, and IL-10 (Carter & Dutton, 1995; 1996; Cerwenka et al., 1998). Both Tc1 and Tc2 have been shown to mediate durable antigen-specific reduction of tumor growth and increased mouse survival in a B16-OVA lung metastasis model. Tc1, however, were shown to be 5-fold more effective at clearance than Tc2, with Tc1 demonstrating superior persistence in the tumor over time (Dobranzski et al., 1999). Based upon this data, we had selected to use OTI Tc1 in our initial treatment model, but found that our cells, unlike those of Dobrzanski and colleagues, were unable to enact long-term immune protection.

Clues to this failure come from a number of recent studies that have evaluated the importance of CD8 phenotype and lineage in protective immunity (Berger et al., 2008; Wherry et al., 2003). It has been suggested that *in vitro* acquisition of an effector phenotype is a large reason for the poor survival often seen in adoptively transferred CD8+ cells (Gattinoni et al., 2005b; 2006; Dudley et al., 2001; Yee et al., 2002; Klebanoff et al., 2005), and transfer of alternative populations of CD8+ cells has been under investigation. Studies within both mouse and human melanomas have shown a superior long-term effect with adoptive transfer of antigen-specific T_{CM} cells over T_{EM}/T_E cells (Klebanoff et al., 2005; Chapuis et al., 2012). T_E derived from T_{CM} have been shown to have greater capacity than T_{EM} to persist *in vivo*, have greater proliferative potential, and are more efficient at mediating long-term protective immunity (Wherry et al., 2003; Berger et al., 2008). Use of T_N populations has also been shown to provide long-term antigen-specific immunity (Chen et al., 2005), likely owing to the ability of these cells to form all major CD8 populations upon antigenic stimulation *in vivo*.

In our second study, we set out to define the phenotype acquired by our OTI+ CD8+ cells following the adoptive transfer of T_N cells into B16.mOVA tumor-bearing mice. We were able to successfully show that our CD8+ cells expanded, trafficked to, and accumulated within the tumor mass. We further demonstrated based upon surface molecule expression that our cells developed into all major CD8+ subpopulations, with secondary lymphoid tissues containing greater percentages of T_N and T_{CM} cells whereas peripheral tumor tissue demonstrated primarily T_{EM}/T_E cells. These tumor resident T_{EM}/T_E cells further demonstrated a high frequency of exhaustion marker expression, which may account for the lack of permanent tumor rejection seen in our model. Finally,

we were able to demonstrate that our CD8+ cells secreted IFNγ and TNFα cytokines consistent with a Tc1 phenotype and were able to effectively lyse antigen-bearing targets throughout the course of tumor progression.

4.2 Materials and Methods

4.2.1 Mice

Mice six to eight weeks old were used for all experiments, with matching of donor/recipient gender whenever possible. All mice were housed and bred in the Johns Hopkins University Cancer Research Building I mouse facility using standard procedures, and all experiments involving the use of mice were performed in accordance with protocols approved by the Animal Care and Use Committee of the Johns Hopkins University School of Medicine.

C57BL/6 WT (C57BL/6NCr) and C57BL/6 45.1+/+ (B6-LY5.2/Cr) mice homozygous for the CD45.1/Ly5.2 congenic marker were purchased from the NCI (Frederick, MD). C57BL/6 I-A^b-/- (B6.129S2-$H2^{dlAB1\text{-}Ea}$/J) mice bearing a homozygous deletion within the *MHCII* gene locus (Madsen et al., 1999) were purchased from Jackson Laboratory (Bar Harbor, ME). C57BL/6 RAG1-/- OTI+/+ (B6.129S7-$Rag1^{tm1Mom}$Tg(TcraTcrb)1100Mjb) mice bearing homozygous knockout of the *Rag1* gene along with homozygous insertion of the OTI αβ TCR specific for chicken ovalbumin peptide 257-264 (OVAI - SIINFEKL) presented by the MHCI molecule H-$2K^b$ (Hogquist et al., 1994) were purchased from Taconic (Germantown, NY). C57BL/6 Luci+/+ mice

expressing firefly luciferase under the control of the β-actin promoter (Cao et al., 2004) were a generous gift from Dr. Leo Luznik.

C57BL/6 RAG1+/- OTI+/- CD45.1+/- and RAG1+/- OTI+/- Luci+/- mice were generated by crossing C57BL/6 RAG1-/- OTI+/+ mice with C57BL/6 45.1+/+ and C57BL/6 Luci+/+, respectively, to create heterozygote F1 progeny which were used as donors in experiments.

4.2.2 Tumor Cell Lines and Culture

All tumor cell lines were grown in 'CTL' media comprised of RPMI 1640 supplemented with 10% fetal bovine serum (FBS), penicillin-streptomycin (100 IU/ml & 100 ug/ml), L-glutamine (2 mM), HEPES buffer (5 mM), and 2-mercaptoethanol (100 uM) at 37°C in a humidified 5% CO_2 incubator. Addition of G418 (1000 ug/ml) was used for selection/maintenance of mOVA expression.

The B16-F10 cell line is a melanoma derived from the C57BL/6 background and was contained within longstanding laboratory stocks. It has virtually undetectable baseline MHCI and MHCII expression, both of which can be induced by exposure to IFNγ. B16.mOVA is a derivative of the B16-F10 line, which has been engineered to express a membrane-bound version of chicken ovalbumin (OVA) via stable transfection with pcDNA3.1(+)/mOVA under neomycin/G418 selection as previously described (Preynat-Seauve et al., 2007) and was a gift from Dr. Bertrand Huard.

4.2.3 OTI Tc0 Isolation

C57BL/6 OTI+ splenocytes were harvested into single cell suspension by crushing through a 100 um cell strainer (BD Biosciences; San Jose, CA) followed by subsequent red blood cell (RBC) lysis using ammonium-chloride-potassium lysis buffer (ACK) (Gibco; Carlsbad, CA). RBC-free splenocytes were then enumerated and washed with ice-cold PBS. CD8+ cells were then purified using negative selection with MACS CD8a+ T-cell Isolation Kit I or II according to manufacturer instruction using MACS LS separation columns (Miltenyi; Auburn, CA). Following purification, cells were stored at 4°C in CTL media until ready for use. Cell purity was analyzed by FACS analysis for CD8, CD4, and Thy1.2 and was consistently greater than 95% CD8+ Thy1.2+ CD4-. Prior to adoptive transfer, cells were washed 3 times in ice-cold PBS, counted, and diluted as needed.

4.2.4 Subcutaneous Tumor Challenge and Treatment

A fresh vial of tumor cells was thawed for each challenge experiment and grown for approximately 7 days with harvest at approximately 70% confluency to ensure exponential growth. For challenge, cells were harvested from adherent culture flasks using 0.25% trypsin-EDTA (Gibco; Carlsbad, CA) and washed in ice-cold CTL media. Cells were washed 3 times in ice-cold PBS, counted, and diluted to 1E6 cells/ml in ice-cold PBS. Mice were then challenged subcutaneously with 1E5 tumor cells in the previously shaved right flank on day 0. On day 6, mice were transferred to fresh clean caging and provided with water containing trimethoprim/sulfamethoxazole (Sulfatrim; dosed for 95 mg/kg/24hr; obtained from the Johns Hopkins Hospital pharmacy) in

preparation for irradiation. On day 7, mice were irradiated at 500 Rads whole body irradiation and then adoptively transferred via tail vein injection with OTI Tc0. Tumor size was then determined with cross-sectional caliper measurement once or twice weekly. Mice were sacrificed at the first sign of suffering or for timed explant sampling as indicated.

4.2.5 *In Vivo* Bioluminescent Imaging

D-Luciferin (Perkin-Elmer; Waltham, MA) was prepared fresh at 15 mg/ml in PBS, sterile filtered using a 0.22 um syringe filter, and stored on ice in the dark prior to injection. Mice were given 200 ul intraperitoneal (i.p.) injection of D-Luciferin to provide an approximate dose of 150 mg/kg. They were then anesthetized using isoflurane in preparation for imaging. Imaging was performed 10 minutes after injection of D-Luciferin in order to optimize light signal per the manufacturer's protocol. Mice were imaged using the IVIS Spectrum (Perkin-Elmer; Waltham, MA) *in vivo* imaging system under real-time isoflurane anesthesia.

To ensure signal accuracy, the longest exposure without pixel saturation was utilized. No more than 5 mice were imaged at a single time to minimize signal bleed. To maximize signal sensitivity, the smallest imaging field that could fit all samples was utilized. For groups demonstrating wide mouse-to-mouse variability, mice bearing large signal intensity were imaged and removed to allow reimaging and uncovering of lower-intensity signals. Image data was acquired and analyzed using Living Image™ software (Perkin-Elmer; Waltham, MA). Regions of Interest (ROIs) were generated based upon a 2% maximum pixel signal threshold within each image, and data expressed as Radiance

(photons/s/cm^2) in order to control for variability in exposure times used. Mice were imaged once or twice weekly, and never more than every other day to avoid anesthesia-induced failure to thrive.

4.2.6 *In Vivo* CTL Kill Assay

C57BL/6 CD45.1+/+ donor mice were sacrificed and spleens harvested for use as target cells. RBC-free, single cell suspensions were then prepared as described previously. Splenocytes were then counted, seeded at 10E6 cells/ml in warmed CTL media with or without 1 ug/ml OVAI peptide (Genscript; Piscataway, NJ) into culture flasks, and incubated 2 hours at 37°C in a humidified 5% CO_2 incubator for peptide loading. Cells were transferred to 50 ml conical tubes and washed with warmed PBS. Cell pellets were then thoroughly resuspended in 1 uM (OVAI targets) or 0.1 uM (unlabeled targets) Carboxyfluorescein Succinimidyl Ester (CFSE)(Invitrogen; Carlsbad, CA) and incubated for 20 minutes in a light-protected 37°C water bath. CFSE labeling was then quenched with ice-fold FBS for 5 minutes on ice and cells washed twice with ice-cold PBS and counted. Peptide loaded (CFSE high) and non-loaded (CFSE low) cells were then mixed 1:1 for a total cell count of 50E6 cells/ml and stored on ice in the dark prior to injection. Recipient mice were i.v. injected with 200 ul target mix via tail vein. Extra cells were stored overnight at 4°C in CTL for use as FACS controls. Recipients were sacrificed and harvested approximately 18 hours later for analysis of target cell killing via flow cytometry. % Lysis was defined as being equal to (1-(target/non-target))x100.

4.2.7 *Ex Vivo* Lymphocyte Isolation and Stimulation

Tumor-bearing mice were sacrificed and spleens, lymph nodes, and tumors harvested into ice-cold CTL media. RBC-free, single cell suspensions of spleens and LNs were prepared as outlined previously. Given the large volume of necrotic debris, tumor tissue samples required more elaborate processing. Single cell tumor suspensions were prepared by crushing tissue through a 100 um cell strainer (BD Biosciences; San Jose, CA). Cells were then washed with ice-cold RPMI and spun at 1000 RPM, leaving smaller dead cell fragments in the supernatant. This step was repeated until the supernatant was grossly clear of pigmented debris. Red blood cell (RBC) lysis was then performed using ammonium-chloride-potassium lysis buffer (ACK) (Gibco; Carlsbad, CA). Dead cell removal was then further performed using one or two rounds of ficoll-paque (GE Life Sciences; Piscataway, NJ) separation. Cells were counted and stored in ice-cold CTL media until ready for FACS staining or *in vitro* stimulation.

For *in vitro* stimulation, 1E6 explant cells were seeded in 1 ml CTL media in a 24-well flat bottom plate (Corning; Tewksbury, MA). 2 ug/ml OVAI peptide (Genscript; Piscataway, NJ) was then seeded into test wells along with 1 ul/ml GolgiPlug™ (brefeldin A) (BD Biosciences; San Jose, CA). Negative controls received GolgiPlug™ without OVAI peptide, and positive controls were treated with 2 ul/ml Leukocyte Activation Cocktail containing PMA/ionomycin and GolgiPlug™ (BD Biosciences; San Jose, CA). Cells were then incubated overnight (~16 hours) at 37°C in a humidified 5% CO_2 incubator. The following morning, cells were harvested and analyzed via flow cytometry.

4.2.8 Antibodies and Flow Cytometry

CD4-APC (clone RM4-5), CD8-PE and CD8-A700 (clone 53-6.7), Thy1.2-FITC (clone 30-H12), TNF-APC (clone MP6-XT22), CD44-V500 (clone IM7), Ki67-PerCP-Cy5.5 (clone B56), and IFNγ-PE (clone XMG1.2) were purchased from BD Biosciences (San Jose, CA). Galectin-9-PE (clone 108A2), CD127-APC (clone A7R34), PD-1-BrilliantViolet™421 (clone 29F.1A12), IL-17a-PacificBlue™ (clone TC11-18H10.1), and TIM-3-PE (clone RMT3-23) were purchased from BioLegend (San Diego, CA). Thy1.1-APC-eFluor™780 (clone HIS51), CD62L-PerCP-Cy5.5 (clone MEL-14), KLRG-1-PE-Cy7 (clone 2F1), IL-2-PE-Cy7 (clone JES6-SH4), and LAG-3-PE (clone C9B7W) were purchased from eBioscience (San Diego, CA). CD4-PE-TexasRed® (clone RM4-5) was purchased from Invitrogen (Camarillo, CA). All antibodies were titrated for optimal staining intensity vs. background signal for 1E6 cells/reaction. All isotype control antibodies were from the same manufacturer and used at the same concentration as their associated test antibody.

Qdot®625-"tetramer" specific for OTI CD8+ cells was prepared in house. Monomer of H-2K^b coupled with the chicken ovalbumin peptide 257-264 SIINFEKL were prepared by the NIH Tetramer Core Facility (Atlanta, GA) and stored at -80°C until ready for tetramerization. For tetramerization, a 25 ul aliquot of approximately 2 ug/ml monomer stock was thawed on ice and diluted to a total volume of 100 ul with sterile 1X PBS. 20 ul of Qdot®625-Streptavidin (Invitrogen; Camarillo, CA) was then added to the monomer, mixed thoroughly, and allowed to incubate on ice in the dark for 20 minutes. This step was repeated a total of 4 times to yield a final solution of 200 ul tetramer at 0.225 ug/ml concentration. Formed tetramer was titrated using RAG-/- OTI+/+

splenocytes and stored at 4°C until use. All formed tetramers were used within one month of preparation. It should be noted that this is in fact not a true tetramer, as each Qdot® has between 5 and 10 streptavidin molecules bound to it, each of which can bind up to 4 monomers. Thus, the end molecule is a large multimer and not a true tetramer.

For all extracellular antibody staining, 1E6 cells were washed with FACS buffer containing 1X Hanks Balanced Salt Solution (HBSS), 10 mM HEPES buffer, 2% FBS, and 0.1% sodium azide and stained with appropriate antibody for 15 minutes at room temperature in the dark followed by two washings with FACS buffer. No more than 5 antibodies were stained at a single time. Cells were similarly washed for tetramer staining but were incubated for 30 minutes. Viability staining using LIVE/DEAD® Yellow and Aqua Fixable Dead Cell Stain Kit (Invitrogen; Camarillo, CA) was performed according to the manufacturer's instructions at a 1:2000 dilution with a 30 minute room temperature incubation and washing steps using PBS. Cellular fixation/permeabilization was performed using the Foxp3 Staining Buffer Set (eBioscience; San Diego, CA) according to manufacturer instructions with fixation performed for 45 minutes at 4°C in the dark. Subsequent intracellular staining was performed for 30 minutes at 4°C in the dark with washes using the staining buffer set. For multi-step staining sequences, the following sequence was always followed: Tetramer, extracellular antibody, Live/Dead stain, fixation/permeabiliation, intracellular stain. Following staining, cells were stored in FACS buffer at 4°C in the dark and were analyzed within 24 hours of staining.

Flow cytometry was performed on the BD FACSCaliber™, FACSAria™, or LSRII™ with data acquisition using CellQuest Pro™ or FACSDiva™ (BD Biosciences;

San Jose, CA). Data analysis was further performed with FACSDiva™ as well as FlowJo (Tree Star Inc.; Ashland, OR).

4.2.9 Histology

Mice were sacrificed and tumors, spleens, and lymph nodes (LN) harvested into ice-cold CTL media. Tissues were then blotted to remove excess CTL and transferred to Intermediate Tissue-Tek CryoMolds (Sakura Finetek; Torrance, CA) containing a small layer of Optimal Cutting Temperature (OCT) media (Sakura Finetek; Torrance, CA) and subsequently covered with OCT media. Tissue chambers were then flash-frozen in a beaker of liquid nitrogen-cooled isopentane (Sigma; St. Louis, MO). Once fully frozen, samples were transferred on dry ice to a -80°C freezer for storage prior to cryosectioning. Tissue was subsequently cryosectioned at 5 um sections onto "Plus" slides, fixed in ice-cold acetone for 10 minutes, and air dried for 30 minutes by the Johns Hopkins Histology Core. Following sectioning and fixation, slides were stored in a -80°C freezer until stained.

Primary antibodies used for staining included: I-A^b-biotin (clone AF6-120.1; Ms IgG2a) and CD45.1-FITC (clone A20; Ms IgG2a)(BD Biosciences; San Jose, CA). All isotype controls were used at the same concentration and were from the same supplier as the test antibody. Fluorescein/Oregon Green® Rabbit IgG Antibody (Invitrogen; Camarillo, CA) was used as a secondary antibody to increase primary antibody-FITC signal. Goat anti-Rabbit AlexaFluor®488 (Invitrogen; Camarillo, CA) and Stretavidin-Cy3 (Sigma; St. Louis, MO) were used for tertiary staining.

For staining, slides were allowed to warm to room temperature for 5 minutes in a laminar flow hood and then tissue demarcated with an ImmunEdge Pen (Vector Labs; Burlingame, CA) prior to rehydration with PBS for 10 minutes at room temperature. All subsequent staining and blocking steps were performed in a light-protected, humidified chamber with three PBS washes between steps. Samples were first treated with 1-2 drops Molecular Probes Endogenous Biotin Blocking Kit (Invitrogen; Camarillo, CA) solutions A and B for 30 minutes each at room temperature. They were then covered with 100 ul isotype-control blocking antibodies at 10 ug/ml in Blocking Buffer (2% IgG-free BSA and 5% normal mouse serum (Jackson Immunoresearch; West Grove, PA) in PBS) for 1 hour at room temperature. This blocking solution was then shaken off without PBS wash and replaced with primary antibodies at 10 ug/ml in Blocking Buffer and incubated overnight at 4°C. Slides were then incubated with 100 ul of 2 ug/ml secondary antibody in PBS/2%BSA for 1 hour at room temperature, washed, and incubated with 100 ul of tertiary antibodies diluted 1:100 in PBS/2%BSA for 1 hour at room temperature. Nuclei were then counterstained with Hoechst 33342 (Invitrogen; Camarillo, CA) diluted 1:50,000 in PBS for 15 minutes at room temperature. Following PBS wash, slides were fixed and mounted using a single drop of Aqua Poly/Mount (Polysciences; Warrington, PA) and cover slips placed and immobilized with nail polish. Slides were then stored face-up in light-protected slide boxes at 4°C until imaging.

Imaging was performed using a Nikon E800 fluorescent microscope using standard DAPI, FITC, Cy3, and Cy5 filter sets. Image acquisition and analysis was performed using Nikon Elements Software (Nikon Metrology; Brighton, MI).

4.3 Results

4.3.1 OTI CD8 Expand and Accumulate within the Tumor

To evaluate the function of our OTI CD8+ cells *in vivo*, we first sought to examine their ability to traffic to and accumulate within the tumor. In order to accomplish this, we initially utilized a bioluminescent imaging (BLI) approach to allow for analysis of OTI accumulation within tumors over multiple sequential time points. Recipient MHCII KO mice were challenged with 1E5 B16.mOVA tumor on day 0 and treated on day 7 with 500 Rads non-myeloablative whole body irradiation followed by adoptive transfer of 2.5E6 Tc0 cells from OTI+/- Luci+/- donor mice. Mice were then subjected to bioluminescent imaging every other day to detect the location of OTI cells via the activity of the luciferase enzyme. As shown in Figure 4.1, OTI cells quickly trafficked to and preferentially accumulated within the tumor mass. With our imaging modality, cells could be detected in what appeared to be draining lymph nodes as early as day 10 (three days post transfer), with OTI clearly evident within the tumor as early as day 12. Accumulation continued through day 14 and appeared to level off after that point. Whether this was due to a slowing of trafficking and accumulation, or perhaps just the detection limit of our system could not be determined. In either case, OTI cells clearly persisted even when tumor treatment effect began to wane.

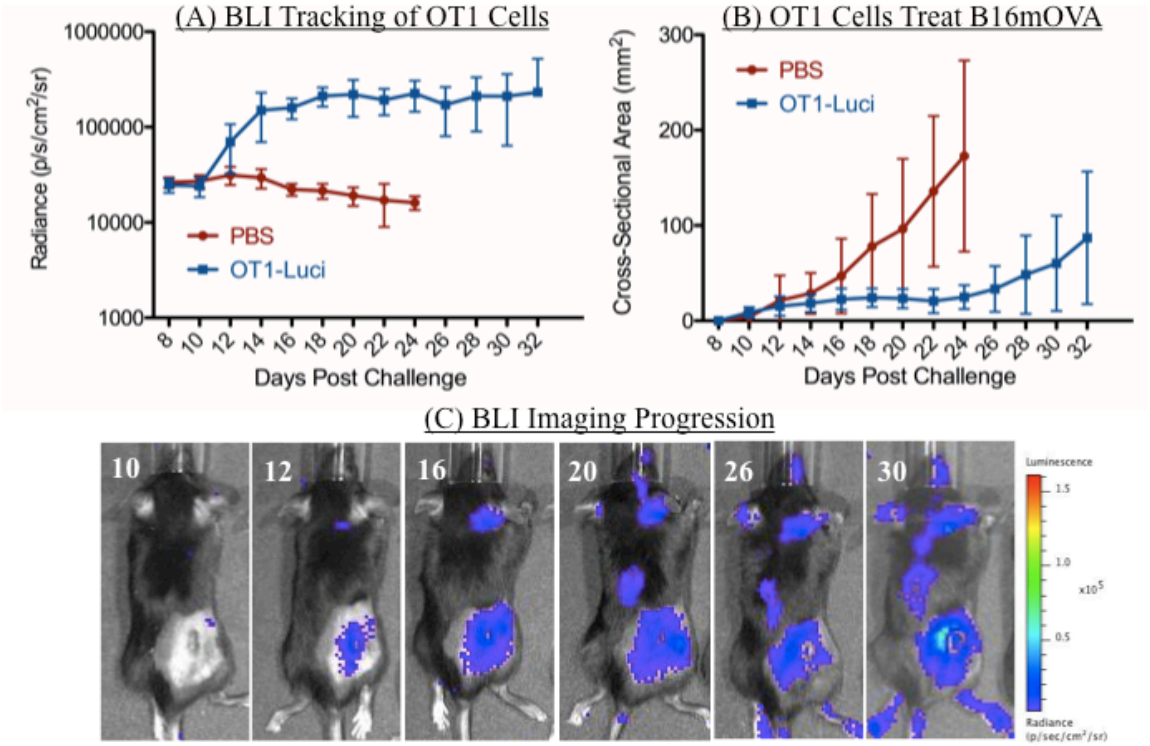

Figure 4.1 OTI CD8+ quickly traffic to and accumulate within B16.mOVA tumors. C57BL/6 MHCII KO mice were challenged with 1E5 B16.mOVA tumor on day 0 and treated on day 7 with 500 Rads non-myeloablative whole body irradiation followed by adoptive transfer of 2.5E6 Tc0 cells from OTI+/- Luci+/- donor mice or PBS control. Mice were then imaged every other day to detect the location of OTI cells, with corresponding caliper measurements of tumor size performed with each round of imaging. Mean +/- Standard Deviation for groups of 3 mice are shown. PBS mice were sacrificed following day 24. (A) BLI of mice over the course of tumor progression. (B) Tumor growth over time as determined by caliper measurements. (C) Representative BLI images of a single mouse over time with experiment day indicated in the upper left corner for each image.

To further expand upon and validate our bioluminescent imaging data, we next performed histologic analysis of tumors to verify that our OTI cells were in fact penetrating and accumulating within the tumor. To accomplish this, mice were similarly challenged and treated as before, only with use of Tc0 from OTI+/- CD45.1+/- as opposed to OTI+/- Luci+/- donors. Mice were sacrificed one week after treatment and tumor masses harvested and processed for histologic evaluation of MHCII and the congenic marker CD45.1 expressed only by OTI cells. As can be seen in Figure 4.2, OTI CD8+ cells were found in large abundance both immediately surrounding as well as deep within the tumor tissue, confirming our BLI data. Also noteworthy within this evaluation, although not depicted here, was the fact that MHCII expression correlated very well with the presence of OTI cells. Regions of tumor with the highest OTI content demonstrated intense MHCII staining, and conversely areas devoid of OTI cells had minimal to no MHCII signal. This finding was well in line with our hypothesis of inflammation-induced MHCII upregulation in our B16.mOVA tumor.

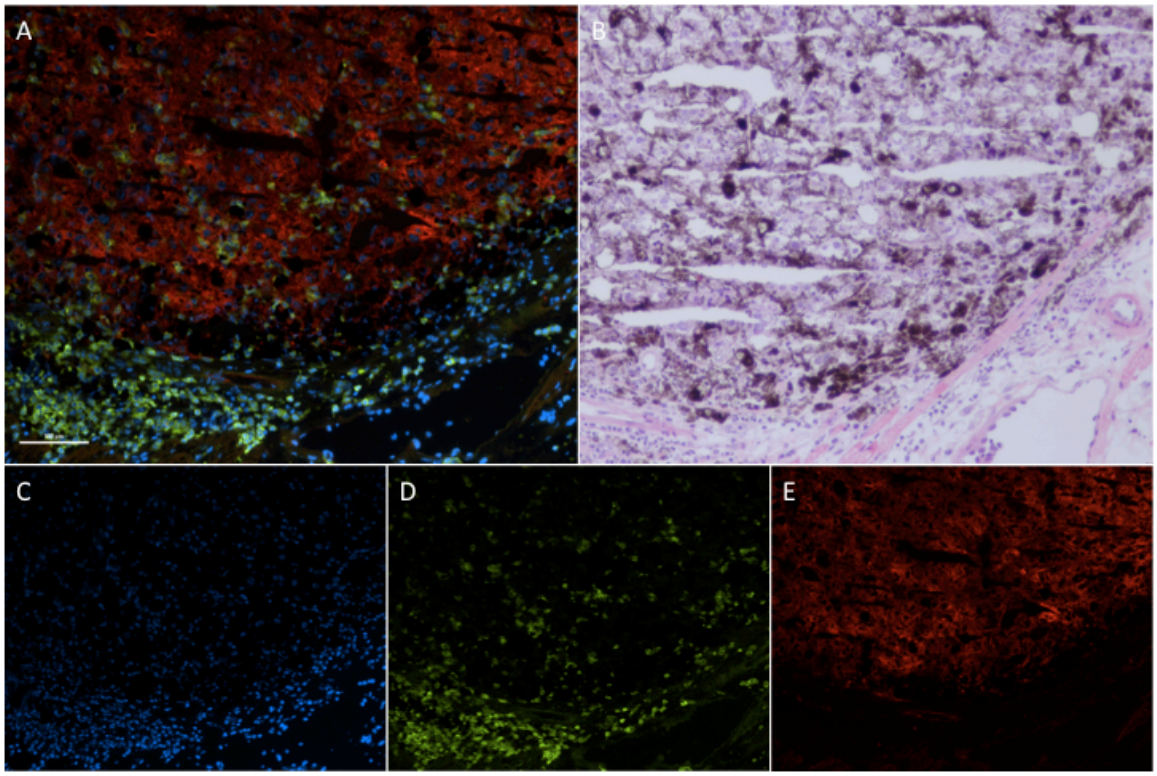

Figure 4.2 OTI CD8+ are readily detectable within tumors.

C57BL/6 WT and MHCII KO mice were challenged with 1E5 B16.mOVA tumor on day 0 and treated on day 7 with 500 Rads non-myeloablative whole body irradiation followed by adoptive transfer of 2.5E6 OTI+/- CD45.1+/- Tc0 or PBS. Mice were sacrificed one week after treatment and tumor masses harvested and processed for histologic evaluation. Displayed here are a Merge (A) of DAPI nuclear stain (C), CD45.1 (D), and MHCII (I-A^b) (E), as well as an H&E stain (B) demonstrating necrotic tumor mass with overlying epidermis. Representative images from I-A^b-/- recipients are shown. 3 mice were used per group.

As a final method to investigate the proliferation and expansion of our OTI cells, we explanted spleens, draining lymph nodes (DLN), and tumors over the course of treatment to assess for total numbers of OTI+ and OTI- CD8+ cells via flow cytometry. Mice were challenged and treated as before, with sacrificing and tissue harvesting performed weekly throughout tumor treatment. Samples were processed to create single cell suspensions and subsequently analyzed via flow cytometry for the expression of CD8 and OTI-specific tetramer. In a second experiment, samples were similarly generated and evaluated for the expression of the proliferation marker Ki67 within CD8+ cells. Unfortunately, due to technical limitations of the staining procedure, we were unable to differentiate between OTI+ and OTI- CD8+ when performing Ki67 analysis. As shown in Figure 4.3(A&B), total OTI+ and OTI- CD8+ cells within spleens and LNs expanded early in the course of tumor treatment with the largest increase occurring between the second and third weeks post treatment. OTI+ CD8+ subsequently plateaued with continued increase in total CD8+ cells indicating ongoing expansion of host-derived CD8+. Due to the large volume of necrotic debris within tumor samples and low relative quantity of tumor infiltrating lymphocytes (TILs), accurate total numbers of TILs could not be determined.

Tumor infiltrating CD8+ cells were, however, able to be identified and analyzed on a percentile basis for analysis of Ki67 staining along with CD8+ cells from spleen and DLNs as shown in Figure 4.3(C&D). Ki67 staining from spleens and DLNs revealed a high level of CD8+ proliferation early in the course of treatment with a dramatic decrease occurring again between the second and third weeks post treatment. This proliferation of CD8+ cells was seen both for OTI-treated mice as well as untreated mice, likely

indicating a large component of homeostatic proliferation following irradiation. Within TIL samples, Ki67 staining was overall lower, but interestingly did not demonstrate the same dramatic drop between weeks two and three post treatment, perhaps suggesting a continued antigen-dependent proliferative stimulus with the tumor.

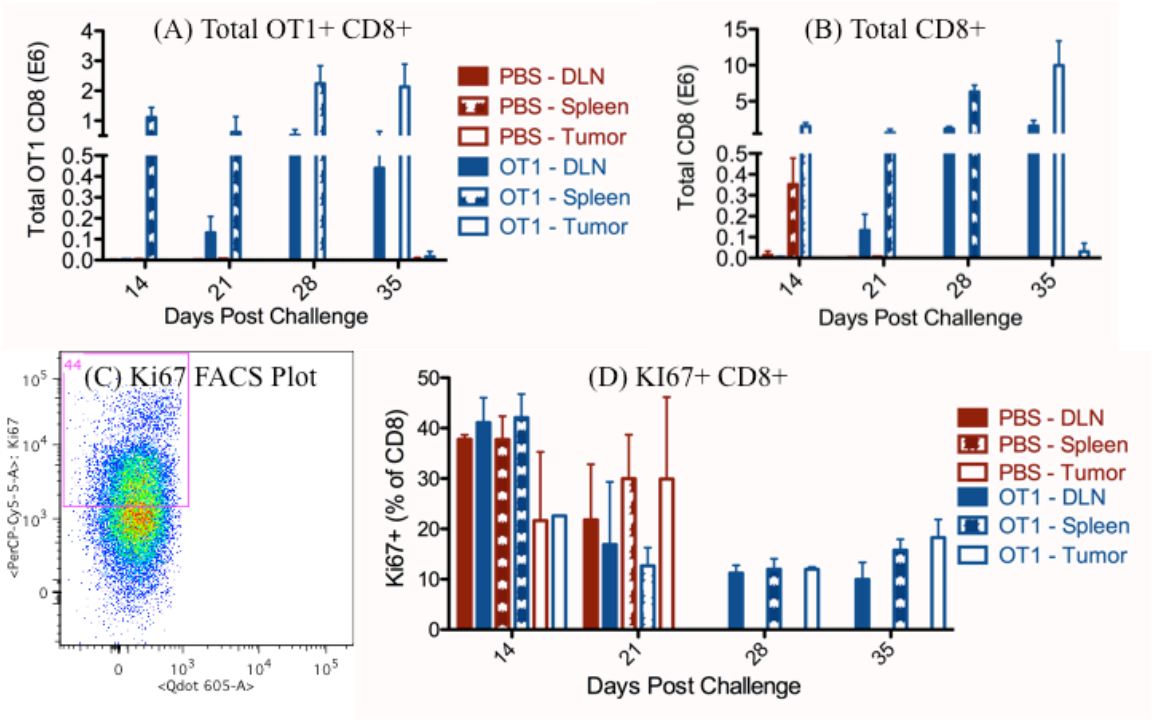

Figure 4.3 Proliferation and accumulation of OTI+ and OTI- CD8+ T-cells in tumor-bearing mice.

C57BL/6 MHCII KO mice were challenged with 1E5 B16.mOVA tumor on day 0 and treated on day 7 with 500 Rads non-myeloablative whole body irradiation followed by adoptive transfer of 2.5E6 OTI cells or PBS. Mice were sacrificed at weekly intervals and spleens, tumor-draining lymph nodes, and tumors harvested. Single cell suspensions were prepared from explanted tissue and subjected to flow cytometric analysis of live cells as determined by scatter profiles and live/dead cell stain. Mean +/- Standard Deviation for 3-5 mice per group are shown. PBS mice were sacrificed following day 21. (A&B) Explanted cells were stained for CD8 and OTI-specific tetramer and total numbers of cells per tissue determined. (C&D) Explanted cells were stained for CD8 and then intracellularly stained for Ki67. Cells with staining above isotype control (C) were considered Ki67+ and expressed as a percentage of total CD8+ cells (D).

4.3.2 Cell Surface Phenotype of OTI CD8+

Having demonstrated that our OTI cells effectively proliferated and trafficked to the site of tumor, we next examined their cell surface phenotype over the course of tumor treatment. To begin with, we examined the expression of the adhesion molecules CD44 and CD62L. Mice were challenged and treated as before, with sacrificing, tissue harvesting, and explant preparation again performed at weekly intervals and analyzed via flow cytometry. As shown in Figure 4.4, OTI CD8+ cells demonstrated CD44 and CD62L patterns consistent with naïve (CD44- CD62L+), central memory (CD44+ CD62L+), and effector/effector memory (CD44+, CD62L-) populations at varying ratios depending on their tissue of origin. DLN explants demonstrated an abundance of naïve cells, very few effector cells, and an intermediate level of central memory cells. TILs, on the other hand, demonstrated a dramatic majority of effector/effector memory cells, while spleens showed intermediate quantities of all three populations.

With our OTI cells demonstrating what appeared to be appropriate patterns of CD44 and CD62L expression, we next turned our attention to examining CD127 and KLRG-1, which have been shown to be variably expressed on different CD8+ populations. As shown in Figure 4.5, OTI CD8+ within DLNs and spleens were almost entirely CD127+ KLRG-1-. TILSs demonstrated an overall majority of these same CD127+ KLRG-1- negative cells, but showed an increased frequency of double negative cells as well. Interestingly, few KLRG-1+ cells were identified within our OTI CD8+. However, evaluation of OTI- host CD8+ cells demonstrated increased numbers of CD127- KLRG-1+ cells (~10-30%) relative to OTI+ CD8+ cells (~0-10%) over the course of tumor progression (data not shown).

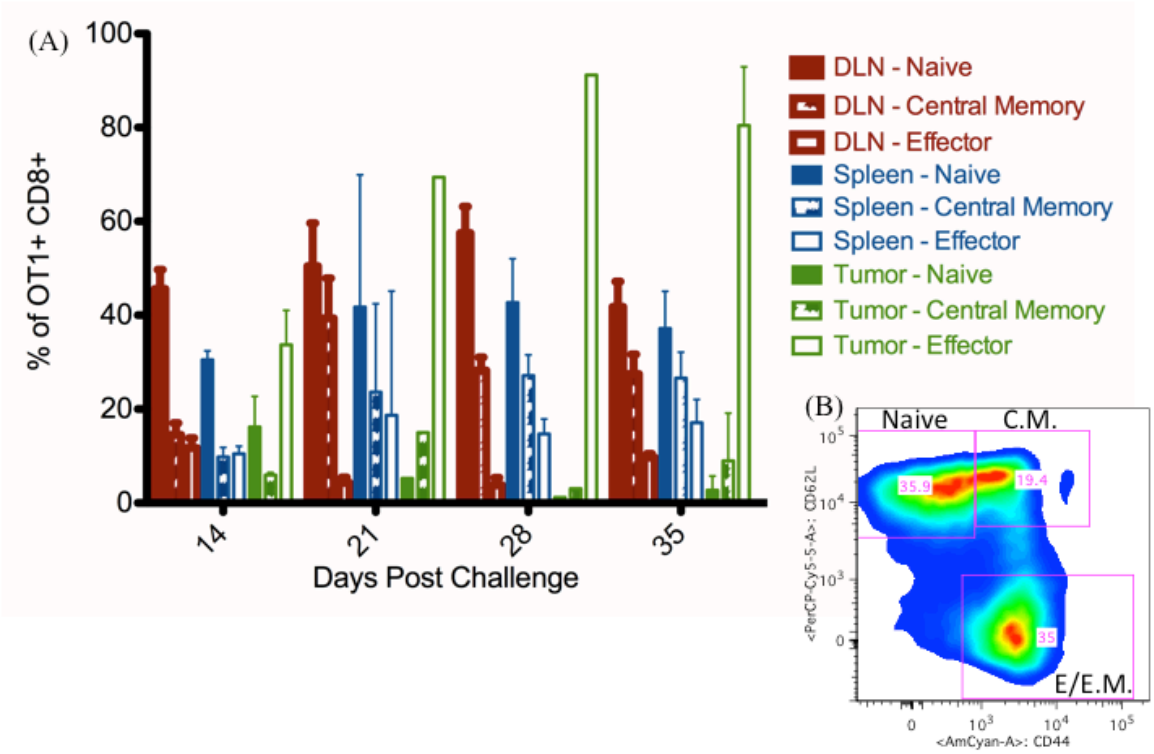

Figure 4.4 CD44 vs. CD62L expression by OTI CD8+ in tumor-bearing mice.

C57BL/6 MHCII KO mice were challenged with 1E5 B16.mOVA tumor on day 0 and treated on day 7 with 500 Rads non-myeloablative whole body irradiation followed by adoptive transfer of 2.5E6 OTI cells. Mice were sacrificed at weekly intervals and spleens, tumor-draining lymph nodes, and tumors harvested. Single cell suspensions were prepared from explanted tissue and subjected to flow cytometric analysis of live cells as determined by scatter profiles and live/dead cell stain. (A) Tetramer+ (OTI+) CD8+ cells were classified as naïve, central memory (CM), or effector/effector memory (E/EM) based upon their CD44 and CD62L expression patterns as shown in (B). Mean +/- Standard Deviation for 3-5 mice per group are shown.

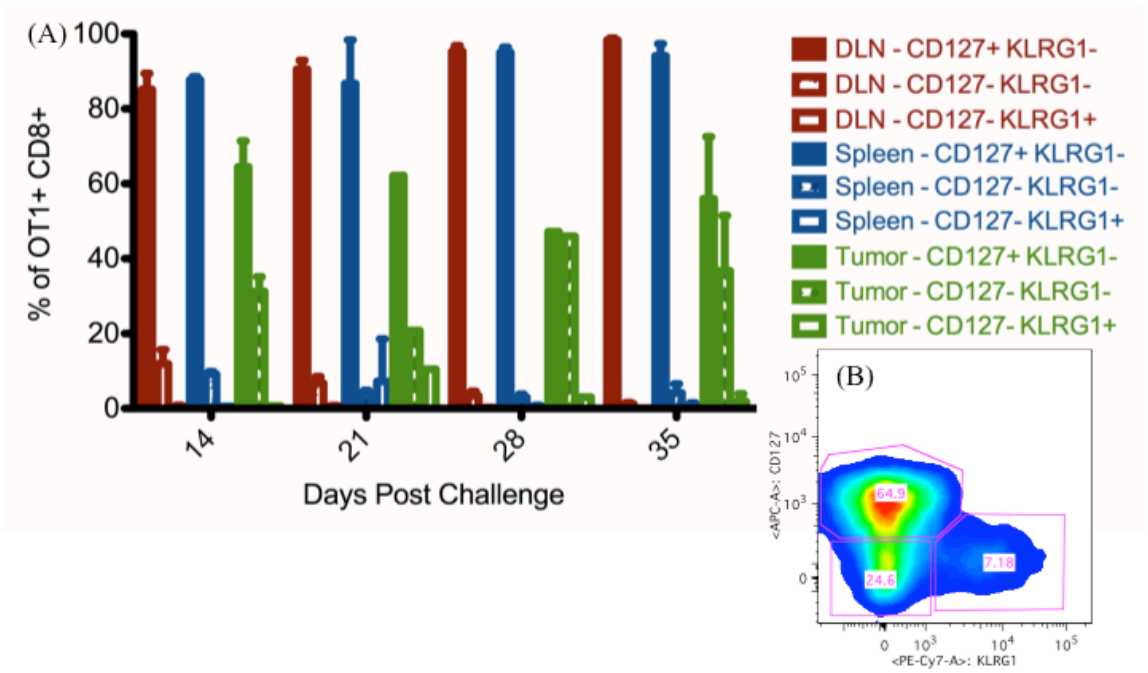

Figure 4.5 CD127 vs. KLRG-1 expression by OTI CD8+ in tumor-bearing mice. C57BL/6 MHCII KO mice were challenged with 1E5 B16.mOVA tumor on day 0 and treated on day 7 with 500 Rads non-myeloablative whole body irradiation followed by adoptive transfer of 2.5E6 OTI cells. Mice were sacrificed at weekly intervals and spleens, tumor-draining lymph nodes, and tumors harvested. Single cell suspensions were prepared from explanted tissue and subjected to flow cytometric analysis of live cells as determined by scatter profiles and live/dead cell stain. (A) Tetramer+ (OTI) CD8+ cells were analyzed for CD127 and KLRG-1 expression patterns as shown in (B). Mean +/- Standard Deviation for 3-5 mice per group are shown.

Finally, having examined markers associated with differing CD8+ populations, we next examined the negative costimulatory molecules PD-1, LAG-3, and TIM-3. These molecules are thought to be involved in T-cell exhaustion and have been further implicated to play roles in Treg function. As shown in Figure 4.6, OTI CD8+ cells from spleens and LNs were primarily negative for all three markers, whereas TILs demonstrated strikingly high percentages of cells expressing these markers, suggesting a high frequency of effector cell exhaustion within our OTI+ TILs.

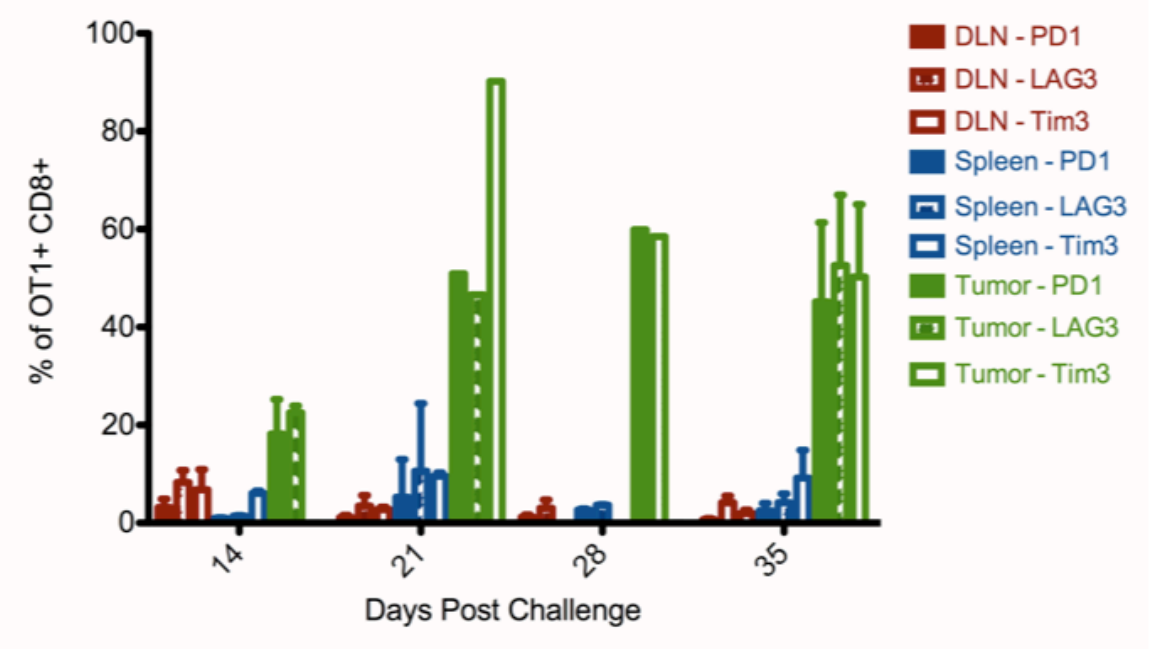

Figure 4.6 Expression of PD-1, LAG-3, and TIM-3 by OTI CD8+ in tumor-bearing mice.

C57BL/6 MHCII KO mice were challenged with 1E5 B16.mOVA tumor on day 0 and treated on day 7 with 500 Rads non-myeloablative whole body irradiation followed by adoptive transfer of 2.5E6 OTI cells. Mice were sacrificed at weekly intervals and spleens, tumor-draining lymph nodes, and tumors harvested. Single cell suspensions were prepared from explanted tissue and subjected to flow cytometric analysis of live cells as determined by scatter profiles and live/dead cell stain. Mean +/- Standard Deviation for 3-5 mice per group are shown. Of note, day 28 samples were unavailable for TIM-3 analysis.

4.3.3 OTI CD8 Develop a Functional Tc1 Phenotype

Having examined the proliferation, trafficking, tumor accumulation, and cell surface phenotype of our OTI+ cells, we turned our attention to their effector capabilities, beginning with the evaluation of their antigen-specific cytokine expression profiles. Mice were challenged and treated as before, with sacrificing, tissue harvesting, and explant preparation again performed at weekly intervals. Cells were then seeded into *in vitro* stimulation with OVAI peptide with subsequent intracellular flow cytometric analysis of the cytokines IFNγ, TNFα, IL-2, and IL-17. As shown in Figure 4.7, CD8+ explants from all three tissues of tumor-bearing mice demonstrated high levels of IFNγ and TNFα expression. IL-2 and IL-17 expression, on the other hand, were found only sparingly and at very low levels (each at ~2%) (data not shown).

We next investigated the ability of our OTI cells to effectively kill antigen-loaded targets *in vivo*. Tumor-bearing mice were given adoptive transfer of a 1:1 mix of $CFSE^{high}$ OVAI peptide-loaded and $CFSE^{low}$ non peptide-loaded target splenocytes and evaluated for killing effect 16 hours later by assessing for target populations in recipient spleens and tumor-draining lymph nodes. Unfortunately, TIL samples yielded inadequate numbers of target events for evaluation. As shown in Figure 4.8, tumor-bearing mice treated with OTI+ CD8+ cells effectively lysed nearly 100% of peptide-loaded targets with no effect on antigen-free targets. Mice treated only with PBS demonstrated only minimal lysis of these same target cells.

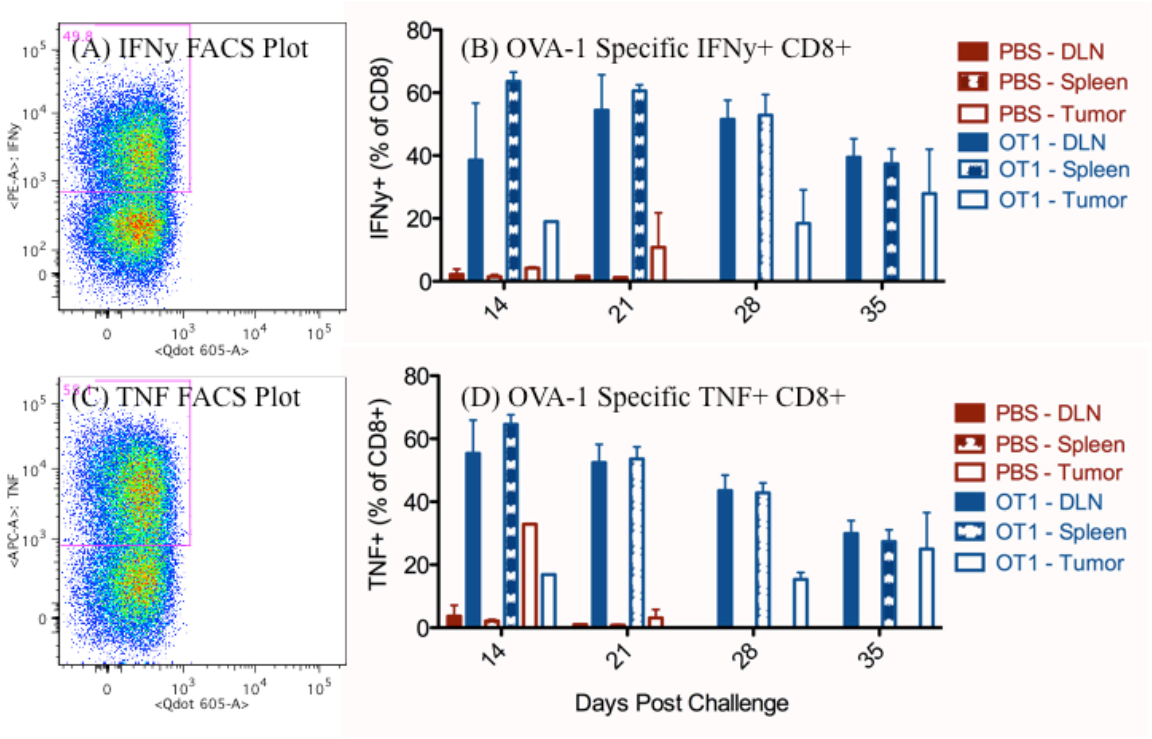

Figure 4.7 OVAI-specific CD8+ develop Tc1 effector cytokine profiles in tumor-bearing mice.

C57BL/6 MHCII KO mice were challenged with 1E5 B16.mOVA tumor on day 0 and treated on day 7 with 500 Rads non-myeloablative whole body irradiation followed by adoptive transfer of 2.5E6 OTI cells or PBS. Mice were sacrificed at weekly intervals and spleens, tumor-draining lymph nodes, and tumors harvested. Single cell suspensions were prepared from explanted tissue and subjected to *in vitro* stimulation with OVAI peptide followed by intracellular flow cytometric analysis of live cells as determined by scatter profiles and live/dead cell stain. Representative FACS profiles of IFNγ (A) and TNFα (C) staining are shown with corresponding Mean +/- Standard Deviation for 3-5 mice per group in (B) and (D), respectively. Of note, all untreated PBS mice were sacrificed following day 21, and day 21 TIL samples were not of adequate numbers to evaluate.

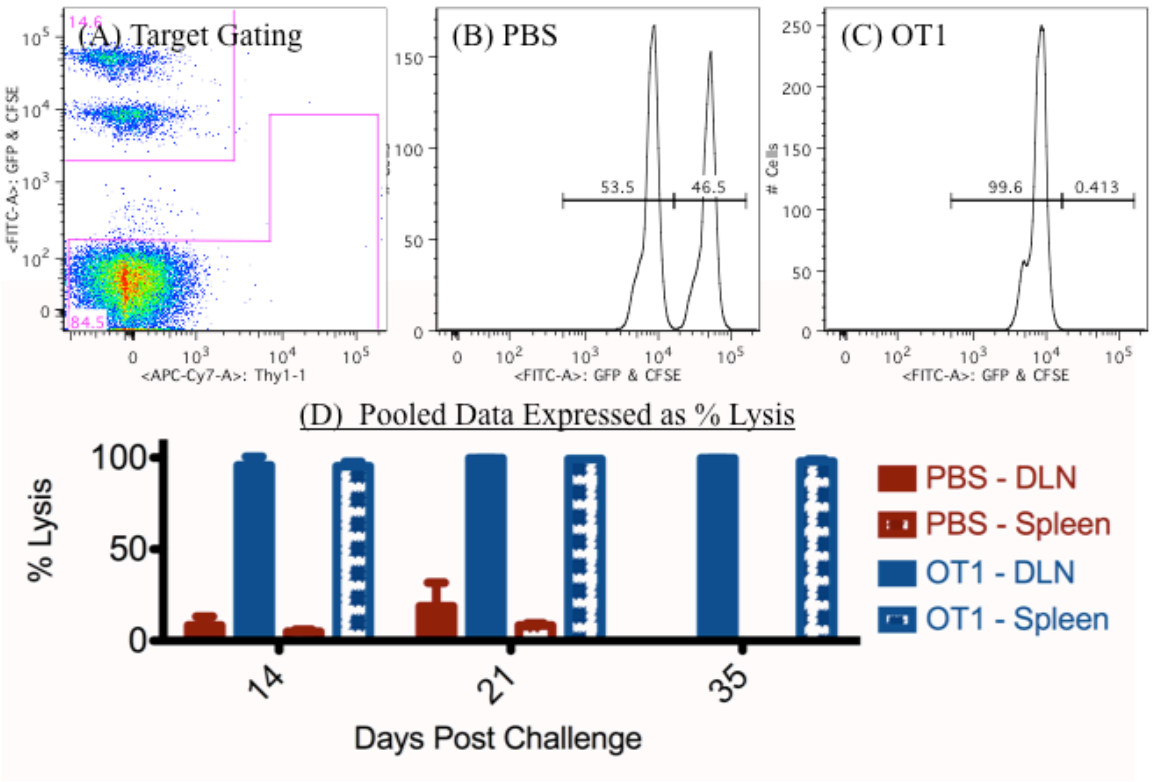

Figure 4.8 OTI CD8+ effectively lyse OVAI peptide-loaded targets *in vivo.*

C57BL/6 MHCII KO mice were challenged with 1E5 B16.mOVA tumor on day 0 and treated on day 7 with 500 Rads non-myeloablative whole body irradiation followed by adoptive transfer of 2.5E6 OTI cells or PBS. Mice were given adoptive transfer of a 1:1 mix of $CFSE^{high}$ OVAI peptide-loaded and $CFSE^{low}$ non peptide-loaded target splenocytes and evaluated for killing effect 16 hours later by assessing for target populations in recipient spleens and tumor-draining lymph nodes (inadequate numbers were obtained from tumor). % Lysis was defined as being equal to (1-(target/non-target))x100. FACS target gating is shown in (A), with representative plots from PBS- (B) and OTI-treated (C) mice along with corresponding Mean +/- Standard Deviation for 3-5 mice per group in (D). Of note, all untreated PBS mice were sacrificed following day 21, and day 28 target labeling failed and thus no data was available for this time point.

4.4 Discussion

In this second study we sought to characterize our adoptively transferred OTI Tc0 cells throughout the course of tumor treatment, with a particular emphasis upon understanding their effector function as a means for later assessing the implications of Treg suppression upon CD8+ cells. In order for an antigen-specific naïve CD8+ cell to enact killing of an appropriate antigen-bearing target tumor cell, the CD8+ cell must proliferate, differentiate, traffic, and enact effector cytolytic function using a number of potential mechanisms. Previous studies utilizing naïve CD8+ cells for this function had been able to demonstrate these very steps taking place (Chen et al., 2005), and we therefore hoped to recapitulate some of the same findings.

To begin with, we examined the expansion, trafficking, and accumulation of our cells. By making use of luciferase-expressing transgenic mice, we were able to utilize *in vivo* bioluminescent imaging to repeatedly monitor these events in tumor-bearing mice. These studies demonstrated that OTI CD8+ cells quickly trafficked to and accumulated within the tumor tissue. As early as 3 days following transfer, cells could be detected within regions consistent with tumor draining lymph nodes, and were further localized within tumor tissue as early as 5 days post transfer. While the accuracy of the timing seen here is certainly dependent upon the detection threshold of our system, 3-5 days from transfer to visible trafficking and accumulation within the tumor mass is reasonable and consistent with previous work. Studies by Rabinovich and colleagues (Rabinovich et al., 2008) comparing tracking of OTI cells using the firefly luciferase used here against an enhanced vector demonstrated OTI cells within the site of OVA vaccination at 5 days

post transfer using the traditional luciferase. They further demonstrated that the minimum number of cells needed for detection using the traditional luciferase was on the order of 10E5, suggesting a reference range for the minimum number of trafficked cells demonstrated in our studies.

Besides the timing of initial trafficking, our BLI studies also gave some insight into the kinetics and durability of CD8+ accumulation within the tumor. Following their initial detection between days 10 and 12 (3-5 days post transfer), cells accumulated rapidly through the 14-16 day time point, but then showed a deceleration in this accumulation. This result may indicate a true slowing of accumulation, but may also reflect technical limitations associated with our BLI platform, as well as changes in the tumors themselves. Subcutaneously growing B16 tumors are well known to develop necrotic and ulcerative cores as they progress (Overwijk & Restifo, 2001), and this was consistently observed within our studies. These necrotic sites would represent a potential dead space for OTI accumulation, and in fact upon close examination of individual mouse images (Figure 4.1), such dead spaces can be demonstrated as early as day 16. Also of note in our BLI studies, while there was a definite early focus of signal within the tumor, as time progressed signal could be detected throughout the body of the mouse, particularly in areas of exposed, non-hairy skin, likely due to decreased light absorbance by the black hair of the mouse. This widespread signal distribution likely represented the systemic expansion of OTI cells in these mice, at least in part due to homeostatic proliferation induced by the whole-body irradiation used in this study.

To further corroborate and expand upon our BLI data, we also performed histologic evaluation of our tumors to confirm that our OTI cells were in fact penetrating

with the tumor and not merely colocalizing in two dimensional space. These studies clearly demonstrated that OTI cells could be found in high volume surrounding the tumor mass, but also could be found deep within the tumor mass itself. Previous studies have indicated that the penetration of adoptively transferred cells into melanoma lesions is very low, on the order of <0.005% per gram of tumor (Pockaj et al., 1994; Goedegebuure et al., 1995), thus making histologic quantification difficult. Our studies also confirmed this finding, showing wide variability in overall TIL prevalence, which was also observed in the aforementioned studies by Rabinovich and colleagues (Rabinovich et al., 2008). Interestingly, however, we anecdotally found a high degree of correlation between the incidence of OTI cells and MHCII staining within our tumor samples. Areas with a high volume of OTI cells demonstrated strong MHCII staining, whereas areas devoid of OTI cells demonstrated low to negative MHCII signal. This finding was consistent with our hypothesis of inflammation-induced upregulation of MHCII by tumor cells, and suggests that our OTI cells were actively producing inflammatory cytokines within the tumor.

As a final means of assessing the proliferation of OTI cells within our model, we performed flow cytometric analysis of explanted spleens, tumor-draining lymph nodes, and tumors to assess for total host OTI- and OTI+ CD8+ cell numbers during tumor progression in conjunction with the use of Ki67 staining. Ki67 is a protein of uncertain function, which has been well documented to be expressed within the nuclei of actively replicating cells (Starborg et al., 1996). Analysis of spleens and tumor draining lymph nodes revealed that the vast majority of CD8+ cells during the first two weeks (day 14 and 21) following irradiation and adoptive transfer were OTI+ cells. Ki67 expression during this time frame was very high within CD8+ cells from both OTI-treated and PBS

mice, suggesting a high degree of proliferation in all CD8+ populations which would be consistent with a picture of lymphopenia-induced homeostatic proliferation caused by our non-myeloablative irradiation. Between the second and third weeks post transfer, both OTI+ and total CD8+ numbers increased dramatically, with the increase in total CD8+ being beyond that accounted for by OTI+ CD8+, suggesting a recovery of host-derived CD8+ cells. Ki67 expression during this interval was decreased relative to earlier time points, suggesting a slowing of overall proliferation. Finally, between the third and fourth week post-transfer, OTI+ CD8+ numbers plateaued while total CD8+ numbers continued to rise, suggesting continued host CD8+ expansion.

Analysis of accurate TIL numbers via flow cytometry proved to be exceedingly challenging, with the low cell yields and large volume of necrotic debris making accurate cell enumeration impossible. However, Ki67 analysis was able to be performed upon TIL samples. While overall lower than the percentages seen early on with spleen and tumor samples, a consistent low-level (10-20%) Ki67 expression level was observed throughout the course of treatment. This consistent low-level proliferation likely represents a continuous antigen-driven proliferative response within the tumor, as opposed to the likely larger influence of homeostatic proliferation seen within the spleen, and to a lesser extent DLN cells.

Having established the effective proliferation and trafficking of our OTI CD8+ cells, we next turned our attention to characterizing their surface phenotype. A number of cell surface molecules have been utilized to classify the various subpopulations of CD8+ cells. One such pairing of molecules are the cell adhesion molecules CD44 and CD62L. Naïve cells are classically thought of as being CD44- and CD62L+, while

antigen-experienced cells become CD44+, being either CD44+ CD62L+ for central memory cells, and CD44+ CD62L- for effector/effector memory cells. These variable expression patterns have functional consequences. Expression of CD62L allows residence within secondary lymphatic tissues, whereas its loss allows migration into peripheral tissues (Butcher & Pickler, 1996). Upon analyzing our explant cells for these two markers, we were able to demonstrate that all three major populations of CD8+ cells were in fact present. Most strikingly within this analysis was the extremely high predominance of CD44+ CD62L- effector/effector memory cells within TIL populations, which was to be expected given their peripheral tissue location and had been previously demonstrated in other models (Chen et al., 2005). Also noteworthy was the large volume of CD44- CD62L+ naïve cells that persisted throughout the course of tumor progression in spleens and DLNs. Despite the tumor burden of these mice, the majority of OTI CD8+ cells remained antigen inexperienced based upon CD44/CD62L staining. Finally, it is important to note that a significant number of CD44+ CD62L+ central memory cells were identified, particularly in spleens and DLNs. As previously mentioned, growing evidence suggests that these cells are critical for the development of a long-lasting, durable immune response (Wherry et al., 2003; Berger et al., 2008). The fact that all three CD8+ populations were found in our model suggests that a failure of CD8+ differentiation from our naïve OTI CD8+ cells was not the cause of the long-term treatment failure seen in this model.

Having established that all three major CD8+ subpopulations were present, we next evaluated two other cell surface molecules: CD127 and KLRG-1. CD127, also known IL7 receptor alpha, is expressed on naïve cells, downregulates in the setting of

active antigen stimulation, and is again found upregulated on central memory cells as well as effector cells destined for future memory development (Bengsch et al., 2007; Boettler et al., 2006; Wherry and Ahmed, 2004). Killer cell lectin-like receptor G1 (KLRG-1) expression classically defines antigen-experienced CD8+ cells capable of enacting effector function but otherwise impaired in long-term proliferative capacity (Voehringer et al., 2002). The combination of these two markers has recently been used to assess CD8+ populations over the course of viral infection, with chronic viral infection demonstrating a majority of CD127- KLRG-1+ CD8+ cells, whereas resolved infections demonstrate primarily CD127+ KLRG-1- CD8+ memory cells (Ibegbu et al., 2005; Thimme et al., 2005).

In analyzing these populations within our own study, we found that the majority of OTI CD8+ cells in all tissues analyzed demonstrated a CD127+ KLRG-1- phenotype, which would be consistent with either naïve cells or central memory cells. Given that the majority of our spleen and DLN OTI CD8+ demonstrated a CD44- CD62L+ naïve phenotype, CD127+ KLRG-1- cells within those tissues also likely represent naïve cells. In TIL samples, however, the largest proportion of cells were shown to be primarily CD44+ CD62L- effector/effector memory cells. This combination suggests that the CD127+ KLRG-1- cells within tumors are not naïve cells, but rather likely effector cells that are either destined for memory cell production, or perhaps more likely have not yet altered CD127/KLRG-1 expression. Perhaps in support of the latter, unlike spleens and DLNs, tumor samples also contained a high fraction of CD127- KLRG-1- OTI CD8+ cells. This expression pattern suggests an active antigen stimulation state without compromise of future proliferative potential seen with KLRG-1 expression. Such a

population has recently been demonstrated on intrahepatic Hepatitis C virus-specific CD8+ cells (Bengsch et al., 2007). Interestingly, as previously mentioned, evaluation of OTI- host CD8+ cells demonstrated increased numbers of CD127- KLRG-1+ cells (~10-30%) relative to OTI+ CD8+ cells (~0-10%) over the course of tumor progression (data not shown). The significance of this finding is unknown at this time, although it at the least validates the technical staining accuracy of our KLRG-1 and CD127 markers.

A third set of cell surface molecules examined were the negative costimulatory ligands PD-1, LAG-3, and TIM-3, which were previously discussed in detail (Chapter 2.7). PD-1 expression is considered a marker of immune exhaustion, and T-cells expressing this molecule are typically dysfunctional in their proliferative and effector capacities (Blackburn et al., 2009; Wherry et al., 2007; Day et al., 2006). LAG-3 is a negative regulator of activated T-cells with close relationship to the CD4 molecule (Huard et al., 1994; Hannier et al., 1998) and has previously been shown to regulate activated T-cell expansion (Workman et al., 2004). Binding of TIM-3 to its ligand, galectin-9, results in Th1 cell death (Zhu et al., 2005). All three of these molecules have been implicated in the function of Tregs (Workman & Vignali 2005; Zhou et al., 2010; Sakuishi et al., 2013), and antibody blockade of each of these molecules alone or in combination has shown improvement in tumor clearance in a number of models (Woo et al., 2012; Ngiow et al., 2011; Duraiswamy et al., 2013). We were able to demonstrate that our OTI CD8+ cells demonstrated minimal expression of these markers in spleens and DLNs, but in contrast TILs expressed high levels of all three molecules in excess of 50% of cells in many cases. Similar high frequency expression of these molecules has been described for TILs from a number of models (Woo et al., 2012; Curran et al., 2010;

Fourcade et al., 2012). This predominance of negative costimulatory molecule expression within or OTI cells may serve as an explanation as to the lack of long-term protective immunity seen in our tumor model.

Finally, having examined the proliferative, homing, and cell surface phenotype of our cells, we turned our attention to examining their effector phenotype. Our initial analysis here focused upon the ability of our CD8+ cells to secrete effector cytokines and to display CTL activity by lysing antigen-loaded targets. Given limitations of the experimental setup used, we could not distinguish in this analysis between adoptively transferred OTI+ CD8+ cells and host-derived CD8+ cells which were also specific for OVAI peptide. Given the large quantity of OTI cells given it is likely that the large majority of effect seen was from these cells. In either case, since our goal was to assess the OVA-specific effector cell activity in our tumor bearing model, a contribution by the host CD8+ T-cells to this pool would not alter the relevance of our findings.

Analysis of cytokine secretion in our model indicated that a large percentage of CD8+ cells were capable of secreting both IFNγ and TNFα in response to OVAI stimulation *in vitro*. The overall frequency of cells secreting these cytokine within total CD8+ cells did decreased over time, particularly later in the course of tumor treatment. Given the late increase of host-derived CD8+ cells demonstrated previously, this decreased frequency of cytokine secretion in response to OVAI stimulation likely represents in large part a dilution effect rather than a loss of secretory capability. Despite this overall decrease frequency of secretion, TIL samples demonstrated maintained and even increased frequency of IFNγ and TNFα secretion in response to OVAI peptide.

Secretion of IFNγ and TNFα is consistent with a Tc1 phenotype as opposed to a Tc2 phenotype (Carter & Dutton, 1995; 1996; Cerwenka et al., 1998), the former of which as mentioned has been previously shown to show superior anti-tumor effects (Dobrzanski et al., 1999). Due to our initial positive results with IFNγ and TNFα, coupled with the inferior technical detection ability of IL-4, IL-5, and IL-10, we did not assess for the production of those Tc2 cytokines in this study. It certainly would be possible that some of our cells developed a Tc2 phenotype as well. Interestingly, besides their secretion of IFNγ and TNFα, our cells secreted only negligible levels of IL-2 and IL-17. While lack of IL-17 secretion was not unexpected, the lack of IL-2 secretion was somewhat surprising, and may suggest another cause for the lack of long-standing immunity seen in our model. Tc1 cells are classically described to secrete IL-2. Further, the superior ability of central memory cells over effector memory cells to promote long-term immune protection has been attributed to the ability of central memory cells to secrete IL-2 in an autocrine fashion, rendering them somewhat independent of T-helper cells (Wherry et al., 2003). The fact that our OVAI-specific CD8+ cells did not secrete significant amounts of IL-2 in any compartment suggests that they may lack this necessary component of long-lasting immunity.

Finally, as a last assessment of our OTI CD8+ cells, we evaluated their ability to lyse OVAI-loaded target cells. Tumor-bearing mice treated with OTI CD8+ demonstrated an impressive ability to lyse OVAI-loaded splenocytes with little non-specific influence upon OVA-free targets. Mice not treated with OTI CD8+ demonstrated only minimal lysis of these same targets, suggesting that this cytotoxic effect was in fact due to our OTI CD8+ cells. Unfortunately, our analysis of *in vivo* CTL

activity was limited to spleens and tumor draining lymph nodes, as insufficient numbers of target cells were isolated from our tumor samples. Given the phenotypic differences seen in our other studies, most notably the high frequency expression of PD-1, LAG-3, and TIM-3 within our TIL samples, coupled with the fact that our tumors were not permanently treated but rather only suffered a treatment lag, it would not be surprising to see a reduction of functional CTL activity within the TIL samples. The fact that the B16.mOVA tumor was not permanently treated despite the presence of OVAI-specific CTL would suggest either a loss of OVA antigen from the tumor (which had previously been ruled out), or perhaps a state of local functional immune impairment within the tumor, which would be supported by our negative costimulatory molecule staining.

In conclusion, in this second study we were able to characterize the trafficking, proliferation, cell surface phenotype, and effector profile of our adoptively transferred naïve OTI Tc0 cells during the course of B16.mOVA tumor progression. Our cells effectively proliferated, trafficked to, and accumulated within tumors. They further developed surface phenotypes consistent with multiple lineages including naïve, central memory, and effector/effector memory cells CD8+ T-cells. These various populations showed variable distributions amongst spleen, DLN, and tumor that were consistent with current dogma. Our cells demonstrated CTL activity and cytokine expression consistent with a Tc1 effector phenotype. Finally, TILs from our study demonstrated a high degree of exhaustion marker expression consistent with the failure of long-term tumor clearance seen. The characterization of out adoptively transferred naïve OTI Tc0 cells performed here will hopefully allow for elucidation of Treg suppressive effects upon CD8+ cells in our future studies.

Chapter 5

Failure of the OTII Treg System

5.1 Introduction

In our first study, we were able to establish a model of antigen-specific immune-mediated tumor rejection of B16.mOVA by OTI CD8+ that could subsequently be suppressed by OTII Tregs in MHCII KO mice. In our second study, we characterized the expansion, tumor trafficking, cell surface phenotype, and effector function our OTI CD8+ in tumor-bearing mice. In this third study, we set out to further examine the influence of tumor MHCII expression upon Treg suppression and to examine the alterations in OTI CD8+ phenotype elicited by Tregs in order to better understand the suppressive mechanisms involved.

It is well established that Tregs can have a negative impact upon anti-tumor immune response. This has been demonstrated both through models where depletion or blocking of Treg function improves tumor response and effector T-cell function (Onizuka et al., 1999; Shimizu et al., 1999; 2002; Turk et al., 2004; Ko et al., 2005; Leach et al., 1996), as well as in models where adoptive transfer of Tregs has been demonstrated to suppress established tumor antigen-specific cytotoxic CD8+ T-cells (Turk et al., 2004; Antony et al., 2005). Understanding of the phenotypic alterations in CD8+ T-cells brought about by Tregs is, however, less understood. Multiple models have

demonstrated that Tregs can impair CD8+ proliferation and IFNγ production *in vitro* (Suvas et al., 2003; Piccirillo & Shevach, 2001; Dittmer et al., 2004; Murakami et al., 2002), but the alterations that occur *in vivo* are somewhat mixed and appear to vary depending on the model used.

Depletion of Tregs prior to HSV infection has been shown to result in improved CD8+ proliferation, increased expression of the activation markers CD44 and CCR5, and increased cytotoxicity, as well as improved memory responses to recall antigens (Suvas et al., 2003). In a recent study utilizing the B16 melanoma model, Treg depletion was associated not only with improved tumor outcome, but specifically with increased absolute numbers of CTLs, a doubling of CD8+ TILs, and significantly increased frequency of activated CD44+ and granzyme B+ CD8+ cells in spleens, DLNs, and most strikingly within the tumor tissue itself (Klages et al., 2010).

Models of transplant tolerance have demonstrated that when transplanted into tolerized animals, antigen-specific CD8+ cells proliferated and accumulated normally, but demonstrated impaired IFNγ secretion and direct cell-mediated cytotoxicity, including failed graft rejection (Lin et al., 2002). In a mouse model of persistent retroviral infection, adoptively transferred CD8+ cells proliferated and became activated but failed to produce IFNγ or decrease viral loads. This failure of effector function was ameliorated upon Treg depletion using anti-GITR antibodies (Dittmer et al., 2004). Studies performed on human melanoma samples have similarly indicated the generation of high avidity tumor antigen-specific CD8+ T-cells that display effective expansion and tissue homing, but impaired production of IFNγ and decreased perforin-mediated cytotoxicity at the site of tumor (Zippelius et al., 2004). This independent regulation of

cytotoxicity versus proliferation and cytokine production has been previously well described for CD8+ T-cells (Snyder et al., 2003; Hernandez et al., 2002). Beyond their effects on effector CD8+ function, Tregs have been suggested to alter the CD8+ recall responses in a number of models (Suvas et al., 2003; Dittmer et al., 2004; Lin et al., 2002), and have further been implicated to inhibit division of memory CD8 T-cells in an IL-2–dependent fashion (Murakami et al., 2002).

Perhaps the most thorough and relevant data to our own study comes from experiments by Chen and colleagues (Chen et al., 2005) who evaluated the effects of influenza hemagluttinin (HA)-specific Tregs upon HA-specific CD8+ cells in HA-expressing tumor-bearing mice. In their study, they demonstrated that the addition of Tregs abrogated the rejection of HA-expressing tumors otherwise elicited by adoptive transfer of naïve HA-specific CD8+ T-cells. They further demonstrated that the presence of these Tregs did not alter the expansion, homing, differentiation, activation, or cytokine secretion by HA-specific CD8+, but did result in a suppression of direct CD8+ T-cell-mediated cytotoxicity.

Thus, in this third study, we sought to evaluate the implications of variable tumor MHCII expression upon the suppressive effects of Tregs as previously seen in Chapter 1, and further to characterize the phenotypic alterations elicited by Tregs upon the OTI CD8+ T-cell phenotype previously characterized in Chapter 2 as a means of better understanding the suppressive mechanisms involved. Unfortunately and to our surprise, we found a complete absence of Treg suppression for all three OVA-expressing B16 variants tested, including the original B16.mOVA, which had previously demonstrated what appeared to be suppression in MHCII KO recipients. Upon examining the

phenotype of our OTI CD8+ cells in the presence of Tregs, we found no differences in the proliferation, homing, cell surface phenotype, cytokine secretion, or cytotoxicity of our OTI CD8+. To evaluate these two negative results, we verified that this lack of suppression or alteration in OTI phenotype occurred despite the persistence and continued expression of Foxp3 by our OTII Tregs. When evaluated *in vitro* it was discovered that, although they expressed functional MHCII, our OVA-bearing tumor cells failed to directly present endogenously produced OVA to OTII cells. Subsequent investigation into the background of our OVA lines and construct revealed that despite the presence of full length OVA within these tumors, through an unknown mechanism they fail to present to or activate OTII T-cells (Preynat-Seauve et al., 2007). Regrettably, this finding therefore makes all Treg studies performed herein uninterpretable.

5.2 Materials and Methods

5.2.1 Mice

Mice six to eight weeks old were used for all experiments, with matching of donor/recipient gender whenever possible. All mice were housed and bred in the Johns Hopkins University Cancer Research Building I mouse facility using standard procedures, and all experiments involving the use of mice were performed in accordance with protocols approved by the Animal Care and Use Committee of the Johns Hopkins University School of Medicine.

C57BL/6 WT (C57BL/6NCr) and C57BL/6 45.1+/+ (B6-LY5.2/Cr) mice homozygous for the CD45.1/Ly5.2 congenic marker were purchased from the NCI

(Frederick, MD). C57BL/6 Thy1.1+/+ (B6.PL-Thy1^{a}/CyJ) mice homozygous for the Thy1.1/CD90.1 congenic marker, C57BL/6 I-A^{b}-/- (B6.129S2-H2$^{dlAB1\text{-}Ea}$/J) mice bearing a homozygous deletion within the *MHCII* gene locus (Madsen et al., 1999), C57BL/6 RAG1-/- (B6.129S7-Rag1^{tm1Mom}/J) mice bearing a homozygous deletion of the *Rag1* gene, and C57BL/6 OTII+/+ (B6.Cg-Tg(TcraTcrb)425Cbn/J) mice bearing homozygous insertion of the OTII αβ TCR specific for chicken ovalbumin peptide 323-339 (OVAII - ISQAVHAAHAEINEAGR) presented by the MHCII molecule I-A^{b} (Barnden et al., 1998) were purchased from Jackson Laboratory (Bar Harbor, ME). C57BL/6 RAG1-/- OTI+/+ (B6.129S7-Rag1^{tm1Mom}Tg(TcraTcrb)1100Mjb) mice bearing homozygous knockout of the *Rag1* gene along with homozygous insertion of the OTI αβ TCR specific for chicken ovalbumin peptide 257-264 (OVAI - SIINFEKL) presented by the MHCI molecule H-2K^{b} (Hogquist et al., 1994) and C57BL/6 RAG1-/- OTII+/+ (B6.129S7-Rag1^{tm1Mom}Tg(TcraTcrb)425Cbn) mice bearing homozygous knockout of the *Rag1* gene along with homozygous insertion of the OTII αβ TCR specific for OVAII were purchased from Taconic (Germantown, NY). C57BL/6 Foxp3-GFP+/+ and +/y mice were a generous gift from Dr. Alexander Rudensky (Fontenot et al., 2005b). C57BL/6 Luci+/+ mice expressing firefly luciferase under the control of the β-actin promoter (Cao et al., 2004) were a generous gift from Dr. Leo Luznik.

C57BL/6 OTII+/+ Thy1.1+/+ mice were created by crossing C57BL/6 OTII+/+ with C57BL/6 Thy1.1+/+ to create OTII+/- Thy1.1+/- F1 progeny. These F1 progeny were then intercrossed and F2 progeny typed according to the presence of Thy1.1, absence of Thy1.2, and increase in CD4:CD8 ratio as seen in CD4 transgenic mice to suggest OTII+/? Thy1.1+/+ status. Since this CD4:CD8 skewing cannot differentiate

between OTII+/- and OTII+/+, F2 offspring were then testcrossed to C57BL/6 WT mice and progeny again typed for CD4, CD8, Thy1.1, and Thy1.2. F2 parents were considered to be OTII+/+ only if all pups showed CD4:CD8 skewing with a minimum of 8 pups typed. Once successfully generated, male and female OTII+/+ Thy.1.1+/+ mice were maintained as an independent colony.

C57BL/6 OTII+/- Thy1.1+/- Foxp3+/y mice were generated by crossing C57BL/6 OTII+/+ Thy1.1+/+ male mice with a C57BL/6 Foxp3-GFP+/+ female. Resultant female progeny were OTII+/- Thy1.1+/- Foxp3-GFP+/- and were not utilized due to decreased frequency of Foxp3 expression resulting from random X-inactivation in Foxp3-GFP heterozygotes. Male progeny on the other hand were Foxp3-GFP hemizygotes (+/y) and thus all Foxp3+ cells expressed the transgenic Foxp3-GFP and were subsequently used as Treg donors.

C57BL/6 RAG1+/- OTI+/- CD45.1+/- and RAG1+/- OTI+/- Luci+/- mice were generated by crossing C57BL/6 RAG1-/- OTI+/+ mice with C57BL/6 45.1+/+ and C57BL/6 Luci+/+, respectively, to create heterozygote F1 progeny which were used as donors in experiments.

5.2.2 Tumor Cell Lines and Culture

All tumor cell lines were grown in 'CTL' media comprised of RPMI 1640 supplemented with 10% fetal bovine serum (FBS), penicillin-streptomycin (100 IU/ml & 100 ug/ml), L-glutamine (2 mM), HEPES buffer (5 mM), and 2-mercaptoethanol (100 uM) at 37°C in a humidified 5% CO_2 incubator. Addition of G418 (1000 ug/ml) was used for selection/maintenance of mOVA expression, and hygromycin (200 ug/ml) was

used for selection/maintenance of C2TA expression. For *in vitro* induction of MHCI & MHCII, cells were cultured in 100 U/ml IFNγ (Peprotech, Rocky Hill, NJ) for three days.

The B16-F10 cell line is a melanoma derived from the C57BL/6 background. It has virtually undetectable baseline MHCI and MHCII expression, both of which can be induced by exposure to IFNγ. The B16-F10-D cell line is a variant of this same B16-F10 tumor that similarly has undetectable baseline MHCI and MHCII, but through unknown mechanisms has lost the ability up-regulate MHCII in the presence of IFNγ. Both of these tumor lines were contained within longstanding laboratory stocks. B16.mOVA is a derivative of the B16-F10 line, which has been engineered to express a membrane-bound version of chicken ovalbumin (OVA) via stable transfection with pcDNA3.1(+)/mOVA under neomycin/G418 selection as previously described (Preynat-Seauve et al., 2007) and was a gift from Dr. Bertrand Huard. B16-F10-D.mOVA and B16.mOVA.CIITA are OVA-expressing derivates of the above B16 lines with non-inducible and constitutive MHCII expression, respectively, that were created in house as previously described in Chapter 3.

5.2.3 OTI Tc0 Isolation

C57BL/6 OTI+ splenocytes were harvested into single cell suspension by crushing through a 100 um cell strainer (BD Biosciences; San Jose, CA) followed by subsequent red blood cell (RBC) lysis using ammonium-chloride-potassium lysis buffer (ACK) (Gibco; Carlsbad, CA). RBC-free splenocytes were then enumerated and washed with ice-cold PBS. CD8+ cells were then purified using negative selection with MACS CD8a+ T-cell Isolation Kit I or II according to manufacturer instruction using MACS LS

separation columns (Miltenyi; Auburn, CA). Following purification, cells were stored at 4°C in CTL media until ready for use. Cell purity was analyzed by FACS analysis for CD8, CD4, and Thy1.2 and was consistently greater than 95% CD8+ Thy1.2+ CD4-. Prior to adoptive transfer, cells were washed 3 times in ice-cold PBS, counted, and diluted as needed.

5.2.4 Regulatory T-Cell Culture & Retroviral Transduction

Regulatory T-cells were generated using two different culture methods which each produced equivalent *in vitro* suppressive ability (data not shown). In the first method, C57BL/6 RAG-/- OTII+/+ splenocytes were harvested into single cell suspension by crushing through a 100 um cell strainer (BD Biosciences; San Jose, CA) followed by subsequent red blood cell (RBC) lysis using ammonium-chloride-potassium lysis buffer (ACK) (Gibco; Carlsbad, CA). RBC-free splenocytes were then enumerated and washed with ice-cold PBS. CD4+ cells were then purified using positive selection with MACS CD4 (L3T4) Microbeads according to manufacturer instruction using MACS LS separation columns (Miltenyi; Auburn, CA). Following purification, cells were stored at 4°C in CTL media in preparation for culture and cell purity was analyzed by FACS analysis for CD4 and Thy1.2 and was typically around 75% CD4+ Thy1.2+. 10 cm tissue culture plates (Corning; Tewksbury, MA) were coated for 2 hours at room temperature with 10 ml PBS containing 2 ug/ml of non-azide, low-endotoxin anti-CD28 (clone 37.51) and anti-CD3 (clone 145-2C11) antibodies (BD Biosciences; San Jose, CA) and subsequently washed twice with 10 ml PBS. Purified CD4+ cells were then seeded into antibody-coated plates at 1E6 CD4+ cells/ml in 10 ml 'Treg media' consisting of

CTL containing 5 ng/ml hTGFβ (R&D Systems; Minneapolis, MN), 500 U/ml hIL-2 (NCI Clinical Repository; Rockville, MD), and 100 nM Retinoic Acid (Sigma; St. Louis, MO). Cells were then cultured for 2 days in a humidified 37°C 5% CO_2 incubator.

For retroviral transduction, a retroviral construct Retro.Luci.Thy1.1 containing the congenic marker Thy1.1 and a codon-optimized firefly luciferase gene (Rabinovich et al., 2008) was utilized. Virus was added at a Multiplicity of Infection (MOI) of 5 directly to day 2 cultured Treg cells in the presence of 0.2 ul/ml polybrene (Sigma; St. Louis, MO) and 2 ul/ml Lipofectamine 2000 (Invitrogen; Carlsbad, CA) and mixed thoroughly by gently swirling plates. Cells were then incubated with virus for a total of 3 hours in a humidified 37°C 5% CO_2 incubator with gentle swirling of plates every 30 minutes.

Following transduction (or for cultures not transduced), 30 ml additional pre-warmed Treg media was added and the culture continued for a total of 6 or 7 days. Cells were harvested, washed in ice-cold PBS, counted, and stored at 4°C in CTL media until ready for use. Cells were analyzed for purity using FACS analysis for Foxp3, CD4, and CD25. Purity usually exceeded 75% Foxp3+ CD4+ CD25+. For transduced cultures, cells were also analyzed for Thy1.1 expression to determine transduction efficiency, which was typically 5-10%. Prior to adoptive transfer, cells were washed 3 times in ice-cold PBS, counted, and diluted as needed.

In the second method of Treg culture, C57BL/6 OTII+/- Thy1.1+/- Foxp3-GFP+/y splenocytes were harvested into single cell suspension and subjected to RBC lysis as above. RBC-free splenocytes were then enumerated and seeded at 1E6 splenocytes/ml in 50 ml Treg media into at T162 flask (Corning; Tewksbury, MA). 2 ug/ml OVAII peptide (Genscript; Piscataway, NJ) was added to each flask and the cells

cultured upright for 4 days. On day 4, an additional 50 ml of pre-warmed Treg media was added and the flasks were laid down for an additional day of culture. On day 5, an additional 20 ml of pre-warmed CTL media containing 500 U/ml hIL-2 was added and the cells cultured a final day. On day 6 cells were harvested, washed with ice-cold PBS, and FACS sorted for CD4+ Foxp3-GFP+ on a BD FACSAria™ (BD Biosciences; San Jose, CA) to a final purity of >98%. Following sorting, cells were stored in CTL at 4°C until ready for use. Prior to adoptive transfer, cells were washed 3 times in ice-cold PBS, counted, and diluted as needed.

5.2.5 Tumor Challenge and Treatment

A fresh vial of tumor cells was thawed for each challenge experiment and grown for approximately 7 days with harvest at approximately 70% confluency to ensure exponential growth. For challenge, cells were harvested from adherent culture flasks using 0.25% trypsin-EDTA (Gibco; Carlsbad, CA) and washed in ice-cold CTL media. Cells were washed 3 times in ice-cold PBS, counted, and diluted to 1E6 cells/ml in ice-cold PBS. Mice were then challenged subcutaneously with 1E5 tumor cells in the previously shaved right flank on day 0. On day 6, mice were transferred to fresh clean caging and provided with water containing trimethoprim/sulfamethoxazole (Sulfatrim; dosed for 95 mg/kg/24hr; obtained from the Johns Hopkins Hospital pharmacy) in preparation for irradiation. On day 7, mice were irradiated at 500 Rads whole body irradiation and then adoptively transferred via tail vein injection with OTI Tc0 and/or OTII Tregs. Tumor size was then determined with cross-sectional caliper measurement

once or twice weekly. Mice were sacrificed at the first sign of suffering or for timed explant sampling as indicated.

5.2.6 *In Vivo* Bioluminescent Imaging

D-Luciferin (Perkin-Elmer; Waltham, MA) was prepared fresh at 15 mg/ml in PBS, sterile filtered using a 0.22 um syringe filter, and stored on ice in the dark prior to injection. Mice were given 200 ul intraperitoneal (i.p.) injection of D-Luciferin to provide an approximate dose of 150 mg/kg. They were then anesthetized using isoflurane in preparation for imaging. Imaging was performed 10 minutes after injection of D-Luciferin in order to optimize light signal per the manufacturer's protocol. Mice were imaged using the IVIS Spectrum (Perkin-Elmer; Waltham, MA) *in vivo* imaging system under real-time isoflurane anesthesia.

To ensure signal accuracy, the longest exposure without pixel saturation was utilized. No more than 5 mice were imaged at a single time to minimize signal bleed. To maximize signal sensitivity, the smallest imaging field that could fit all samples was utilized. For groups demonstrating wide mouse-to-mouse variability, mice bearing large signal intensity were imaged and removed to allow reimaging and uncovering of lower-intensity signals. Image data was acquired and analyzed using Living Image™ software (Perkin-Elmer; Waltham, MA). Regions of Interest (ROIs) were generated based upon a 2% maximum pixel signal threshold within each image, and data expressed as Radiance (photons/s/cm^2) in order to control for variability in exposure times used. Mice were imaged once or twice weekly, and never more than every other day to avoid anesthesia-induced failure to thrive.

5.2.7 *In Vivo* CTL Kill Assay

C57BL/6 CD45.1+/+ donor mice were sacrificed and spleens harvested for use as target cells. RBC-free, single cell suspensions were then prepared as described previously. Splenocytes were counted, seeded at 10E6 cells/ml in warmed CTL media with or without 1 ug/ml OVAI peptide (Genscript; Piscataway, NJ) into culture flasks, and incubated 2 hours at 37°C in a humidified 5% CO_2 incubator for peptide loading. Cells were transferred to 50 ml conical tubes and washed with warmed PBS. Cell pellets were then thoroughly resuspended in 1 uM (OVAI targets) or 0.1 uM (unlabeled targets) Carboxyfluorescein Succinimidyl Ester (CFSE)(Invitrogen; Carlsbad, CA) and incubated for 20 minutes in a light-protected 37°C water bath. CFSE labeling was then quenched with ice-fold FBS for 5 minutes on ice and cells washed twice with ice-cold PBS and counted. Peptide loaded (CFSE high) and non-loaded (CFSE low) cells were then mixed 1:1 for a total cell count of 50E6 cells/ml and stored on ice in the dark prior to injection. Recipient mice were i.v. injected with 200 ul target mix via tail vein. Extra cells were stored overnight at 4°C in CTL for use as FACS controls. Recipients were sacrificed and harvested approximately 18 hours later for analysis of target cell killing via flow cytometry. % Lysis was defined as being equal to (1-(target/non-target))x100.

5.2.8 *Ex Vivo* Lymphocyte Isolation and Stimulation

Tumor-bearing mice were sacrificed and spleens, lymph nodes, and tumors harvested into ice-cold CTL media. RBC-free, single cell suspensions of spleens and LNs were prepared as outlined previously. Given the large volume of necrotic debris, tumor tissue samples required more elaborate processing. Single cell tumor suspensions

were prepared by crushing tissue through a 100 um cell strainer (BD Biosciences; San Jose, CA). Cells were then washed with ice-cold RPMI and spun at 1000 RPM, leaving smaller dead cell fragments in the supernatant. This step was repeated until the supernatant was grossly clear of pigmented debris. RBC lysis was then performed using ACK lysis (Gibco; Carlsbad, CA). Dead cell removal was then further performed using one or two rounds of ficoll-paque (GE Life Sciences; Piscataway, NJ) separation. Cells were counted and stored in ice-cold CTL media until ready for FACS staining or *in vitro* stimulation.

For *in vitro* stimulation, 1E6 explant cells were seeded in 1 ml CTL media in a 24-well flat bottom plate (Corning; Tewksbury, MA). 2 ug/ml OVAI peptide (Genscript; Piscataway, NJ) was then seeded into test wells along with 1 ul/ml GolgiPlug™ (brefeldin A) (BD Biosciences; San Jose, CA). Negative controls received GolgiPlug™ without OVAI peptide, and positive controls were treated with 2 ul/ml Leukocyte Activation Cocktail containing PMA/ionomycin and GolgiPlug™ (BD Biosciences; San Jose, CA). Cells were then incubated overnight (~16 hours) at 37°C in a humidified 5% CO_2 incubator. The following morning, cells were harvested and analyzed via flow cytometry.

5.2.9 Antibodies and Flow Cytometry

I-A^b-FITC (clone AF6-120.1), I-E^k-FITC (clone 14-4-4S), H-2K^b-FITC (clone AF6-88.5), H-2D^d-FITC (clone 34-2-12), CD25-PE (clone PC61), CD4-APC (clone RM4-5), CD8-PE and CD8-A700 (clone 53-6.7), Thy1.1-PerCP (clone OX-7), Thy1.2-FITC (clone 30-H12), TNF-APC (clone MP6-XT22), CD44-V500 (clone IM7), Ki67-

PerCP-Cy5.5 (clone B56), and IFNγ-PE (clone XMG1.2) were purchased from BD Biosciences (San Jose, CA). PD-L1-BrilliantViolet™421 (clone 10F.9G2), Galectin-9-PE (clone 108A2), CD127-APC (clone A7R34), PD-1-BrilliantViolet™421 (clone 29F.1A12), IL-17a-PacificBlue™ (clone TC11-18H10.1), and TIM-3-PE (clone RMT3-23) were purchased from BioLegend (San Diego, CA). Thy1.1-APC-eFluor™780 (clone HIS51), CD62L-PerCP-Cy5.5 (clone MEL-14), KLRG-1-PE-Cy7 (clone 2F1), IL-2-PE-Cy7 (clone JES6-SH4), Foxp3-FITC (clone FJK-16s), and LAG-3-PE (clone C9B7W) were purchased from eBioscience (San Diego, CA). CD4-PE-TexasRed® (clone RM4-5) was purchased from Invitrogen (Camarillo, CA). All antibodies were titrated for optimal staining intensity vs. background signal for 1E6 cells/reaction. All isotype control antibodies were from the same manufacturer and used at the same concentration as their associated test antibody.

Qdot®625-"tetramer" specific for OTI CD8 cells was prepared in house. Monomer of H-2K^b coupled with the chicken ovalbumin peptide 257-264 SIINFEKL were prepared by the NIH Tetramer Core Facility (Atlanta, GA) and stored at -80°C until ready for tetramerization. For tetramerization, a 25 ul aliquot of approximately 2 ug/ml monomer stock was thawed on ice and diluted to a total volume of 100 ul with sterile 1X PBS. 20 ul of Qdot®625-Streptavidin (Invitrogen; Camarillo, CA) was then added to the monomer, mixed thoroughly, and allowed to incubate on ice in the dark for 20 minutes. This step was repeated a total of 4 times to yield a final solution of 200 ul tetramer at 0.225 ug/ml concentration. Formed tetramer was titrated using RAG-/- OTI+/+ splenocytes and stored at 4°C until use. All formed tetramers were used within one month of preparation. It should be noted that this is in fact not a true tetramer, as each

Qdot® has between 5 and 10 streptavidin molecules bound to it, each of which can bind up to 4 monomers. Thus, the end molecule is a large multimer and not a true tetramer.

For all extracellular antibody staining, 1E6 cells were washed with FACS buffer containing 1X Hanks Balanced Salt Solution (HBSS), 10 mM HEPES buffer, 2% FBS, and 0.1% sodium azide and stained with appropriate antibody for 15 minutes at room temperature in the dark followed by two washings with FACS buffer. No more than 5 antibodies were stained at a single time. Cells were similarly washed for tetramer staining but were incubated for 30 minutes. Viability staining using LIVE/DEAD® Yellow and Aqua Fixable Dead Cell Stain Kit (Invitrogen; Camarillo, CA) was performed according to the manufacturer's instructions at a 1:2000 dilution with a 30 minute room temperature incubation and washing steps using PBS. Cellular fixation/permeabilization was performed using the Foxp3 Staining Buffer Set (eBioscience; San Diego, CA) according to manufacturer instructions with fixation performed for 45 minutes at 4°C in the dark. Subsequent intracellular staining was performed for 30 minutes at 4°C in the dark with washes using the staining buffer set. For multi-step staining sequences, the following sequence was always followed: Tetramer, extracellular antibody, Live/Dead stain, fixation/permeabiliation, intracellular stain. Following staining, cells were stored in FACS buffer at 4°C in the dark and were analyzed within 24 hours of staining.

Flow cytometry was performed on the BD FACSCaliber™, FACSAria™, or LSRII™ with data acquisition using CellQuest Pro™ or FACSDiva™ (BD Biosciences; San Jose, CA). Data analysis was further performed with FACSDiva™ as well as FlowJo (Tree Star Inc.; Ashland, OR).

5.2.10 Histology

Mice were sacrificed and tumors, spleens, and lymph nodes (LN) harvested into ice-cold CTL media. Tissues were then blotted to remove excess CTL and transferred to Intermediate Tissue-Tek CryoMolds (Sakura Finetek; Torrance, CA) containing a small layer of Optimal Cutting Temperature (OCT) media (Sakura Finetek; Torrance, CA) and subsequently covered with OCT media. Tissue chambers were then flash-frozen in a beaker of liquid nitrogen-cooled isopentane (Sigma; St. Louis, MO). Once fully frozen, samples were transferred on dry ice to a -80°C freezer for storage prior to cryosectioning. Tissue was subsequently cryosectioned at 5 um sections onto "Plus" slides, fixed in ice-cold acetone for 10 minutes, and air dried for 30 minutes by the Johns Hopkins Histology Core. Following sectioning and fixation, slides were stored in a -80°C freezer until stained.

Primary antibodies used for staining included: I-A^b-biotin (clone AF6-120.1; Ms IgG2a), CD45.1-FITC (clone A20; Ms IgG2a), and Thy1.1-APC (clone OX-7; Ms IgG1) (BD Biosciences; San Jose, CA). All isotype controls were used at the same concentration and were from the same supplier as the test antibody. Fluorescein/Oregon Green® Rabbit IgG Antibody (Invitrogen; Camarillo, CA) was used as a secondary antibody to increase primary antibody-FITC signal. Goat anti-Rabbit AlexaFluor®488 (Invitrogen; Camarillo, CA) and Stretavidin-Cy3 (Sigma; St. Louis, MO) were used for tertiary staining.

For staining, slides were allowed to warm to room temperature for 5 minutes in a laminar flow hood and then tissue demarcated with an ImmunEdge Pen (Vector Labs; Burlingame, CA) prior to rehydration with PBS for 10 minutes at room temperature. All

subsequent staining and blocking steps were performed in a light-protected, humidified chamber with three PBS washes between steps. Samples were first treated with 1-2 drops Molecular Probes Endogenous Biotin Blocking Kit (Invitrogen; Camarillo, CA) solutions A and B for 30 minutes each at room temperature. They were then covered with 100 ul isotype-control blocking antibodies at 10 ug/ml in Blocking Buffer (2% IgG-free BSA and 5% normal mouse serum (Jackson Immunoresearch; West Grove, PA) in PBS) for 1 hour at room temperature. This blocking solution was then shaken off without PBS wash and replaced with primary antibodies at 10 ug/ml in Blocking Buffer and incubated overnight at 4°C. Slides were then incubated with 100 ul of 2 ug/ml secondary antibody in PBS/2%BSA for 1 hour at room temperature, washed, and incubated with 100 ul of tertiary antibodies diluted 1:100 in PBS/2%BSA for 1 hour at room temperature. Nuclei were then counterstained with Hoechst 33342 (Invitrogen; Camarillo, CA) diluted 1:50,000 in PBS for 15 minutes at room temperature. Following PBS wash, slides were fixed and mounted using a single drop of Aqua Poly/Mount (Polysciences; Warrington, PA) and cover slips placed and immobilized with nail polish. Slides were then stored face-up in light-protected slide boxes at 4°C until imaging.

Imaging was performed using a Nikon E800 fluorescent microscope using standard DAPI, FITC, Cy3, and Cy5 filter sets. Image acquisition and analysis was performed using Nikon Elements Software (Nikon Metrology; Brighton, MI).

5.2.11 OTII Th1 T-Cell Culture

C57BL/6 OTII+/- Thy1.1+/- Foxp3-GFP+/y splenocytes were harvested into single cell suspension and subjected to RBC lysis as above. RBC-free splenocytes were

then enumerated and seeded at 1E6 splenocytes/ml in 40 ml 'Th1 media' (CTL containing 10 ng/ml IL-12, 10 ng/ml IFNγ (Peprotech; Rocky Hill, NJ), 2 U/ml hIL-2, and 2 ug/ml anti-IL-4 (NCI Clinical Repository; Rockville, MD)) into a T162 flask (Corning; Tewksbury, MA). 2 ug/ml OVAII peptide (Genscript; Piscataway, NJ) was added to each flask and the cells cultured upright for 4 days. On day 4, an additional 40 ml of pre-warmed Th1 media was added and the flasks were laid down for an additional day of culture. On day 5, an additional 20 ml of pre-warmed CTL media containing 2 U/ml hIL-2 was added and the cells cultured a final day. On day 6 cells were harvested, washed with ice-cold PBS, and FACS sorted for CD4+ Foxp3-GFP- on a BD FACSAria™ (BD Biosciences; San Jose, CA) to a final purity of >98%. Following sorting, cells were stored in CTL at 4°C until ready for use.

5.2.12 *In Vitro* Direct Tumor Recognition

B16 tumor variants were grown for three days in the presence or absence of 100 U/ml IFNγ (Peprotech; Rocky Hill, NJ) and 5E5 cells seeded in 500 ul CTL media into 24-well flat-bottom plates (Corning; Tewksbury, MA). 1E6 *in vitro* polarized, sorted OTII Th1 cells were added to each well for a total volume of 1 ml CTL. 2 ug/ml OVAII peptide (Genscript; Piscataway, NJ) was added to tumor-containing wells as an antigen positive control, as well as to wells containing only Th1 cells to verify absence of MHCII in our sorted Th1 cells. 1 ul/ml GolgiPlug™ was added to all tumor-stimulated wells, and 2 ul/ml Leukocyte Activation Cocktail containing PMA/ionomycin and GolgiPlug™ (BD Biosciences; San Jose, CA) was used as a positive control for Th1 cytokine staining.

Cells were incubated for 6 hours at 37°C in a humidified 5% CO_2 incubator, harvested, and analyzed for cytokine expression via flow cytometry.

5.3 Results

5.3.1 Failed Tumor Suppression with B16 Variants

In our first series of studies, we developed a model in which OTII Tregs were capable of suppressing treatment of the MHCII-inducible B16.mOVA tumor line by OTI CD8+ in MHCII KO mice (Figure 3.5). Based upon those findings, we had hypothesized that by altering the expression pattern of MHCII within the tumor, we would also alter the suppressive pattern demonstrated by our Tregs. To accomplish this goal, we had set out to create B16.mOVA variants that demonstrated constitutive and non-inducible MHCII expression, which were successfully created in the form of the MHCII-constitutive line B16.mOVA.CIITA and the MHCII-non-inducible B16-F10-D.mOVA as previously described and characterized in Chapter 3. With those tools now in hand and validated, and with a better understanding of out OTI treatment system, we set out to examine the implications of variable MHCII expression upon the ability of OTII Tregs to suppress the treatment effect of OTI CD8+. As modeled in Figure 5.1, we hypothesized that the constitutive expression of MHCII in our B16.mOVA.CIITA line would result in improved Treg suppression (orange curve) relative to our inducible variant B16.mOVA (blue curve), whereas non-inducible MHCII expression by our B16-F10-D.mOVA line would result in little to no detectable suppression (yellow curve).

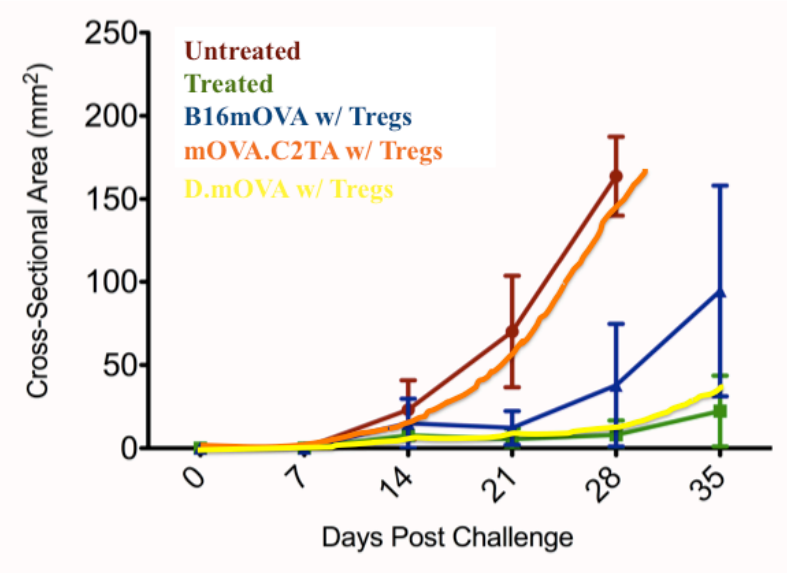

Figure 5.1 Hypothesized effect of variable MHCII expression upon suppression of OTI CD8+ by OTII Tregs.

Thus, recipient C57BL/6 MHCII KO mice were challenged subcutaneously with 1E5 B16.mOVA, B16.mOVA.CIITA, or B16-F10-D.mOVA tumor on day 0 and treated on day 7 with 500 Rads non-myeloablative whole body irradiation followed by adoptive transfer of 2.5E6 OTI Tc0 cells with or without co-administration of 7.5E6 OTII Tregs. Tumors were then measured at weekly intervals using cross-sectional caliper measurements. As shown in Figure 5.2, OTII Tregs failed to demonstrate suppression in any of the three tumor systems. This failure within the B16.mOVA system was in contrast to results previously obtained. Complicating this result further was the observation that the treatment effect of OTI CD8+ within each of the tumor lines was quite different. While these lines had previously been grown and treated *in vivo* as part of their creation and validation, they had not previously been done so in the same experiment to allow for direct comparison. Also evident within this figure is the wide range of tumor sizes in some groups as evidenced by the large standard deviation bars shown, further complicating the evaluation of this data.

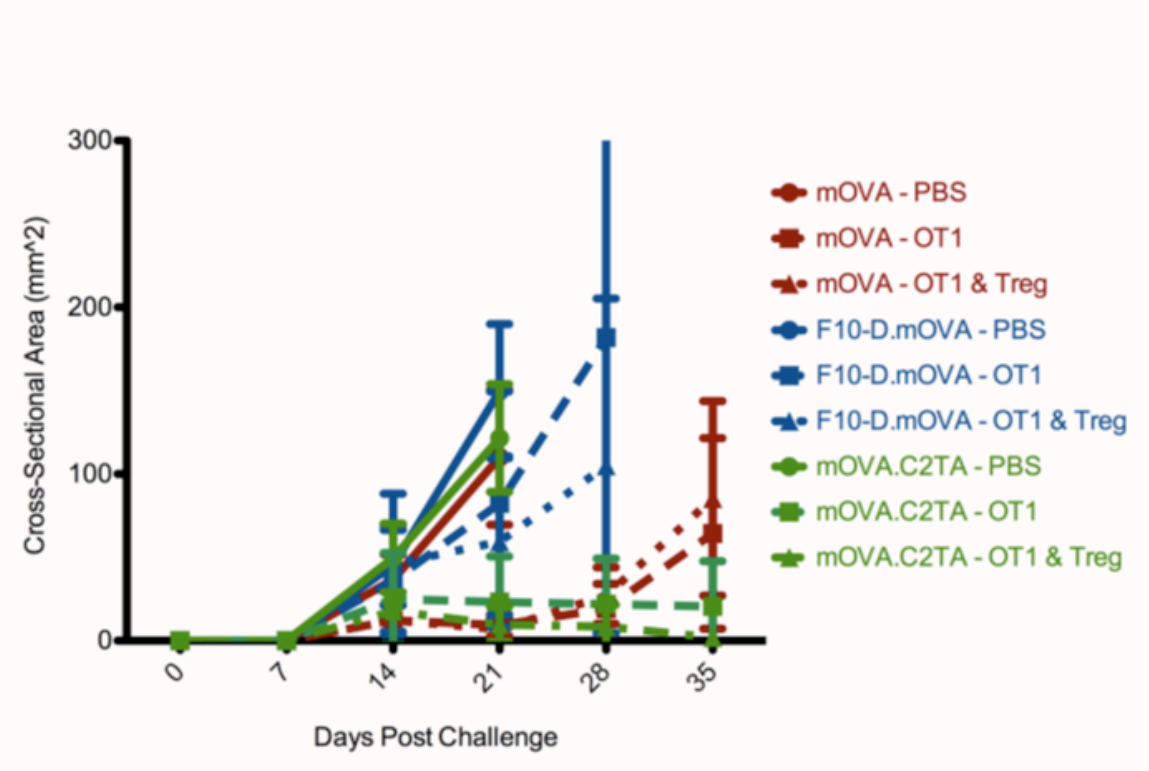

Figure 5.2 OTII Tregs fail to suppress treatment of B16.mOVA variants by OTI CD8+ in MHCII KO mice.

C57BL/6 MHCII KO mice were challenged with 1E5 B16.mOVA, B16.mOVA.CIITA, or B16-F10-D.mOVA tumor on day 0 and treated on day 7 with 500 Rads non-myeloablative whole body irradiation followed by adoptive transfer of 2.5E6 OTI cells with or without co-administration of 7.5E6 OTII Tregs. Tumors were then measured at weekly intervals using cross-sectional caliper measurements. Mean +/- Standard Deviation for 5 mice per group are shown.

5.3.2 Lack of Treg Accumulation within the Tumor

Having failed to demonstrate any suppression with our B16.mOVA variants, we next sought to examine the activity of our Tregs *in vivo*. We first examined the trafficking of our Tregs in a manner similar to that done previously for our OTI CD8+. Recipient MHCII KO mice were challenged with 1E5 B16.mOVA, B16.mOVA.CIITA, B16-F10D.mOVA, or parental non-OVA-expressing B16-F10 on day 0 and treated on day 7 with 500 Rads non-myeloablative whole body irradiation followed by adoptive transfer of 7.5E6 OTII Tregs bearing the luciferase enzyme via *in vitro* transduction with a retroviral luciferase construct with or without co-administration of 2.5E6 OTI cells. Bioluminescent imaging (BLI) was then performed twice weekly to detect the location of OTII Tregs via activity of the luciferase enzyme. As shown in Figure 5.3, OTII Tregs were detected in the area surrounding the tumor as early as the first day post transfer (day 8), but unlike the accumulation seen for OTI cells, the OTII Tregs demonstrated a steady decline of signal in the area of the tumor. Also unlike the OTI cells, the OTII cells appeared to never perfectly co-localize with the tumor, but rather were persistently found in the tissue immediately surrounding the tumor mass. This accumulation by Tregs within the tumor surroundings appeared to be antigen non-specific and independent of MHCII expression, as OTII cells were found with equal intensity in OTI-treated or untreated tumors as well as in non OVA-bearing B16-F10 tumors.

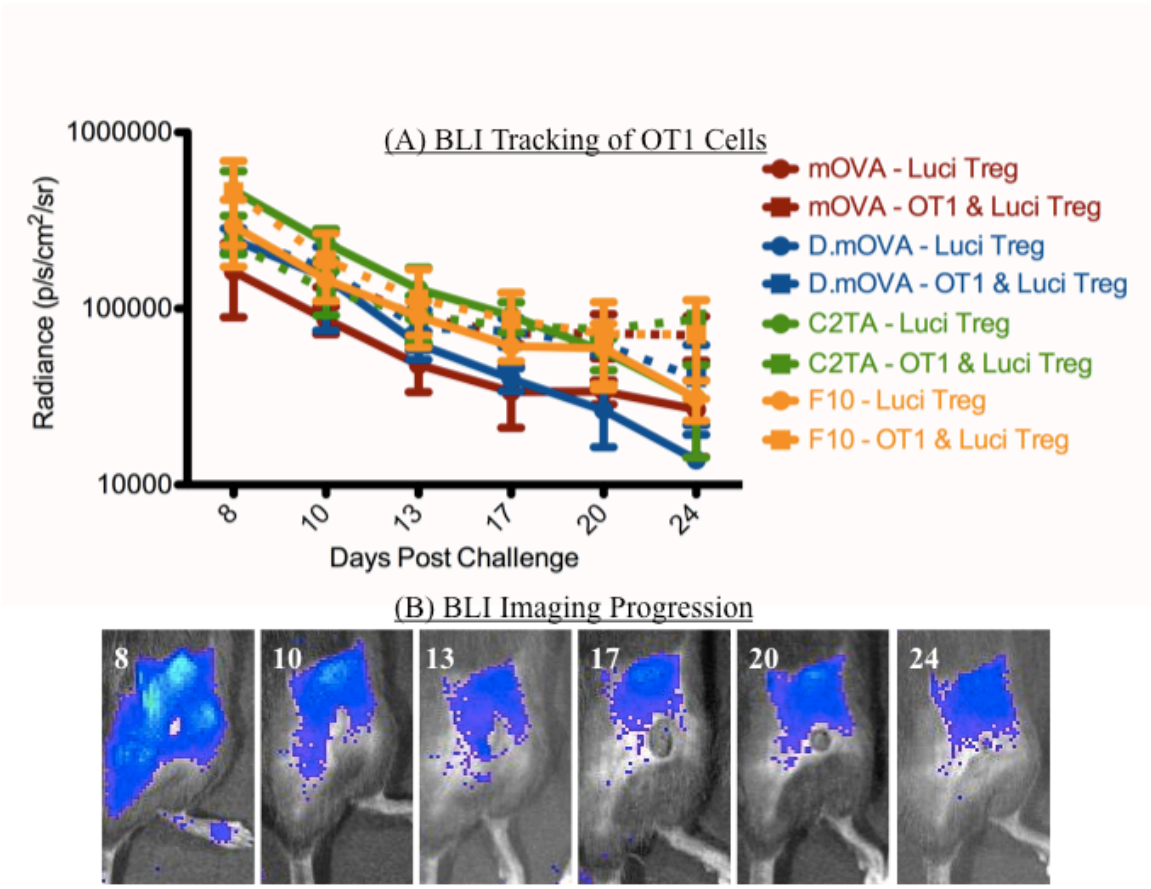

Figure 5.3 OTII Tregs demonstrate an MHCII-independent, antigen non-specific and fading accumulation around, but not within B16 tumor variants.

C57BL/6 MHCII KO mice were challenged with 1E5 B16.mOVA, B16.mOVA.CIITA, B16-F10D.mOVA, or parental non-OVA-expressing B16-F10 on day 0 and treated on day 7 with 500 Rads non-myeloablative whole body irradiation followed by adoptive transfer of 7.5E6 OTII Luci+ Tregs with or without co-administration of 2.5E6 OTI cells. Mice were imaged twice weekly to detect the location of OTII cells. Mean +/- Standard Deviation for groups of 3 mice are shown. (A) BLI of mice over the course of tumor progression. (B) Representative BLI images of a single mouse over time with experiment day indicated in the upper left corner for each image.

To verify the results from our BLI data, we next sought to examine the tumors histologically for the presence of OTII Tregs. MHCII KO recipients were challenged with B16.mOVA and treated as before with OTI CD8+ and OTII+/- Thy1.1+/- Foxp3-GFP+/y mice as Treg donors. Mice were sacrificed one week after treatment and tumor masses harvested and processed for histologic evaluation of MHCII and the congenic marker Thy1.1 expressed only by OTII Tregs. These slides demonstrated a complete absence of Tregs within the tumor mass, even in areas with high MHCII expression (data not shown), validating the findings from our BLI data suggesting that Tregs were in fact not migrating into and accumulating within the actual tumor mass.

With our BLI and histologic data suggesting that our Tregs were not accumulating within the tumor mass, we next set out to determine if they were persisting in other tissues, namely spleens and tumor-draining lymph nodes (DLN). MHCII KO recipient mice were again challenged with B16mOVA and treated as above using OTI CD8+ and OTII+/- Thy1.1+/- Foxp3-GFP+/y Tregs. Mice were sacrificed and spleens, DLNs, and tumors harvested for explant analysis at weekly intervals via flow cytometric analysis. As shown in Figure 5.4, OTII Tregs were successfully identified via CD4+ Thy1.1+ staining, and the vast majority of these cells maintained Foxp3 expression. OTII cells persisted and maintained Foxp3 expression throughout the course of tumor progression, although their total numbers were consistently far lower than those seen for our OTI cells in prior studies. Also, significant numbers of Tregs could not be identified within TIL samples (data not shown), further supporting their absence in tumor tissue.

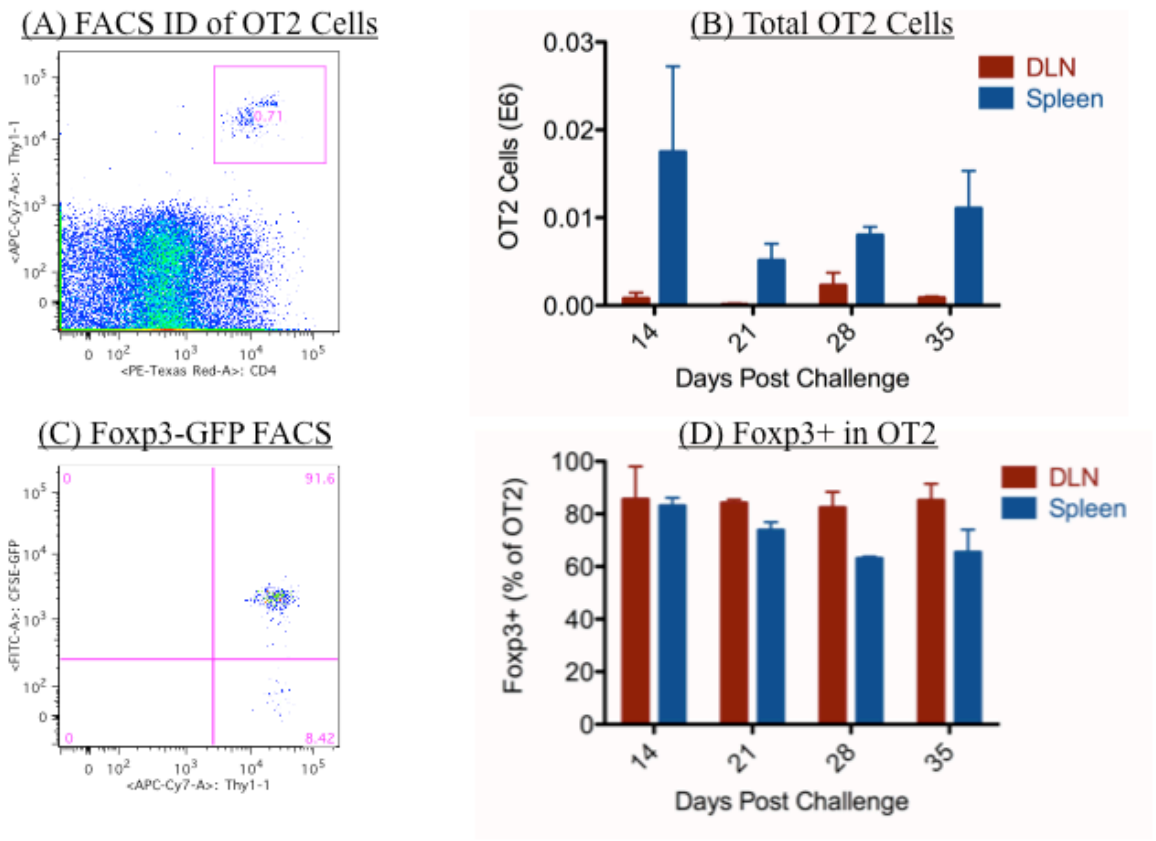

Figure 5.4 OTII cells persist and maintain Foxp3 expression within B16.mOVA tumor-bearing mice.

C57BL/6 MHCII KO mice were challenged with 1E5 B16.mOVA tumor on day 0 and treated on day 7 with 500 Rads non-myeloablative whole body irradiation followed by adoptive transfer of 2.5E6 OTI and 7.5E6 OTII Tregs. Mice were sacrificed at weekly intervals and spleens, tumor-draining lymph nodes, and tumors harvested. Single cell suspensions were prepared from explanted tissue and subjected to flow cytometric analysis of live cells as determined by scatter profiles and live/dead cell stain. OTII cells were identified by expression of CD4+ and Thy1.1 (A) and total numbers enumerated in (B). Foxp3 expression within OTII cells was verified as in (C) and quantified (D). Mean +/- Standard Deviation for 3-5 mice per group are shown.

5.3.3 Tregs Fail to Alter OTI CD8+ Phenotype

Having demonstrated persistence of OTII Tregs within spleens and DLNs despite their absence in tumors and failed suppression of tumor immune rejection, we next examined whether the phenotype of our OTI cells was altered by the presence of OTII Tregs. To perform this analysis, we in essence repeated the studies previously described in Chapter 4 with inclusion of OTII Tregs alongside our OTI treatment only groups. Recipient MHCII KO mice were challenged and treated as before with or without addition of OTII Tregs. To analyze the trafficking and accumulation of OTI cells within the tumor, OTI+/- Luci+/- CD8+ were used along with OTII Tregs with imaging performed every other day following adoptive transfer. These studies, as shown in Figure 5.5(A), showed that Tregs failed to significant alter the trafficking to or accumulation within B16.mOVA tumors by Luci-expressing OTI CD8+. Similarly, analysis of total OTI CD8+ numbers via flow cytometric analysis of explanted spleen and DLN tissues revealed no difference in total OTI CD8+ numbers with administration of OTII Tregs as shown in Figure 5.5(B).

Assessment of OTI CD8+ effector phenotype was similarly examined with inclusion of OTII Tregs along with OTI CD8+. As shown in Figure 5.5(C), levels of IFNγ expression were not altered with addition of OTII Tregs. TNFα expression levels were also unchanged (data not shown). Similarly, evaluation of OTI CD8+ cell surface phenotype was performed and demonstrated no changes in CD44/CD62L, CD127/KLRG-1, or PD-1/LAG-3/TIM-3 expression levels upon OTI CD8+ when OTII Tregs were included (data not shown). Finally, evaluation of the *in vivo* cytotoxicity of our OTI CD8+ was examined in the presence of OTII Tregs as performed previously. As

shown in Figure 5.5(D), these data showed no decrease in *in vivo* CTL activity of our OTI CD8+ in the presence of OTII Tregs.

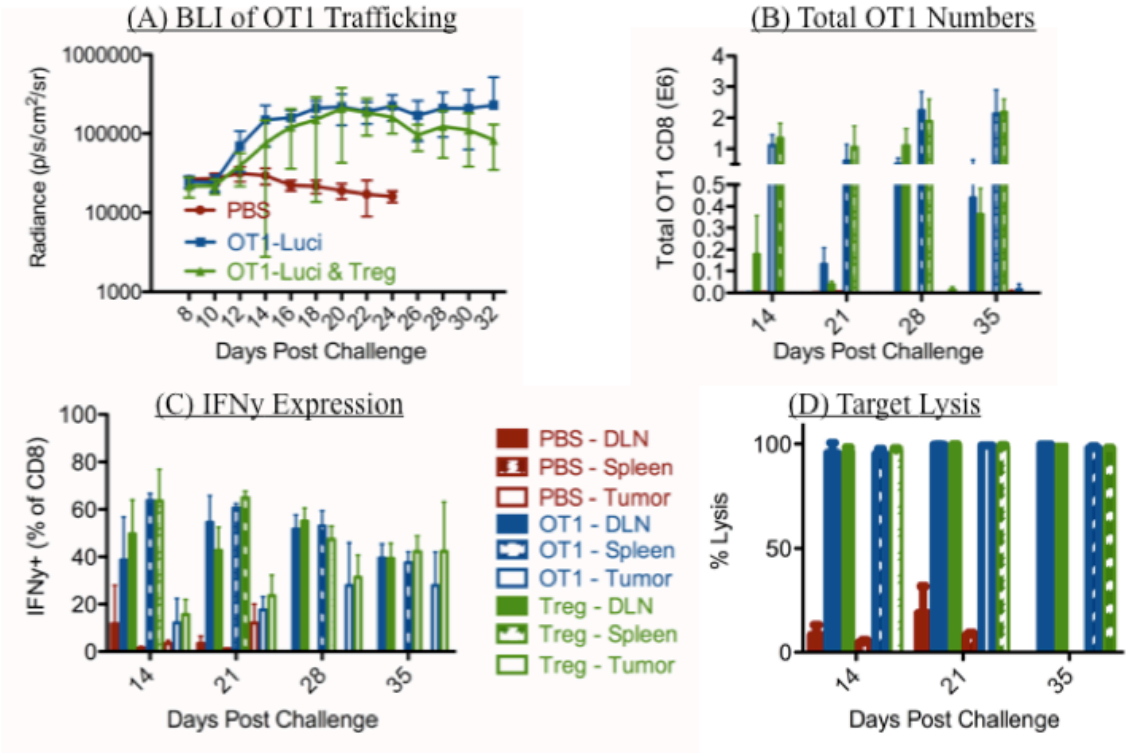

Figure 5.5 OTII Tregs do not alter the phenotype of OTI CD8+ in tumor-bearing mice.

C57BL/6 MHCII KO mice were challenged with 1E5 B16.mOVA tumor on day 0 and treated on day 7 with 500 Rads non-myeloablative whole body irradiation followed by adoptive transfer of 2.5E6 OTI and 7.5E6 OTII Tregs. Mean +/- Standard Deviation for 3-5 mice per group are shown. (A) BLI was performed every other day to analyze *in vivo* trafficking of OTI+/- Luci+/- CD8+ cells in the presence or absence of OTII Tregs. (B) Weekly explants of spleens and DLNs were assessed for total OTI CD8+ cells via FACS analysis using CD8 and OVAI-specific tetramer. (C) Weekly explants of spleens, DLN, and TILs were subjected to *in vitro* stimulation with OVAI peptide and analyzed for expression of IFNγ by CD8+ cells. (D) Tumor-bearing mice were given adoptive transfer of a 1:1 mix of $CFSE^{high}$ OVAI peptide-loaded and $CFSE^{low}$ non peptide-loaded target

splenocytes and evaluated for killing effect 16 hours later by assessing for target populations in recipient spleens and tumor-draining lymph nodes. % Lysis was defined as being equal to (1-(target/non-target))x100.

5.3.4 OTII Th1 Do Not Recognize B16 Variants

Given the failure of our OTII Tregs to alter the phenotype of our OTI CD8+ cells as well as their inability to suppress OTI CD8-mediated tumor treatment, we decided to take a step back and evaluate the interaction between our OTII cells and tumor cells *in vitro*. Specifically, we sought to assess whether our tumor cells were capable of directly presenting OVAII antigen to our OTII cells. To accomplish this, tumor cells were cultured for 72 hours with and without 100 U/ml IFNγ and then cocultured for 6 hours with *in vitro* polarized OTII Th1 cells with or without addition of exogenous OVAII peptide. Th1 cells were then harvested and analyzed via intracellular cytokine staining for production of IFNγ, TNFα, and IL-2. As shown in Figure 5.6, OTII Th1 displayed cytokine production only when exogenous OVAII peptide was added to tumors that had previously been shown to express MHCII (B16.mOVA and B16.mOVA.CIITA treated with IFNγ, and B16.mOVA.CIITA without IFNγ treatment). Importantly, despite the presence of MHCII (previously shown and verified again here; data not shown) none of these OVA-containing tumors was able to present endogenously-contained OVA antigen to OTII Th1 cells.

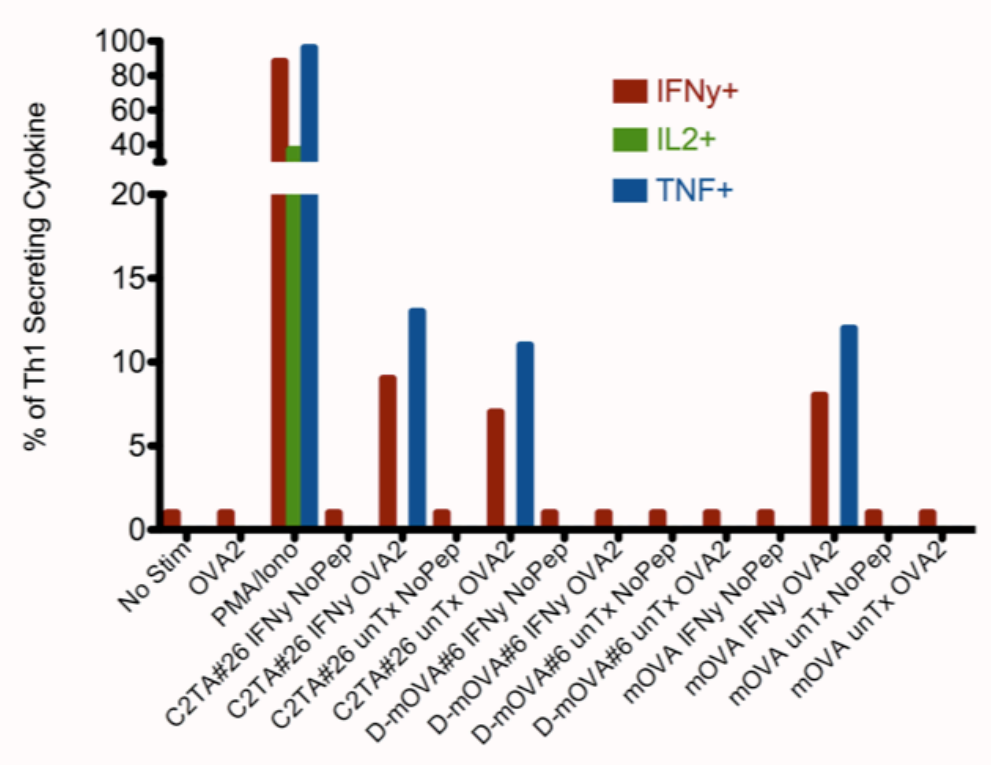

Figure 5.6 B16.mOVA variants fail to directly present endogenous OVA but can present exogenous OVAII peptide to OTII Th1 cells *in vitro*.

OVA-containing B16 tumor lines B16-F10-D.mOVA, B16.mOVA, and B16.mOVA.CIITA were cultured for 72 hours with or without 100 U/ml IFNγ and then cocultured for 6 hours with *in vitro* polarized, sorted OTII Th1 cells with or without addition of 2 ug/ml exogenous OVAII peptide as indicated. Following coculture, Th1 cells were harvested and analyzed for cytokine production via intracellular cytokine staining and flow cytometry.

5.4 Discussion

In this third study we sought to expand upon the findings from our first two studies to explore the implications of variable tumor MHCII expression upon Treg suppression along with evaluating the phenotype of suppressed CD8+ cells in our model as a means of understanding the potential suppressive mechanisms utilized. Unfortunately, despite our results in the first study, which had indicated a suppressive effect of OTII Tregs upon OTI CD8+ in MHCII KO mice, we were unable to replicate these findings when all three tumor lines were utilized. The cause for this failure, particularly for the B16.mOVA line, left us largely at a loss for explanation given that none of our reagents or protocols had changed.

Closer assessment of each of the tumor curves revealed that each of our three tumor variants grew at comparable rates when untreated, but demonstrated widely variable treatment responses even without Treg inclusion. The B16-F10-D.mOVA line demonstrated the least treatment response while the B16.mOVA.CIITA line demonstrated the greatest and most durable treatment response. We had previously demonstrated that B16.mOVA.CIITA was the only tumor of the three evaluated that expressed baseline MHCII as well as MHCI (Figure 3.6), owing likely to the fact that CIITA has been shown to play a minor role in MHCI expression (Holling et al., 2006; LeibundGut-Landmann et al., 2004). This prolonged availability of MHCI expression may explain the increased treatment effect seen for the B16.mOVA.CIITA tumor. As to why the B16-F10-D.mOVA line responded less to treatment can only be speculated at, but given that this particular B16-F10 line was a different derivative than our other

B16.mOVA variants, may represent the previously described variability displayed by B16-F10 derivative lines (Overwijk and Restifo, 2001).

Given the complexity of our experimental design, including use of multiple tumor lines, multiple adoptively transferred TCR-transgenic cell populations, and the use of a number of genetically engineered and inbred mice, we considered it entirely possible that the failure of suppression of tumor growth reflected not a failure of Treg function, but rather perhaps was due to the numerous variables in our system not aligning appropriately and making consistent results difficult. This seemed particularly plausible given that we had previously shown suppression in our first studies. Therefore, while suppression of tumor rejection was our main and idealized result, it was not the only method we had to determine if our Tregs were in fact suppressing OTI CD8+.

To this end, we first chose to evaluate the trafficking and accumulation of our OTII Tregs in a manner similar to what had previously been performed for our OTI CD8+ cells. MHCII KO mice were challenged with our three OVA-expressing B16 variants as well as the parental B16-F10 non-OVA-expressing line and then given adoptive transfer of OTII Luci+ Tregs with or without OTI CD8+. Our results here demonstrated an early trafficking of Treg cells to what appeared to be the peri-tumoral tissue with lack of penetration into the primary tumor mass. These results further demonstrated a persistent decline of Treg signal over the course of tumor growth, and what's more failed to demonstrate a separation of any of the treatment groups. This lack of separation of groups was of particular concern. Trafficking to the non-OVA-expressing B16-F10 group suggested a lack of antigen-dependence. Further trafficking to the Treg only B16.mOVA group as well as to either of the B16-F10-D.mOVA groups

suggested that MHCII was not involved, as none of these three groups should have expressed MHCII. The fact that we saw the greatest signal immediately following adoptive transfer with subsequent waning also suggested a non-specific response, as we had envisioned the upregulation of MHCII during the course of tumor progression would allow direct interaction with Tregs that would result in increased signal intensity. Thus, collectively, these studies suggested that Tregs were only transiently trafficking to peri-tumoral area and were not interacting with tumor cells in an antigen-specific, MHCII-dependent manner. Histologic examination of tumor explants confirmed the lack of Tregs within the tumor despite the presence of high-level MHCII expression in appropriate samples.

Having failed to demonstrate appropriate trafficking and accumulation of OTII Tregs, we evaluated their persistence within tumor-draining lymph nodes and spleens. This analysis revealed that OTII cells were in fact present within these tissues, but at very low numbers. Those OTII cells that were present, however, by and large maintained expression of Foxp3, indicating that they had not become 'ex-Tregs' (Zhou et al., 2009b) capable of potentially providing helper function to our OTI CD8+.

With our OTII Tregs persisting and maintaining Foxp3 expression within spleens and DLNs, we next evaluated for alterations of OTI phenotype in the presence of Tregs. While unable to alter the tumor growth outcome in these studies, it remained a possibility that our OTI CD8+ phenotype had been altered by Tregs. Evaluation of OTI CD8+ tumor trafficking and accumulation, proliferation, cell surface phenotype, cytokine expression, and *in vivo* cytotoxicity all failed to demonstrate any differences in the presence of OTII Tregs. This was in stark contrast to studies by others that had

demonstrated primarily the ability of Tregs to suppress the cytotoxic function of CD8+ effector cells while leaving trafficking, proliferation, maturation, and polarization largely unaltered (Lin et al., 2002; Dittmer et al., 2004; Zippelius et al., 2004; Chen et al., 2005).

The inability of our Tregs to suppress tumor rejection, alter OTI phenotype, or demonstrate antigen- and MHCII-dependent tumor interactions raised serious questions about the validity of our OVA-expressing tumor model. A critical component of our hypothesis was that tumor cells could directly present antigen to Tregs via tumor-expressed MHCII. While we had previously documented tumor MHCII expression *in vitro* (Figures 3.6) and *in vivo* (Figure 3.9), as well as OVA expression via MHCI-dependent *in vitro* (Figure 3.8) and *in vivo* (Figure 3.4) T-cell recognition, we had yet to directly evaluate the ability of our tumors to directly present antigen to OTII cells. While our results from Figure 3.5(B) suggesting suppression in the MHCII KO mice inferred this interaction, they did not prove it, and further had since failed to be replicated.

Therefore, to better assess this question we evaluated the ability of OTII Th1 cells to directly recognize tumor cells via *in vitro* coculture experiments. Tumor variants were cultured with or without IFNγ in order to induce MHCII expression and, with or without exogenous addition of OVAII peptide, were then cocultured with *in vitro* polarized, sorted OTII Th1 cells, which were subsequently evaluated for intracellular cytokine expression. Tumor MHCII expression and MHCI-dependent OVA recognition were also confirmed and were as previously demonstrated (Figures 3.6 and 3.8, respectively; repeat data not shown). Despite their ability to express MHCII and be recognized by OVA-specific, MHCI-restricted T-cells, none of the B16 variants were able to directly stimulate OTII Th1 cells with endogenously expressed OVA antigen. The fact that cells expressing

MHCII could stimulate OTII Th1 in the presence of exogenous OVAII peptide suggested that this was not a failure of MHCII:peptide:TCR interaction, but rather a failure of endogenous antigen content or perhaps endogenous antigen processing and presentation within the tumor cells.

With this finding, we referred back to the original work by Preynat-Seauve and colleagues (Preynat-Seauve et al., 2007) who had previously generated our B16.mOVA cell line and *mOVA* DNA construct. In their work, despite demonstrating that B16 cells expressed full-length OVA protein derived from a DNA construct containing the OVAII peptide 323-339 coding sequence recognized by the OTII TCR (also confirmed in our lab upon receipt of the *mOVA* DNA construct), they failed to demonstrate the recognition of tumor-derived OVA by OTII cells *in vivo*. This occurred for their B16.mOVA lines as well as several other tumor lines also expressing their OVA construct. They did not investigate this finding further, and attributed it to an inefficiency of tumor associated OVA antigen cross-presentation within host tumor-draining lymph nodes, citing work by Dudziak and colleagues that had demonstrated inefficient MHCII antigen presentation by some subsets of DCs (Dudziak et al., 2007). While our *in vitro* data would suggest that this failure of recognition is not due merely to a shortcoming of antigen cross-presentation, it is in alignment with their findings.

Our results, coupled with the findings of Preynat-Seauve (Preynat-Seauve et al., 2007) and colleagues, convincingly demonstrate that, despite the presence of full length OVA protein, its recognition by OTI cells, and the expression of functional MHCII by our tumor cells, the OVA protein expressed by our tumor cells is unable to stimulate OTII T-cells. Whether this is the result of altered protein expression, post-translation

modification, insufficient protein quantity, or perhaps altered/inadequate antigen processing within our tumor cells is unknown. It is interesting to note that Preynat-Seauve and colleagues demonstrated the failure of OVA recognition to occur using a several different tumor lines all created from their same DNA construct. This is in contrast to other works utilizing tumor-produced OVA that have been shown to be recognized by OTII T-cells (Schreiber et al., 2012), which may suggest something specific to the Preynat-Seauve construct used in our studies. Other groups (Quatromoni et al., 2011) have also recently reported data consistent with failed OTII recognition of a different OVA-expressing B16 line, however, suggesting that this may in fact be a broader reaching issue with variable tumor to tumor relevance. Regardless of the mechanism for this lack of recognition, its result is a complete inability to interpret any and all Treg studies performed within our studies, sadly making a large body of this work null.

Chapter 6

Conclusions and Future Directions

6.1 Conclusions

The motivation for this study was derived primarily from two sets of findings. The first of these is the growing body of literature suggesting that regulatory T-cells exert superior suppressive effects when both Treg and Teffector are specific for antigens within the same target cell. This was further expanded upon by prior work within the lab, which demonstrated that Tregs are capable of antigen-specific suppression in the setting of a heterogeneous mixed-tumor model. The second set of observations driving our thesis involved the increasing awareness that tumor cells, particularly in the setting of an active immune response, are capable of undergoing a number of cellular alterations that allow them to interact with and manipulate immune cells, including the upregulation of molecules involved in antigen presentation pathways. The increased ability of tumors to present self-antigens could allow not only for the presentation of novel antigens, but also the ability of tumors to potentially present antigen directly to T-cells, thus providing a mechanism for antigen specificity of tumor suppression. This study was therefore designed to test the hypothesis that the upregulation of MHCII by tumor cells allows for direct antigen presentation to regulatory T-cells with resultant suppression of immune-mediated tumor rejection.

In Chapter 3, we were able to develop a novel subcutaneous B16 tumor challenge system in which MHCII-inducible B16.mOVA cells were treated by a combination of non-myeloablative whole body irradiation and adoptive transfer of naïve OTI CD8+ cells in both WT and MHCII KO recipients. While this model did not afford a permanent cure to our tumor-bearing mice, it provided an adequate treatment effect for the subsequent evaluation of Treg suppression. Addition of OTII Tregs to this model resulted in a suppressive effect with MHCII KO recipients that failed to be demonstrated in WT mice. Our interpretation of this dichotomy at the time was that the recovery of host lymphopoeisis within the WT recipients, but not MHCII KO recipients, would result in production of polyclonal Tregs capable of suppressing our treatment effect. Thus, MHCII KO mice demonstrated a prolonged treatment effect that allowed for unmasking of suppression by our OTII Tregs that was not afforded by the shortened treatment effect seen in WT mice. Further noteworthy within this study was the fact that the suppression within our MHCII KO recipients demonstrated a lag relative to untreated mice. This lag fit nicely into our hypothesis of inflammation-induced MHCII upregulation as a requirement for Treg suppression with the MHCII-inducible B16.mOVA tumor line. To exploit and expand upon this finding in future studies, we successfully generated the MHCII-constitutive B16.mOVA.CIITA and MHCII-non-inducible B16-F10-D.mOVA tumor lines and subsequently validated their *in vitro* and *in vivo* MHC and OVA expression.

In Chapter 4, we stepped away from our Treg studies to further examine the phenotype of our OTI CD8+ treatment cells over the course of tumor progression. We were able to successfully demonstrate that, upon adoptive transfer, our naïve OTI CD8+

cells effectively proliferated, trafficked to, and accumulated within the B16.mOVA tumor. These cells developed cell surface marker phenotypes consistent with all major lineages of CD8+ T-cells including naïve, central memory, and effector/effector memory cells, and these populations demonstrated appropriate distributions within spleens, DLN, and tumor. Tumor infiltrating OTI CD8+ further demonstrated high frequencies of exhaustion marker expression, perhaps providing a clue to the lack of long-term treatment maintenance in our model. Analysis of effector cell function demonstrated that our OTI CD8+ possessed cytokine expression profiles consistent with a Tc1 phenotype and were effective mediators of target cell lysis. Overall, our OTI CD8+ cells developed a phenotype appropriate for the tumor treatment effect seen and further one that we felt would be amenable to multiple potential mechanisms of Treg suppression.

In Chapter 5, we aimed to bring together the findings from our first two chapters to further understand the ability of tumors to directly present antigen to Tregs along with the suppressive implications of this interaction upon the phenotype of an otherwise productive CD8+ T-cell-mediated immune response. However, we were unable to replicate the suppressive findings from our first study. Probing of this result revealed that our Tregs persisted and maintained Foxp3 expression within recipient mice, but displayed antigen non-specific, MHCII-independent tumor trafficking with poor long-term accumulation. Further, our Tregs failed to alter the proliferation, trafficking, cell surface phenotype, or effector function of our OTI CD8+ cells. *In vitro* analysis revealed that our OVA-expressing tumor lines were unable to directly present endogenous OVA to OTII cells. Subsequent review of the original work describing our B16.mOVA tumor line

corroborated this finding *in vivo*, but like us could only speculate as to the mechanism of this failure.

Collectively, the studies described herein have developed and characterized a novel tumor challenge and treatment system along with a series of OVA-expressing B16 tumors with variable MHCII expression patterns that should provide invaluable to future studies aimed at elucidating the ability of tumor cells to directly present class II antigens. Unfortunately, given the failure of our tumor cells to directly present endogenous OVA antigen to OTII cells, the studies involving the direct presentation by tumors to Tregs are sadly uninterpretable and ultimately invalid. This model and the concepts developed herein remain poised for future exploitation using an alternative class II antigen for CD4+ T-cell recognition.

6.2 Future Directions

Our study developed a novel tumor challenge and treatment model along with a set of B16 tumors with variable MHCII expression patterns, but due to the inability of our tumor cells to present endogenous OVA antigen to OTII cells, ultimately failed to address its primary hypothesis. The model itself, however, remains valid and capable of answering this question if an appropriate class II antigen within B16 cells can be identified.

In fact, such a system has been identified in the form of the endogenous melanocyte differentiation antigen tyrosinase-related protein 1 (TRP-1 or gp75). TRP-1 is present in normal melanocytes as well as melanoma cells, and has been considered as a

potential target for immunotherapy within humans (Overwijk et al., 1999). Muranski and colleagues (Muranski et al., 2008) developed a transgenic mouse expressing a MHCII-restricted TCR, which recognizes an epitope within the TRP-1 protein, and subsequently were able to demonstrate the ability to treat B16 tumors *in vivo* using *in vitro* polarized Th17 TRP-1 cells. Two recent studies utilizing this model further support its applicability to our system. In the first of these, Xie and colleague (Xie et al., 2010) were able to demonstrate that the combination of non-myeloablative whole body irradiation along with adoptive transfer of naïve TRP-1 CD4+ cells resulted in the development of a Th1 phenotype within TRP-1 cells and a substantial treatment effect upon established B16 tumors. This treatment resulted in an upregulation of MHCII expression by B16 tumor cells and importantly was not seen when MHCII KO recipient mice were used.

In the second recent study utilizing this model, Quezada and colleagues (Quezada et al., 2010) were able to elicit long-standing B16 tumor rejection using adoptive transfer of these same naïve TRP-1 CD4+ cells in conjunction with non-myeloablative whole body irradiation and CTLA-4 blockade. They further showed that this treatment effect was antigen-specific and resulted in an IFNγ-dependent upregulation of MHCII upon tumor cells. Even more importantly, they demonstrated that the use of *in vitro* polarized TRP-1 Th1 cells could treat tumors in MHCII KO mice, an effect that was abrogated with addition of MHCII-blocking antibodies.

Collectively, these two studies indicate that TRP-1 CD4+ cells can directly recognize B16 tumors in an MHCII-dependent fashion. Inability of direct tumor recognition by our OTII+ T-cells was the key failure in our prior Tregs studies, and thus use of TRP-1 CD4+ cells as Treg donors could potentially solve this problem. Therefore,

the immediate next step to follow our studies should be to evaluate the ability of TRP-1 Tregs to suppress OTI CD8+ cells in our tumor model.

A second line of evaluation that should be undertaken to expand upon the findings within our model surrounds the phenotype of our OTI CD8+ cells, specifically as it pertains to their inability to provide long-lasting tumor immunity within recipient mice. Besides making elucidation of Treg effects more difficult in our studies, this failure of long-term tumor immunity despite the presence of tumor antigen-specific effector cells is one of the hallmarks of tumor progression and one of the major shortcomings of adoptive immunotherapy in cancer (Rosenberg, 2001; Zippelius et al., 2004; Dudley & Rosenberg, 2003). A large volume of research is currently investigating this issue, with a number of observations indicating that molecules involved in T-cell exhaustion and costimulation are crucial mediators in this process. Several such molecules, including PD-1, LAG-3, and TIM-3, were shown to be expressed at high frequency by tumor-infiltrating OTI CD8+ cells in our own study. The understanding of the function and importance of these molecules in tumor progression is increasing (Blackburn et al., 2009; Workman et al, 2004; Zhu et al., 2005), and the use of antibody blockade of these molecules, along with CTLA-4, (Woo et al., 2012; Ngiow et al., 2011; Duraiswamy et al., 2013; Ott et al., 2013) has resulted in dramatic tumor responses that are changing the frontier of cancer immunotherapy. Further evaluation of these markers, along with potential incorporation of antibody-blocking strategies, may allow for improved treatment responses and understanding of OTI phenotype and Treg function within our model.

A final set of studies that should prove to be insightful would be to further evaluate the failure of our OVAII-OTII system, with particular emphasis upon analyzing

the antigen processing and presentation pathways within our B16.mOVA tumor. As previously mentioned, despite the fact that our B16.mOVA cells had been previously shown to produce full length OVA protein (Preynat-Seauve et al., 2007) which was transcribed from a DNA construct that included the OVAII amino acid sequence, our tumor cells failed to present this epitope to OVAII-specific OTII cells. This same finding was also observed by the above authors as well as by other groups utilizing a different OVA-expressing B16 line (Quatromoni et al., 2011), and yet other groups (Schreiber et al., 2012) have reported the successful recognition of tumor-expressed OVA by OTII cells, suggesting that this is not a universal phenomenon with the OVA protein. These results may be explained by the previously-mentioned observations of Tsuji and colleagues (Tsuji et al., 2012) who have identified a novel HSP90-dependent antigen presentation pathway within tumor cells. In their model, this observation resulted in the ability of melanoma cells to directly present novel antigens to CD4+ cells via tumor-expressed MHCII. Ironically, their observation of a novel tumor antigen processing pathway, which had previously served as support for the motivation to pursue our own experiments, may in fact provide an explanation for their failure.

6.3 Concluding Remarks

In this study, we hypothesized that the inflammation-induced upregulation of MHCII by tumor cells could allow for direct presentation of tumor-derived antigens to Tregs with resultant antigen-specific suppression of immune-mediated tumor rejection. In the end, we were unsuccessful at answering this question due to the inability of our

tumor cells to directly present endogenously expressed OVA antigen to our Treg cells. Despite this failure, this work is not without merit, and a number of positives can be taken from this study. The novel treatment model along with the panel of variable MHCII-expressing B16 tumor lines developed and characterized herein will serve as valuable tools going forth in future experiments. A framework for this evaluation has been laid here, and incorporation of an appropriate Treg source, perhaps from the TRP-1 mouse, should allow for the efficient evaluation of our original hypothesis. Although unanswered here, the question of direct interaction between tumors and Tregs remains an important question in the field of cancer immunology worthy of continued investigation.

Bibliography

Ahmadzadeh M, Felipe-Silva A, Heemskerk B, Powell DJ, Wunderlich JR, Merino MJ, & Rosenberg SA. (2008). Foxp3 expression accurately defines the population of intratumoral regulatory T-cells that selectively accumulate in metastatic melanoma lesions. Blood. 112(13): 4953-4960.

Ahmadzadeh M, Johnson LA, Heemskerk B, Wunderlich JR, Dudley ME, White DE, & Rosenberg SA. (2009). Tumor antigen-specific CD8 T-cells infiltrating the tumor express high levels of PD-1 and are functionally impaired. Blood. 114(8): 1537-1544.

Anderson AC, Anderson DE, Bregoli L, Hastings WD, Kassam N, Lei C, Chandwaskar R, Karman J, Su EW, Hirashima M, Bruce JN, Kane LP, Kuchroo VK, & Hafler DA. (2007a). Promotion of tissue inflammation by the immune receptor Tim-3 expressed on innate immune cells. Science. 318(5853): 1141-1143.

Anderson CF, Oukka M, Kuchroo VJ, & Sacks D. (2007b). CD4(+)CD25(-)Foxp3(-) Th1 cells are the source of IL-10-mediated immune suppression in chronic cutaneous leishmaniasis. J Exp Med. 204(2): 285-297.

Antony PA, Piccirillo CA, Akpinarli A, Finkelstein SE, Speiss PJ, Surman DR, Palmer DC, Chan CC, Klebanoff CA, Overwijk WW, Rosenberg SA, & Restifo NP. (2005). CD8+ T-cell immunity against a tumor/self-antigen is augmented by CD4+ T helper cells and hindered by naturally occuring T regulatory cells. J Immunol. 174(5): 2591-2601.

Aoudjit F, Guo W, Gagnon-Houde JV, Castaigne JG, Alcaide-Loridan C, Charron D, & Al-Daccak R. (2004). HLA-DR signalling inhibits Fas-mediated apoptosis in A375 melanoma cells. Exp Cell Res. 299(1): 79-80.

Apostolou I, Sarukhan A, Klein L, & von Boehmer H. (2002). Origin of regulatory T-cells with known specificity for antigen. Nat Immunol. 3(8): 756-763.

Arnold B, Schönrich G, & Hämmerling GJ. (1993). Multiple levels of peripheral tolerance. Immunol Today. 14(1): 12-14.

Asseman C, Mauze S, Leach MW, Coffman RL, & Powrie F. (1999). An essential role for interleukin 10 in the function of regulatory T-cells that inhibit intestinal inflammation. J Exp Med. 190(7): 995-1004.

Attia P, Maker AV, Haworth LR, Rogers-Freezer L, & Rosenberg SA. (2005). Inability of a fusion protein of IL-2 and diphtheria toxin (Denileukin Diftitox, DAB389IL-2, ONTAK) to eliminate regulatory T lymphocytes in patients with melanoma. J Immunother. 28(6): 582-592.

Awwad M & North RJ. (1989). Cyclophosphamide-induced immunologically mediated regression of a cyclophosphamide-resistant murine tumor: a consequence of eliminating precursor L3T4+ suppressor T-cells. Cancer Res. 49(7): 1649-1654.

Bacher P, Kniemeyer O, Schönbrunn A, Sawitzki B, Assenmacher M, Rietschel E, Steinback A, Cornely OA, Brakhage AA, Thiel A, & Scheffold A. (2013). Antigen-specific expansion of human regulatory T-cells as a major tolerance mechanism against mucosal fungi. Mucosal Immunology. 2013 Dec 4. Epub ahead of print.

Baecher-Allan C, Wolf E, & Hafler DA. (2006). MHC class II expression identifies functionally distinct human regulatory T-cells. J Immunol. 176(8): 4622-4631.

Barnden MJ, Allison J, Heath WR, & Carbone FR. (1998). Defective TCR expression in transgenic mice constructed using cDNA-based α- and β-chain genes under the control of heterologous regulatory elements. Immunol Cell Biol. 76(1): 34-40.

Barnett B, Kryczek I, Cheng P, Zou W, & Curiel TJ. (2005). Regulatory T-cells in ovarian cancer: biology and therapeutic potential. Am J Reprod Immunol. 54(6): 369-377.

Belkaid Y. (2007). Regulatory T-cells and infection: a dangerous necessity. Nat Rev Immunol. 7(11): 875-888.

Benacerraf B. (1981). Role of MHC gene products in immune regulation. Science. 212(4500): 1229-1238.

Bengsch H, Spangenberg HC, Kersting N, Neumann-Haefelin C, Panther E, Von Weizsacker F, Blum HE, Piercher H, & Thimme R. (2007). Analysis of CD127 and KLRG1 expression on hepatitis C virus-specific CD8+ T-cells reveals the existence of different memory T-cell subsets in the peripheral blood and liver. J Virol. 81(2): 945-953.

Bennett CL, Christie J, Ramsdell F, Brunkow ME, Ferguson PJ, Whitesell L, Kelly TE, Saulsbury FT, Chance PF, & Ochs HD. (2001). The immune dysregulation, polyendocrinopathy, enteropathy, X-linked syndrome (IPEX) is caused by mutations of FOXP3. Nat Genet. 27(1): 20-21.

Berd D & Mastrangelo MJ. (1988). Effect of low dose cyclophosphamide on the immune system of cancer patients: depletion of CD4+ 2H4+ suppressor-induced T-cells. Cancer Res. 48(6): 1671-1675.

Berger C, Jensen MC, Lansdorp PM, Gough M, Elliott C, & Riddell SR. (2008). Adoptive transfer of effector CD8+ T-cells derived from central memory cells establishes persistent T-cell memory in primates. J Clin Invest. 118(1): 294-305.

Bernsen MR, Hakansson L, Gustafsson B, Krysander L, Rettrup B, Ruiter D, & Hakansson A. (2003). On the biological relevance of MHC clas II and B7 expression by tumour cells in melanoma metastasis. Br J Cancer. 88(3): 424-431.

Bioanconi E, Piovesan A, Facchin F, Beraudi A, Casadei R, Frabetti F, Vitale L, Pelleri MC, Tassani S, Piva F, Perez-Amodio S, Strippoli P, & Canaider S. (2013). An estimation of the number of cells in the human body. Ann Hum Biol. 40(6): 463-471.

Blackburn SD, Shin H, Haining WN, Zou T, Workman CJ, Polley A, Betts MR, Freeman GH, Vignali DA, & Wherry EJ. (2009). Coregulation of CD8+ T-cell exhaustion by multiple inhibitory receptors during chronic viral infection. Nat Immunol. 10(1): 29-37.

Blank C & Mackensen A. (2007). Contribution of the PD-L1/PD-1 pathway to T-cell exhaustion: an update on implications for chronic infections and tumor evasion. Cancer Immunol Immunother. 56(5): 739-745.

Boettler T, Panther E, Bengsch B, Nazarova N, Spangenberg HC, Blum HE, & Thimme R. (2006). Expression of the interleukin-7 receptor alpha chain (CD127) on virus-specific CD8+ T-cells identifies functionally and phenotypically defined memory T-cells during acute resolving hepatitis B virus infection. J Virol. 80(7): 3532-3540.

Bonertz A, Weitz J, Pietsch DHK, Rahbari NN, Schlude C, Ge Y, Juenger S, Vlodavsky I, Khazaie K, Jaeger D, Reissfelder C, Antolovic D, Aigner M, Koch M, & Bechhove P. (2009). Antigen-specific Tregs control T-cell responses against a limited repertoire of tumor antigens in patients with colorectal carcinoma. J Clin Invest. 119(11): 3311-3321.

Bopp T, Becker C, Klein M, Klein-Hessling S, Palmetshofer A, Serfling E, Heib V, Becker M, Kubach J, Schmitt S, Stoll S, Schild H, Staege MS, Stassen M, Jonuleit H, & Schmitt E. (2007). Cyclic adenosine monophosphate is a key component of regulatory T-cell-mediated suppression. J Exp Med. 204(6): 1303-1310.

Borsellino G, Kleinewietfeld M, Di Mitri D, Sternjak A, Diamantini A, Giometto R, Hopner S, Centonze D, Bernardi G, Dell'acqua ML, Rossini PM, Battistini L, Rotzschke O, & Falk K. (2007). Expression of ectonucleotidase CD39 by Foxp3+ Treg cells: hydrolysis of extracellular ATP and immune suppression. Blood. 110(4): 1225-1232.

Brunkow ME, Jeffery EW, Hjerrild KA, Paeper B, Clark LB, Yasayko SA, Wilkinson JE, Galas D, Ziegler SF, & Ramsdell F. (2001). Disruption of a new forkhead/winged-helix protein, scurfin, results in the fatal lymphoproliferative disorder of the scurfy mouse. Nat Genet. 27(1): 68-73.

Burnett FM. (1957). Cancer – a biological approach. Brit Med J. 1(5023): 841-847.

Butcher EC & Pickler LJ. (1996). Lymphocyte homing and homeostasis. Science. 272(5258): 60-66.

Camby I, Le Mercier M, Lefranc F, & Kiss R. (2006). Galectin-1: a small protein with major functions. Glycobiology. 16(11): 137R-157R.

Cao X, Cai SF, Fehniger TA, Song J, Collins LI, Piwnica-Worms DR, & Ley TJ. (2007). Granzyme B and perforin are important for regulatory T-cell-mediated suppression of tumor clearance. Immunity. 27(4): 635-646.

Cao YA, Wagers AJ, Beilhack A, Dusich J, Bachmann MH, Negrin RS, Weissman IL, & Contag CH. (2004). Shifting foci of hematopoiesis during reconstitution from single stem cells. Proc Natl Acad Sci. 101(1): 221-226.

Carter LL & Dutton RW. (1995). Relative perforin- and Fas-mediated lysis in T1 and T2 CD8 effector populations. J Immunol. 155(3): 1028-1031.

Carter LL & Dutton RW. (1996). Type 1 and type 2: a fundamental dichotomy for all T-cell subsets. Curr Opin Immunol. 8(3): 336-342.

Cederbom L, Hall H, & Ivars F. (2000). CD4+CD25+ regulatory T-cells down-regulate co-stimulatory molecules on antigen-presenting cells. Eur. J. Immunol. 30(6): 1538-1543.

Cerwenka A, Carter LL, Reome JB, Swain SL, & Dutton RW. (1998). In vivo persistence of CD8 polarized T-cell subsets producing type 1 or type 2 cytokines. J Immunol. 161(1): 97-105.

Chapuis AG, Thompson JA, Margolin KA, Rodmyre R, Lai IP, Dowdy K, Farrar EA, Bhatia S, Sabath DE, Cao J, Li Y, & Yee C. (2012). Transferred melanoma-specific CD8+ T-cells persist, mediate tumor regression, and acquire central memory phenotype. Proc Natl Acad Sci. 109(12): 4592-4597.

Chen M, Pittet M, Gorelik L, Flavell RA, Weissleder R, von Boehmer H, & Khazaie K. (2005). Regulatory T-cells suppress tumor-specific CD8 T-cell cytotoxicity through TGF-β signals in vivo. Proc Natl Acad Sci. 102(2): 419-424.

Chen W, Jin W, Hardegen N, Lei KJ, Li L, Marinos N, McGrady G, & Wahl SM. (2003). Conversion of peripheral CD4+CD25- naïve T-cells to CD4+CD25+ regulatory T-cells by TGF-beta induction of transcription factor Foxp3. J Exp Med. 198(12): 1875-1886.

Collison LW, Workman CJ, Kuo TT, Boyd K, Wang Y, Vignali KM, Cross R, Sehy D, Blumberg RS, & Vignali DAA. (2007). The inhibitory cytokine IL-35 contributes to regulatory T-cell function. Nature. 450(7169): 566-569.

Coombes JL, Siddiqui KRR, Arancibia-Cárcamo CV, Hall J, Sun CM, Belkaid Y, & Powrie F. (2007). A functionally specialized population of mucosal CD103+ DCs induces Foxp3+ regulatory T-cells via a TGF-beta and retinoic acid-dependent mechanism. J Exp Med. 204(8): 1757-1764.

Cuenca A, Cheng F, Wang H, Brayer J, Horna P, Gu L, Bien H, Borrello IM, Levitsky HI, & Sotomayor EM. (2003). Extra-lymphatic solid tumor growth is not immunologically ignored and results in early induction of antigen-specific T-cell anergy: dominant role of cross-tolerance to tumor antigens. Cancer Research. 63(24): 9007-9015.

Curiel TJ, Coukos G, Zou L, Alvarez X, Cheng P, Mottram P, Evdemon-Hogan M, Conejo-Garcia JR, Zhang L, Burow M, Zhu Y, Wei S, Kryczek I, Daniel B, Gordon A, Myers L, Lackner A, Disis ML, Knutson KL, Chen L, & Zou W. (2004). Specific recruitment of regulatory T-cells in ovarian carcinoma fosters immune privilege and predicts reduced survival. Nat Med. 10(9): 942-949.

Curotto De Lafaille MA & Lafaille JJ. (2009). Natural and adaptive Foxp3+ regulatory T-cells: more of the same or a division of labor? Immunity. 30(5): 626-635.

Curran MA, Montalvo W, Yagita H, & Allison JP. (2010). PD-1 and CTLA-4 combination blockage expands infiltrating T-cells and reduces regulatory T and myeloid cells within B16 melanoma tumors. Proc Natl Acad Sci. 107(9): 4275-4280.

Dannull J, Su Z, Rizzieri D, Yang BK, Coleman D, Yancey D, Zhang A, Dahm P, Chao N, Gilboa E, Vieweg J. (2005). Enhancement of vaccine-mediated antitumor immunity in cancer patients after depletion of regulatory T-cells. J Clin Invest. 115(12): 3623-3633.

Day CL, Kaufmann DE, Kiepiela P, Brown JA, Moodley ES, Reddy S, Machey EW, Miller JD, Leslie AJ, DePierres C, Mncube Z, Duraiswamy J, Zhu B, Eichbaum Q, Altfeld M, Wherry EJ, Coovadia HM, Goulder PJ, Klenerman P, Ahmed R, Freeman GJ, & Walker BD. (2006). PD-1 expression on HIV-specific T-cells is associated with T-cell exhaustion and disease progression. Nature. 443(7109): 350-354.

de la Rosa M, Rutz S, Dorninger H, & Scheffold A. (2004). Interleukin-2 is essential for CD4+CD25+ regulatory T-cell function. Eur. J. Immunol. 34(9): 2480-2488.

Deaglio S, Dwyer KM, Gao W, Friedman D, Usheva A, Erat A, Chen JF, Enjyoji K, Linden J, Oukka M, Kuchroo VK, Strom TB, & Robson SC. (2007). Adenosine generation catalyzed by CD39 and CD73 expressed on regulatory T-cells mediates immune suppression. J Exp Med. 204(6): 1257-1265.

Deffrennes V, Vedrenne J, Stolzenberg MC, Piskurich J, Barbieri G, Ting JP, Charron D, & Alcaide-Loridan C. (2001). Constitutive expression of MHC class II genes in melanoma cell lines results from the transcription of class II transactivator abnormally initiated from its B cell-specific promoter. J Immunol. 167(1): 98-106.

Derre L, Rivals JP, Jandus C, Pastor S, Rimoldi D, Romero P, Michielin O, Olive D, & Speiser DE. (2010). BTLA mediates inhibition of human tumor-specific CD8+ T-cells that can be partially reversed by vaccination. J Clin Invest. 120(1): 157-167.

Dittmer U, He H, Messer RJ, Schimmer S, Olbrich AR, Ohlen C, Greenberg PD, Stromnes IM, Iwashiro M, Sakaguchi S, Evans LH, Petersson KE, Yang G, & Hasenkrug KJ. (2004). Functional impairment of CD8(+) T-cells by regulatory T-cells during persistent retroviral infection. Immunity. 20(3): 293-303.

Dobrzanski MJ, Reome JB, & Dutton RW. (1999). Therapeutic effects of tumor-reactive type 1 and type 2 CD8+ T-cell subpopulations in established pulmonary metastases. J Immunol. 162(11): 6671-6680.

Dobrzanski MJ, Reome JB, & Dutton RW. (2000). Type 1 and type 2 CD8+ effector T-cell subpopulations promote long-term tumor immunity and protection to progressively growing tumor. J Immunol. 164(2): 916-925.

Dobrzanski MJ, Reome JB, & Dutton RW (2001). Immunopotentiating role of IFN-gamma in early and late stages of type 1 CD8 effector cell-mediated tumor rejection. Clin Immunol. 98(1): 70-84.

Dong H, Strome SE, Salomao DR, Tamura H, Hirano F, Flies DB, Roche PC, Lu J, Zhu G, Tamada K, Lennon VA, Celis E, & Chen L. (2002). Tumor-associated B7-H1 promotes T-cell apoptosis: a potential mechanism of immune evasion. Nat Med. 8(8): 793-800.

Drake CG, Jaffee E, & Pardoll DM. Mechanisms of immune evasion by tumors. Adv Immunol. 90: 51-81.

Dudley ME & Rosenberg SA. (2003). Adoptive-cell-transfer therapy for the treatment of patients with cancer. Nat Rev Cancer. 3(9): 666-675.

Dudley ME, Wunderlich J, Nishimura MI, Yu D, Yang JC, Topalian SL, Schwartzentruber DJ, Hwu P, Marincol FM, Sherry R, Leitman SF, & Rosenberg SA. (2001). Adoptive transfer of cloned melanoma-reactive T lymphocytes for the treatment of patients with metastatic melanoma. J Immunother. 24(4): 363-373.

Dudley ME, Yang JC, Shery R, Hughes MS, Royal R, Kammula U, Robbins PF, Huang J, Citrin DE, Leitman SF, Wunderlich J, Restifo NP, Thomasian A, Downey SG, Smith FO, Klapper J, Morgon K, Laurencot C, White DE, & Rosenberg SA. (2008). Adoptive cell therapy for patients with metastatic melanoma: evaluation of intensive myeloablative chemoradiation preparative regimens. J Clin Oncol. 26(32): 5233-5239.

Dudziak D, Kamphorst AO, Heidkamp GF, Buchholz VR, Trumpfheller C, Yamazaki S, Cheong C, Liu K, Lee HW, Park CG, Steinman RM, & Nussenzweig MC. (2007). Differential antigen processing by dendritic cell subsets in vivo. Science. 315(5808): 107-111.

Dunn GP, Bruce AT, Ikeda H, Old LJ, & Schreiber RD. (2002). Cancer immunoediting: from immunosurveillance to tumor escape. Nat Immunol. 3(11): 991-998.

Dunn GP, Old LJ, & Schreiber RD. (2004). The immunobiology of cancer immunosurveillance and immunoediting. Immunity. 21(2): 137-148.

Duraiswamy J, Kaluza KM, Freeman GJ, & Coukos G. (2013). Dual blockade of PD-1 and CTLA-4 combined with tumor vaccine effectively restores T-cell rejection function in tumors. Cancer Res. 73(12): 3591-3603.

Ehrlich P. (1909). Ueber den jetzigen stand der Karzinomforschung. Ned Tijdschr Geneeskd. 5: 273-290.

Esteller M. (2003). Cancer epigenetics: DNA methylation and chromatin alterations in human cancer. Adv Exp Med Biol. 532: 39-49.

Fallarino F, Grohmann U, Hwang KW, Orabona C, Vacca C, Bianchi R, Belladonna ML, Fioretti MC, Alegre ML, & Puccetti P. (2003). Modulation of tryptophan catabolism by regulatory T-cells. Nat Immunol. 4(12): 1206-1212.

Fantini MC, Becker C, Monteleone G, Pallone F, Galle PR, & Neurath MF. (2004). Cutting edge: TGF-beta induces a regulatory phenotype in CD4+CD25- T-cells through Foxp3 induction and downregulation of Smad7. J Immunol. 172(9): 5149-5153.

Fearon DT, Manders P, & Wagner SD. (2001). Arrested differentiation, the self-renewing memory lymphocyte, and vaccination. Science. 293(5528): 248-250.

Fidler IJ & Bucana C. (1977). Mechanism of tumor cell resistance to lysis by syngeneic lymphocytes. Cancer Res. 37(11):3945-3956.

Fidler IJ, Gersten DM, & Budmen MB. (1976). Characterization in vivo and in vitro of tumor cells selected for resistance to syngeneic lymphocyte-mediated cytotoxicity. Cancer Res. 36(9 pt. 1): 3160-3165.

Fontenot JD, Gavin MA, & Rudensky AY. (2003). Foxp3 programs the development and function of CD4+ CD25+ regulatory T-cells. Nat Immunol. 4(4): 330-336.

Fontenot JD, Rasmussen JP, Gavin MA, & Rudensky AY. (2005a). A function for interleukin 2 in Foxp3-expressing regulatory T-cells. Nat Immunol. 6(11): 1142-1151.

Fontenot JD, Rasmussen JP, Williams LM, Dooley JL, Farr AG, & Rudensky AY. (2005b). Regulatory T-cell lineage specification by the forkhead transcription factor Foxp3. Immunity. 22(3): 329-341.

Fourcade J, Sun Z, Pagliano O, Guillaume P, Luescher IF, Sander C, Kirkwood JM, Olive D, Kuchroo V, & Zarour HM. (2012). CD8+ T-cells specific for tumor antigens can be rendered dysfunctinoal by the tumor microenvironment through upregulation of the inhibitory receptors BTLA and PD-1. Cancer Res. 72(4): 887-896.

Freeman GJ, Long AJ, Iwai Y, Bourque K, Chernova T, Nishimura H, Fitz LJ, Malenkovich N, Okazaki T, Byrne MC, Horton HF, Fouser L, Carter L, Ling V, Bowman MR, Carreno BM, Collins M, Wood CR, & Honjo T. (2000). Engagement of the PD-1 immunoinhibitory receptor by a novel B7 family member leads to negative regulation of lymphocyte activation. J Exp Med. 192(7): 1027-1034.

Fujimoto S, Greene M, & Sehon AH. (1975). Immunosuppressor T-cells in tumor bearing host. Immunol Commun. 4(3): 201-217.

Gabrilovich D. (2004). Mechanisms and functional significance of tumour-induced dendritic cell defects. Nat Rev Immunol. 4(12): 941-952.

Gao Q, Wang XY, Qiu SJ, Yamato I, Sho M, Nakajima Y, Zhou J, Li BZ, Shi YH, Xiao YS, Xu Y, & Fan J. (2009). Overexpression of PD-L1 significantly associates with tumor aggressiveness and postoperative recurrence in human hepatocellular carcinoma. Clin Cancer Res. 15(3): 971-979.

Gattinoni L, Finkelstein SE, Klebanoff CA, Antony PA, Palmer DC, Spiess PJ, Hwang LN, Yu Z, Wrzesinksi C, Heimann DM, Surh CD, Rosenberg SA, & Restifo NP. (2005a). Removal of homeostatic cytokine sinks by lymphodepletion enhances the efficacy of adoptively transferred tumor-specific CD8+ T-cells. J Exp Med. 202(7): 907-912.

Gattinoni L, Klebanoff CA, Palmer DC, Wrzesinksi C, Kerstann K, Zhiya Y, Finkelstein SE, Theoret MR, Rosenberg SA, & Restifo NP. (2005b). Acquisition of full effector function in vitro paradoxically impairs the in vivo antitumor efficacy of adoptively transferred CD8+ T-cells. J Clin Invest. 115(6): 1616-1626.

Gattinoni L, Powell DJ, Rosenberg SA, & Restifo NP. (2006). Adoptive immunotherapy for cancer: building on success. Nat Rev Immunol. 6(5): 383-393.

Gavin MA, Rasmussen JP, Fontenot JD, Vasta V, Manganiello VC, Beavo JA, & Rudensky AY. (2007). Foxp3-dependent programme of regulatory T-cell differentiation. Nature. 445(7129): 771-775.

Gavin MA, Torgerson TR, Houston E, DeRoos P, Ho WY, Stray-Pedersen A, Ocheltree EL, Greenberg PD, Ochs HD, & Rudensky AY. (2006). Single-cell analysis of normal and FOXP3-mutant human T-cells: FOXP3 expression without regulatory T-cell development. Proc Natl Acad Sci. 103(17): 6659-6664.

Geng L, Huang D, Liu J, Qian Y, Deng J Li D, Hu Z, Zhang J, Jiang G, & Zheng S. (2008). B7-H1 up-regulated expression in human pancreatic carcinoma tissue associates with tumor progression. J Cancer Res Clin Oncol. 134(9): 1021-1027.

Gershon RK & Kondo K. (1970). Cell interactions in the induction of tolerance: the role of thymic lymphocytes. Immunology. 18(5): 723-737.

Gershon RK & Kondo K. (1971). Infectious immunological tolerance. Immunology. 21(6): 903-914.

Ghebeh H, Barhoush E, Tulbah A, Eikum N, Al-Tweigeri T, & Dermime S. (2008). Foxp3+ Tregs and B7-H1/PD-1+ T lymphocytes co-infiltrate the tumor tissues of high-risk breast cancer patients: Implications for immunotherapy. BMC Cancer. 8:57.

Ghiringhelli F, Puig PE, Roux S, Parcellier A, Schmitt E, Solary E, Kroemer G, Martin F, Chauffert B, & Zitvogel L. (2005). Tumor cells convert immature myeloid dendritic cells into TGF-beta-secreting cells inducing CD4+CD25+ regulatory T-cell proliferation. J Exp Med. 202(7): 919-929.

Glaser M. (1979). Augmentation of specific immune response against a syngeneic SV40-induced sarcoma in mice by depletion of suppressor T-cells with cyclophosphamide. Cell Immunol. 48(2): 339-345.

Gobert M, Treilleux I, Bendriss-Vermare N, Bachelot T, Goddard-Leon S, Arfi V, Biota C, Doffin AC, Durand I, Olive D, Perez S, Pasqual N, Faure C, Ray-Coquard I, Puisieux A, Caux C, Blay JY, & Menetrier-Caux C. (2009). Regulatory T-cells recruited through CCL22/CCR4 are selectively activated in lymphoid infiltrates surrounding primary breast tumors and lead to an adverse clinical outcome. Cancer Research. 69(5): 2000-2009.

Goedegebuure PS, Douville LM, Li H, Richmond GC, Schoof DD, Scavone M, & Eberlein TJ. (1995). Adoptive immunotherapy with tumor-infiltrating lymphocytes and interleukin-2 in patients with metastatic malignant melanoma and renal cell carcinoma: a pilot study. J Clin Oncol. 13(8): 1939-1949.

Gondek DC, Lu LF, Quezada SA, Sakaguchi S, & Noelle RJ. (2005). Cutting edge: contact-mediated suppression by CD4+CD25+ regulatory cells involves a granzyme B-dependent, perforin-independent mechanism. J Immunol. 174(4): 1783-1786.

Goodwin BL, Xi H, Tejiram R, Eason DD, Ghosh N, Wright KL, Nagarajan U, Boss JM, & Blanck G. (2001). Varying functions of specific major histocompatibility class II transactivator promoter III and IV elements in melanoma cell lines. Cell Growth Differ. 12(6): 327-335.

Green EA, Gorelik L, McGregor CM, Tran EH, & Flavell RA. (2003). CD4+CD25+ T regulatory cells control anti-islet CD8+ T-cells through TGF-beta-TGF-beta receptor interactions in type 1 diabetes. Proc Natl Acad Sci. 100(19): 10878-10883.

Groh V, Wu J, Yee C, & Spies T. (2002). Tumour-derived soluble MIC ligands impair expression of NKG2D and T-cell activation. Nature. 419(6908): 734-738.

Grossman WJ, Verbsky JW, Barchet W, Colonna M, Atkinson JP, & Ley TJ (2004a). Human T regulatory cells can use the perforin pathway to cause autologous target T-cell death. Immunity. 21(4): 589-601.

Grossman WJ, Verbsky JW, Tollefsen BL, Kemper C, Atkinson JP, & Ley TJ. (2004b). Differential expression of granzymes A and B in human cytotoxic lymphocyte subsets and T regulatory cells. Blood. 104(9): 2840-2848.

Groux H, O'Garra A, Bigler M, Rouleau M, Antonenko S, de Vries JE, & Roncarolo MG. (1997). A CD4+ T-cell subset inhibits antigen-specific T-cell responses and prevents colitis. Nature. 389(6652): 737-742.

Guleria I, Khosroshahi A, Ansari MJ, Habicht A, Azuma M, Yagita H, Noelle RJ, Coyle A, Mellor AL, Khoury SJ, & Sayegh MH. (2005). A critical role for the programmed death ligand 1 in fetomaternal tolerance. J Exp Med. 202(2): 231-237.

Hannier S, Tournier M, Bismuth G, & Triebel F. (1998). CD3/TCR complex-associated lymphocyte activation gene-3 molecules inhibit CD3/TCR signalling. J Immunol. 161(8): 4058-4065.

Haribhai D, Lin W, Edwards B, Ziegelbauer J, Salzman NH, Carlson MR, Li SH, Simpson PM, Chatila TA, & Williams CB. (2009). A central role for induced regulatory T-cells in tolerance induction in experimental colitis. J Immunol. 182(6): 3461-3468.

Hawrylowicz CM & O'Garra A. (2005). Potential role of interleukin-10-secreting regulatory T-cells in allergy and asthma. Nat Rev Immunol. 5(4): 271-283.

Hernandez J, Aung S, Marquardt K, & Sherman LA. (2002). Uncoupling of proliferative potential and gain of effector funciton by CD8(+) T-cells responding to self-antigens. J Exp Med. 196(3): 323-333.

Hicklin DJ, Marincola FM, & Ferrone S. (1999). HLA class I antigen downregulation in human cancers: T-cell immunotherapy revives an old story. Mol Med Today. 5(4): 178-186.

Hill JA, Feuerer M, Tash K, Haxhinasto S, Perez J, Melamed R, Mathis D, & Benoist C. (2007). Foxp3 transcription-factor-dependent and -independent regulation of the regulatory T-cell transcriptional signature. Immunity. 27(5): 786-800.

Hodi FS, Mihm MC, Soiffer RJ, Haluska FG, Butler M, Seidon MV, Davis T, Henry-Spires R, MacRae S, Willman A, Padera R, Jaklitsch MT, Shankar S, Chen TC, Korman A, Allison JP, & Dranoff G. (2003). Biologic activity of cytotoxic T lymphocyte-associated antigen 4 antibody blockade in previously vaccinated metastatic melanoma and ovarian carcinoma patients. Proc Natl Acad Sci. 100(8): 4712-4717.

Hogquist KA, Jameson SC, Heath WR, Howard JL, Bevan MJ, & Carbone FR. (1994). T-cell receptor antagonist peptides induce positive selection. Cell. 76(1):17-27.

Holling TM, van Eggermond CJA, Jager MJ, & van den Elsen PJ. (2006). Epigenetic silencing of MHC2TA transcription in cancer. Biochem Pharmacol. 72(11): 1570-1576.

Holzmann B, Brocker EB, Lehmann JM, Ruiter DJ, Sorg C, Riethmuller G, & Johnson JP. (1987). Tumor progression in human malignant melanoma: five stages defined by their antigenic phenotypes. Int J Cancer. 39(4): 466-471.

Hori S, Haury M, Coutinho A, & Demengeot J. (2002). Specificity requirements for selection and effector functions of CD25+4+ regulatory T-cells in anti-myelin basic protein T-cell receptor transgenic mice. Proc Natl Acad Sci. 99(12): 8213-8218.

Hori S, Nomura T, & Sakaguchi S. (2003). Control of regulatory T-cell development by the transcription factor Foxp3. Science. 299(5609): 1057-1061.

Huang CT, Workman CJ, Flies D, Pan X, Marson AL, Zhou G, Hipkiss EL, Ravi S, Kowalski J, Levitsky HI, Powell JD, Pardoll DM, Drake CG, & Vignali DAA. (2004). Role of LAG-3 in regulatory T-cells. Immunity. 21(4): 503-513.

Huard B, Prigent P, Tournier M, Bruniquel D, & Triebel F. (1995). CD4/major histocompatibility complex class II interaciton analyzed with CD4- and lymphocyte activation gene-3(LAG-3)-Ig fusion proteins. Eur J Immunol. 25(9): 2718-2721.

Huard B, Tournier M, Hercend T, Triebel F, & Faure F. (1994). Lymphocyte-activation gene 3/major histocompatibility complex II interaction modulates the antigenic response of CD4+ lymphocytes. Eur J Immunol. 24(12): 3216-3221.

Ibegbu CC, Yu YX, Harris W, Maggio D, Miller JD, & Kourtis AP. (2005). Expression of killer cell lectin-like receptor G1 on antigen-specific human CD8+ T lymphocyes during active, latent, and resolved infection and its relation with CD57. J Immunol. 174(10): 6088-6094.

Isogawa M, Furuichi Y, & Chisari FV. (2005). Oscillating CD8(+) T-cell effector functions after antigen recognition in the liver. Immunity. 23(1): 53-63.

Jandus C, Bioley G, Dojcinovic D, Derre L, Baitsch L, Wieckowski S, Rufer N, Kwok WW, Tiercy JM, Luescher IF, Speiser DE, & Romero P. (2009). Tumor antigen-specific FOXP3+ CD4 T-cells identified in human metastatic melanoma: peptide vaccination results in selective expansion of Th1-like counterparts. Cancer Research. 69(20): 8085-8093.

Janeway CA, Carding S, Jones B, Murray J, Portoles P, Rasmussed R, Rojo J, Saizawa K, West J, & Bottomly K. (1988). CD4+ T cells: specificity and function. Immunol Rev. 101: 39-80.

Janssens W, Carlier V, Wu B, VanderElst L, Jacquemin MG, & Saint-Remy JMR. (2003). CD4+CD25+ T-cells lyse antigen-presenting B cells by Fas-Fas ligand interaction in an epitope-specific manner. J Immunol. 171(9): 4604-4612.

Jonuleit H, Schmitt E, Schuler G, Knop J, & Enk AH. (2000). Induction of interleukin 10-producing, nonproliferating CD4+ T-cells with regulatory properties by repetitive stimulation with allogeneic immature human dendritic cells. J Exp Med. 192(9): 1213-1222.

Kappler JW, Roehm N, & Marrack P. (1987). T-cell tolerance by clonal elimination in the thymus. Cell. 49(2): 273-280.

Karim R, Jordanova ES, Piersma SJ, Kenter GG, Chen L, Boer JM, Melief CJ, & van der Burg SH. (2009). Tumor-expressed B7-H1 and B7-DC in relation to PD-1+ T-cell infiltration and survival of patients with cervical carcinoma. Clin Cancer Res. 15(20): 6341-6347.

Khong HT & Restifo NP. (2002). Natural selection of tumour variants in the generation of ‘tumour escape’ phenotypes. Nat Immunol. 3(11): 999-1005.

Klages K, Mayer CT, Lahl K, Loddenkemper C, Teng MWL, Ngiow SF, Smyth MJ, Hamann A, Huehn J, & Sparwasser T. (2010). Selective depletion of Foxp3+ regulatory T-cells improves effective therapeutic vaccination against established melanoma. Cancer Res. 70(20): 7788-7799.

Klebanoff CA, Gattinoni L, Torabi-Parizi P, Kerstann K, Cardones AR, Finkelstein SE, Palmer DC, Antony PA, Hwang ST, Rosenberg SA, Waldmann TA, & Restifo NP. (2005). Central memory self/tumor-reactive CD8+ T-cells confer superior antitumor immunity compared with effector memory T-cells. Proc Natl Acad Sci. 102(27): 9571-9576.

Kirberg J, Baron A, Jakob S, Rolink A, Karjalainen K, & von Boehmer H. (1994). Thymic selection of CD8+ single positive cells with a class II major histocompatibility complex-restricted receptor. J Exp Med. 180(1): 25-34.

Ko K, Yamazaki S, Nakamura K, Nishioka T, Hirota K, Yamaguchi T, Shimizu J, Nomura T, Chiba T, & Sakaguchi S. (2005). Treatment of advaced tumors with agonistic anti-GITR mAb and its effects on tumor-infiltrating Foxp3+CD25+CD4+ regulatory T-cells. J Exp Med. 202(7): 885-891.

Kobie JJ, Shah PR, Yang L, Rebhahn JA, Fowell DJ, & Mosmann TR. (2006). T regulatory and primed uncommitted CD4 T-cells express CD73, which suppresses effector CD4 T-cells by converting 5'-adenosine monophosphate to adenosine. J Immunol. 177(10): 6780-6786.

Kretschmer K, Apostolou I, Jaeckel E, Khazaie K, & von Boehmer H. (2006). Making regulatory T-cells with defined antigen specificity: role in autoimmunity and cancer. Immunol Rev. 212: 163-169.

Kryczek I, Wei S, Zou L, Zhu G, Mottram P, Xu H, Chen L, & Zou W. (2006). Cutting edge: induction of B7-H4 on APCs through IL-10: novel suppressive mode for regulatory T-cells. J Immunol. 177(1): 40-44.

Kühn R, Löhler J, Rennick D, Rajewsky K, & Müller W. (1993). Interleukin-10-deficient mice develop chronic enterocolitis. Cell. 75(2): 263-274.

Kursar M, Koch M, Mittrücker HW, Nouailles G, Bonhagen K, Kamradt T, & Kaufmann SHE. (2007). Cutting Edge: Regulatory T-cells prevent efficient clearance of Mycobacterium tuberculosis. J Immunol. 178(5): 2661-2665.

Lanier LL. (2005). NK cell recognition. Annu Rev Immunol. 23: 225-274.

Latchman Y, Wood CR, Chernova T, Chaudhary D, Borde M, Chernova I, Iwai Y, Long AJ, Brown JA, Nunes R, Greenfield EA, Bourque K, Boussiotis VA, Carter LL, Carreno BM, Malenkovich N, Nishimura H, Okazaki T, Hongo T, Sharpe AH, & Freeman GJ. (2001). PD-L2 is a second ligand for PD-1 and inhibits T-cell activation. Nat Immunol. 2(3): 261-268.

Leach DR, Krummel MF, & Allison JP. (1996). Enhancement of antitumor immunity by CTLA-4 blockade. Science. 271(5256): 1734-1736.

LeibundGut-Landmann S, Waldenburger JM, Krawczyk M, Otten LA, Suter T, Fontana A, Acha-Orbea H, & Reith W. (2004). Mini-review: Specificity and expression of CIITA, the master regulator of MHC class II genes. Eur J Immunol. 34(6): 1513-1525.

Lewkowich IP, Herman NS, Schleifer KW, Dance MP, Chen BL, Dienger KM, Sproles AA, Shah JS, Köhl J, Belkaid Y, & Wills-Karp M. (2005). CD4+CD25+ T-cells protect against experimentally induced asthma and alter pulmonary dendritic cell phenotype and function. J Exp Med. 202(11): 1549-1561.

Liang B, Workman C, Lee J, Chew C, Dale BM, Colonna L, Flores M, Li N, Schweighoffer E, Greenberg S, Tybulewicz V, Vignali D, & Clynes R. (2008). Regulatory T-cells inhibit dendritic cells by lymphocyte activation gene-3 engagement of MHC class II. J Immunol. 180(9): 5916-5926.

Lin CY, Graca L, Cobbold SP, & Waldmann H. (2002). Dominant transplantation tolerace impairs CD8+ T-cell function but not expansion. Nat Immunol. 3(12): 1208-1213.

Liu FT & Rabinovich GA. (2005). Galectins as modulators of tumour progression. Nat Rev Cancer. 5(1): 29-41.

Liu VC, Wong LY, Jang T, Shah AH, Park I, Yang X, Zhang Q, Lonning S, Teicher BA, & Lee C. (2007). Tumor evasion of the immune system by converting CD4+CD25- T-cells into CD4+CD25+ T regulatory cells: role of tumor-derived TGF-beta. J Immunol. 178(5): 2883-2892.

Loos M, Giese NA, Kleeff J, Giese T, Gaida MM, bergmann F, Laschinger M, W Buchler M, & Friess H. (2008). Clinical significance and regulation of the costimulatory molecule B7-H1 in pancreatic cancer. Cancer Lett. 268(1): 98-109.

Madsen L, Labrecque N, Engberg J, Dierich A, Svejgaard A, Benoist C, Mathis D, & Fugger L. (1999). Mice lacking all conventional MHC class II genes. Proc Natl Acad Sci. 31(96): 10338-10343.

Maizels RM. (2005). Infections and allergy - helminths, hygiene and host immune regulation. Curr Opin Immunol. 17(6): 656-661.

Marincola FM, Jaffee EM, Hicklin DJ, & Ferrone S. (2000). Escape of human solid tumors from T-cell recognition: molecular mechanisms and functional significance. Adv Immunol. 74: 181-273.

Martins I, Deshayes F, Baton F, Forget A, Ciechomska I, Sylla K, Aoudjit F, Charron D, Al-Daccak R, & Alcaide-Loridan C. (2007). Pathologic expression of MHC class II is driven by mitogen-activated protein kinases. Eur J Immunol. 37(3): 788-797.

Mellor AL & Munn DH. (2004). IDO expression by dendritic cells: tolerance and tryptophan catabolism. Nat Rev Immunol. 4(10): 762-774.

Menetrier-Caux C, Gobert M, & Caux C. (2009). Differences in tumor regulatory T-cell localization and activation status impact patient outcome. Cancer Res. 69(20): 7895-7898.

Misra N, Bayry J, Lacroix-Desmazes S, Kazatchkine MD, & Kaveri SV. (2004). Cutting edge: human CD4+CD25+ T-cells restrain the maturation and antigen-presenting function of dendritic cells. J Immunol. 172(8): 4676-4680.

Monney L, Sabatos CA, Gaglia JL, Ryu A, Waldner H, Chernova T, Manning S, Greenfield EA, Coyle AJ, Sobel RA, Freeman GH, & Kuchroo VK. (2002). Th1-specific cell surface protein Tim-3 regulates macrophage activation and severity of an autoimmune disease. Nature. 415(6871): 536-541.

Morgan ME, van Bilsen JHM, Bakker AM, Heemskerk B, Schilham MW, Hartgers FC, Elferink BG, van der Zanden L, de Vries RRP, Huizinga TWJ, Ottenhoff THM, & Toes REM. (2005). Expression of FOXP3 mRNA is not confined to CD4+CD25+ T regulatory cells in humans. Hum Immunol. 66(1): 13-20.

Murakami M, Sakamoto A, Bender J, Kappler J, & Marrack P. (2002). CD25+CD4+ T-cells contribute to the control of memory CD8+ T-cells. Proc Natl Acad Sci. 99(13): 8832-8837.

Muranski P, Boni B, Antony PA, Cassard L, Irvine KR, Kaiser A, Paulos CM, Palmer DC, Touloukian CI, Ptak K, Gattinoni L, Wrzesinski C, Hinrichs CS, Kerstann KW, Feigenbaum L, Chan CC, & Restifo NP. (2008). Tumor-specific Th17-polarized cells eradicate large established melanoma. Blood. 112(2): 362-373.

Murphy KM, Heimberger AB, & Loh DY. (1990). Induction by antigen of intrathymic apoptosis of CD4+CD8+TCRlo thymocytes in vivo. Science. 250(4988): 1720-1723.

Murphy TL & Murphy KM. (2010). Slow down and survive: Enigmatic immunoregulation by BTLA and HVEM. Annu Rev Immunol. 28: 389-411.

Nakamura K, Kitani A, & Strober W. (2001). Cell contact-dependent immunosuppression by CD4(+)CD25(+) regulatory T-cells is mediated by cell surface-bound transforming growth factor beta. J Exp Med. 194(5): 629-644.

Natali PG, Nicotra MR, Bigotti A, Venturo I, Marcenaro L, Giacomini P, & Russo C. (1989). Selective changes in expression of HLA class I polymorphic determinants in human solid tumors. Proc Natl Acad Sci. 86(17): 6719-6723.

Ngiow SF, von Scheidt B, Akiba H, Yagita H, Teng MW, & Smyth MJ. (2011). Anti-TIM3 antibody promotes T-cell IFN-y-mediated antitumor immunity and suppresses established tumors. Cancer Res. 71(10): 3540-3551.

Nishikawa H, Jäger E, Ritter G, Old LJ, & Gnjatic S. (2005a). CD4+ CD25+ regulatory T-cells control the induction of antigen-specific CD4+ helper T-cell responses in cancer patients. Blood. 106(3): 1008-1011.

Nishikawa H, Kato T, Tawara I, Saito K, Ikeda H, Kuribayashi K, Allen PM, Schreiber RD, Sakaguchi S, Old LJ, & Shiku, H. (2005b). Definition of target antigens for naturally occurring CD4(+) CD25(+) regulatory T-cells. J Exp Med. 201(5): 681-686.

Oberle N, Eberhardt N, Falk CS, Krammer PH, & Suri-Payer E. (2007). Rapid suppression of cytokine transcription in human CD4+CD25 T-cells by CD4+Foxp3+ regulatory T-cells: independence of IL-2 consumption, TGF-beta, and various inhibitors of TCR signaling. J Immunol. 179(6): 3578-3587.

Oderup C, Cederbom L, Makowska A, Cilio CM, & Ivars F. (2006). Cytotoxic T lymphocyte antigen-4-dependent down-modulation of costimulatory molecules on dendritic cells in CD4+ CD25+ regulatory T-cell-mediated suppression. Immunology. 118(2): 240-249.

Okudaira K, Hokari R, Tsuzuki Y, Okada Y, Komoto S, Watanabe C, Kurihara C, Kawaguchi A, Nagao S, Asuma M, Yagita H, & Miura S. (2009). Blockade of B7-H1 or B7-DC induces an anti-tumor effect in a mouse pancreatic cancer model. Int J Oncol. 35(4): 741-749.

Onizuka S, Tawara I, Shimizu J, Sakaguchi S, Fujita T, & Nakayama E. (1999). Tumor rejection by in vivo administration of anti-CD25 (interleukin-2 receptor alpha) monoclonal antibody. Cancer Res. 59(13): 3128-3133.

Ostmeier H, Fuchs B, Otto F, Mawick R, Lippold A, Krieg V, & Suter L. (2001). Prognostic immunohistochemical markers of primary human melanomas. Br J Dermatol. 145(2): 203-209.

Ott PA, Hodi FS, & Robert C. (2013). CTLA-4 and PD-1/PD-L1 blockade: new immunotherapeutic modalities with durable clinical benefit in melanoma patients. Clin Cancer Res. 19(19): 5300-5309.

Overwijk WW, Tsung A, Irvine KR, Parkhurst MR, Goletz TJ, Tsung K, Carroll MW, Liu C, Moss B, Rosenberg SA, & Restifo NP. (1998). gp100/pmel 17 is a murine tumor rejection antigen: induction of "self"-reactive, tumoricidal T-cells using high-affinity, altered peptide ligand. J Exp Med. 188(2): 277-286.

Overwijk WW, Lee DS, Surman DR, Irvine KR, Touloukian CE, Chan CC, Carroll MW, Moss B, Rosenberg SA, & Restifo NP. (1999). Vaccination with a recombinant vaccinia virus encoding a "self" antigen induces autoimmune vitiligo and tumor cell destruction in mice: requirement for CD4(+) T lymphocytes. Proc Natl Acad Sci. 96(6): 2982-2987.

Overwijk WW and Restifo NP. (2001). B16 as a mouse model for human melanoma. Curr Protoc Immunol. Chapter: Unit-20.1: 1-35.

Pandiyan P, Zheng L, Ishihara S, Reed J, & Lenardo MJ. (2007). CD4+CD25+Foxp3+ regulatory T-cells induce cytokine deprivation-mediated apoptosis of effector CD4+ T-cells. Nat Immunol. 8(12): 1353-1362.

Phan GQ, Yang JC, Sherry RM, Hwu P, Topoalian SL, Schwartzentruber DJ, Restifo NP, Haworth LR, Seipp CA, Freezer LJ, Morton KE, Mavroukakis SA, Duray PH, Steinberg SM, Allison JP, Davis TA, & Rosenberg SA. (2003). Cancer regression and autoimmunity induced by cytotoxic T lymphocyte associated antigen 4 blockade in patients with metastatic melanoma. Proc Natl Acad Sci. 100(14): 8372-8377.

Piccirillo CA, Letterio JJ, Thornton AM, McHugh RS, Mamura M, Mizuhara H, & Shevach EM. (2002). CD4(+)CD25(+) regulatory T-cells can mediate suppressor function in the absence of transforming growth factor beta1 production and responsiveness. J Exp Med. 196(2): 237-246.

Piccirillo CA & Shevach EM. (2001). Cutting edge: control of CD8+ T-cell activation by CD4+ CD25+ immunoregulatory cells. J Immunol. 167(3): 1137-1140.

Pockaj BA, Sherry RM, Wei JP, Yannelli JR, Carter CS, Leitman SF, Carasquillo JA, Steinberg SM, Rosenberg SA, & Yang JC. (1994). Localization of 111indium-labeled tumor infiltrating lymphocytes to tumor in patients receiving adoptive immunotherapy. Augmentation with cyclophosphamide and correlation with response. Cancer. 73(6): 1731-1737.

Preynat-Seuve O, Contassot E, Schuler P, Piguet V, French LE, & Huard B. (2007). Extralymphatic tumors prepare draining lymph nodes to invasion via a T-cell cross-tolerance process. Cancer Res. 67(10): 5009-5016.

Quatromoni JG, Morris LF, Donahue TR, Wang Y, Mcbride W, Chatila T, & Economou JS. (2011). T-cell receptor transgenic lymphocytes infiltrating murine tumors are not induced to express Foxp3. J Hematol Oncol. 4:48.

Quezada SA, Simpson TR, Peggs KS, Merghoub T, Vider J, Fan X, Blasberg R, Yagita H, Muranski P, Antony PA, Restifo NP, and Allison JP. (2010). Tumor-reactice CD4+ T-cells develop cytotoxic activity and eradicate large established melanoma after transfer into lymphopenic hosts. J Exp Med. 207(3): 637-650.

Rabinovich BA, Yang YE, Etto T, Chen JQ, Levitsky HI, Overwijk WW, Cooper LJN, Gelovani J, & Hwu P. (2008). Visualizing fewer than 10 mouse T-cells with an enhanced firefly luciferase in immunocompetent mouse models of cancer. Proc Natl Acad Sci. 105(38): 14342-14346.

Rabinovich GA, Gabrilovich D, & Sotomayor EM. (2007). Immunosuppressive strategies that are mediated by tumor cells. Annu Rev Immunol. 25(1): 267-296.

Read S, Malmström V, & Powrie F. (2000). Cytotoxic T lymphocyte-associated antigen 4 plays an essential role in the function of CD25(+)CD4(+) regulatory cells that control intestinal inflammation. J Exp Med. 192(2): 295-302.

Rees RC & Mian S. (1999). Selective MHC expression in tumours modulates adaptive and innate antitumor responses. Cancer Immunol Immunother. 48(7): 374-381.

Rivoltini L, Carrabba M, Huber V, Castelli C, Novellino L, Dalerba P, Mortarini R, Arancia G, Anichini A, Fais S, & Parmiani G. (2002). Immunity to cancer: attack and escape in T lymphocyte-tumor cell interaction. Immunol Rev. 188: 97-113.

Rollinghoff M, Starzinski-Powitz A, Pfizenmaier K, & Wagner H. (1977). Cyclophosphamide-sensitive T lymphocytes suppress the in vivo generation fo antigen-specific cytotoxic T lymphocytes. J Exp Med. 145(2): 455-459.

Roncarolo MG, Bacchetta R, Bordignon C, Narula S, & Levings MK. (2001). Type 1 T regulatory cells. Immunol Rev. 182: 68-79.

Rosenberg SA. (2001). Progress in human tumour immunology and immunotherapy. Nature. 411(6835): 380-384.

Rouse BT, Sarangi PP, & Suvas S. (2006). Regulatory T-cells in virus infections. Immunol Rev. 212: 272-286.

Rubenstein N, Alvarez M, Zwirner NW, Toscano MA, Ilarregui JM, Bravo A, Mordoh J, Fainboim L, Podhajcer OL, & Rabinovich GA. (2004). Targeted inhibition of galectin-1 gene expression in tumor cells results in heightened T-cell mediated rejection; a potential mechanism of tumor-immune privilege. Cancer Cell. 5(3): 241-251.

Ruiter DJ, Bergman W, Welvaart K, Scheffer E, van Vloten WA, Russo C, & Ferrone S. (1984). Immunohistochemical analysis of malignant melanomas and nevocellular nevi with monoclonal antibodies to distinct monomorphic determinants of HLA antigens. Cancer Res. 44(9): 3930-3935.

Ruiter DJ, Mattijssen V, Broecker EB, & Ferrone S. (1991). MHC antigens in human melanomas. Semin Cancer Biol. 2(1): 35-45.

Sabatos CA, Chakravarti S, Cha E, Schubart A, Sanchez-Fueyo A, Zheng XX, Coyle AJ, Stron TB, Freeman GJ, & Kuchroo VK. (2003). Interaction of Tim-3 and Tim-3 ligand regulates T helper type 1 responses and induction of peripheral tolerance. Nat Immunol. 4(11): 1102-1110.

Sakaguchi S, Sakaguchi N, Shimizu J, Yamazaki S, Sakihama T, Itoh M, Kuniyasu Y, Nomura T, Toda M, & Takahashi T. (2001). Immunologic tolerance maintained by CD25+ CD4+ regulatory T-cells: their common role in controlling autoimmunity, tumor immunity, and transplantation tolerance. Immunol Rev. 182: 18-32.

Sakuishi K, Ngiow SF, Sullivan JM, Teng MWL, Kuchroo VK, Smyth MJ, & Anderson AC. (2013). Tim3+ Foxp3+ regulatory T-cells are tissue-specific promoters of T-cell dysfunction in cancer. Oncoimmunology. 2(4): e23849.

Sallusto F, Geginat J, & Lanzavecchia A. (2004). Central memory and effector memory T-cell subsets: function, generation, and maintenance. Annu Rev Immunol. 22: 745-763.

Samy ET, Parker LA, Sharp CP, & Tung KSK. (2005). Continuous control of autoimmune disease by antigen-dependent polyclonal CD4+CD25+ regulatory T-cells in the regional lymph node. J Exp Med. 202(6): 771-781.

Sánchez-Fueyo A, Sandner S, Habicht A, Mariat C, Kenny J, Degauque N, Zheng XX, Strom TB, Turka LA, & Sayegh MH. (2006). Specificity of CD4+CD25+ regulatory T-cell function in alloimmunity. J Immunol. 176(1): 329-334.

Sarris M, Andersen KG, Randow F, Mayr L, & Betz AG. (2008). Neuropilin-1 expression on regulatory T-cells enhances their interactions with dendritic cells during antigen recognition. Immunity. 28(3): 402-413.

Schreiber TH, Wolf D, Bodero M, & Podack E. (2012). Tumor antigen specific iTreg accumulate in the tumor microenvironment and suppress therapeutic vaccination. Oncoimmunology. 1(5): 642-648.

Seo N, Hayakawa S, Takigawa M, & Yokura Y. (2001). Interleukin-10 expressed at early tumour sites induces subsequent generation of CD4+ T-regulatory cells and systemic collapse of antitumour immunity. Immunology. 103(4): 449-457.

Serra P, Amrani A, Yamanouchi J, Han B, Thiessen S, Utsugi T, Verdaguer J, & Santamaria P (2003). CD40 ligation releases immature dendritic cells from the control of regulatory CD4+CD25+ T-cells. Immunity. 19(6): 877-889.

Sfanos KS, Bruno TC, Meeker AK, De Marzo AM, Isaacs WB, & Drake CG. (2009). Human prostate-infiltrating CD8+ T lymphocytes are oligoclonal and PD-1+. Prostate. 69(15): 1694-1703.

Shastri N & Gonzalez F. (1993). Endogenous generation and presentation of the ovalbumin peptide/Kb complex to T-cells. J Immunol. 150(7): 2724-2736.

Shevach EM. (2009). Mechanisms of Foxp3+ T regulatory cell-mediated suppression. Immunity. 30(5): 636-645.

Shimizu J, Yamazaki S, & Sakaguchi S. (1999). Induction of tumor immunity by removing CD25+ CD4+ T cells: a common basis between tumor immunity and autoimmunity. J Immunol. 163(10): 5211-5218.

Shimizu J, Yamazaki S, Takahashi T, Ishida Y, & Sakaguchi S. (2002). Stimulation of CD25(+)CD4(+) regulatory T-cells through GITR breaks immunological self-tolerance. Nat Immunol. 3(2): 135-142.

Snyder JE, Bowers WJ, Livingstone AM, Lee FE, Federoff JH, & Mossmann TR. (2003). Measuring the frequency of mouse and human cytotoxic T-cells by the Lysispot assay: independent regulation of cytokine secretion and short-term killing. Nat Med. 9(2): 231-235.

Sotomayor EM, Borrello I, Rattis FM, Cuenca AG, Abrams J, Staveley-O'Carroll K, & Levitsky HI. (2001). Cross-presentation of tumor antigens by bone marrow-derived antigen-presenting cells is the dominant mechanism in the induction of T-cell tolerance during B-cell lymphoma progression. Blood. 98(4): 1070-1077.

Starborg M, Gell K, Brundell E, & Hoog C. (1996). The murine Ki-67 cell proliferation antigen accumulates in the nucleolar and heterochromatic regions of interphase cells and at the periphery of the mitotic chromosomes in a process essential for cell cycle progression. J Cell Sci. 109(1): 143-153.

Staveley-O'Carroll K, Sotomayor E, Montgomery J, Borrello I, Hwang L, Fein S, Pardoll D, & Levitsky H. (1998). Induction of antigen-specific T-cell anergy: An early event in the course of tumor progression. Proc Natl Acad Sci. 95(3): 1178-1183.

Strome SE, Dong H, Tamura H, Voss SG, Flies DB, Tamada K, Salomao D, Cheville J, Hirano F, Lin W, Kasperbauer JL, Ballman KV, & Chen L. (2003). B7-H1 blockade augments adoptive T-cell immunotherapy for squamous cell carcinoma. Cancer Res. 63(19): 6501-6505.

Sun CM, Hall JA, Blank RB, Bouladoux N, Oukka M, Mora JR, & Belkaid Y. (2007). Small intestine lamina propria dendritic cells promote de novo generation of Foxp3 Treg cells via retinoic acid. J Exp Med. 204(8): 1775-1785.

Suvas S, Kumaraguru U, Pack CD, Lee S, & Rouse BT. (2003). CD4+CD25+ T-cells regulate virus-specific primary and memory CD8+ T-cell responses. J Exp Med. 198(6): 889-901.

Taams LS, Palmer DB, Akbar AN, Robinson DS, Brown Z, & Hawrylowicz CM. (2006). Regulatory T-cells in human disease and their potential for therapeutic manipulation. Immunology. 118(1): 1-9.

Taams LS, van Amelsfort JMR, Tiemessen MM, Jacobs KMG, de Jong EC, Akbar AN, Bijlsma JWJ, & Lafeber FPJG. (2005). Modulation of monocyte/macrophage function by human CD4+CD25+ regulatory T-cells. Hum Immunol. 66(3): 222-230.

Tadokoro CE, Shakhar G, Shen S, Ding Y, Lino AC, Maraver A, Lafaille JJ, Dustin ML. (2006). Regulatory T-cells inhibit stable contacts between CD4+ T-cells and dendritic cells in vivo. J Exp Med. 203(3): 505-511.

Tai AK, Zhou G, Chau K, & Ono SJ. (1999). Cis-element dependence and occupancy of the human invariant chain promotoer in CIITA-dependent and –independent transcription. Mol Immunol. 36(7). 447-460.

Tang Q, Adams JY, Tooley AJ, Bi M, Fife BT, Serra P, Santamaria P, Locksley RM, Krummel MF, & Bluestone JA. (2006). Visualizing regulatory T-cell control of autoimmune responses in nonobese diabetic mice. Nat Immunol. 7(1): 83-92.

Tarbell KV, Yamazaki S, Olson K, Toy P, & Steinman RM. (2004). CD25+ CD4+ T-cells, expanded with dendritic cells presenting a single autoantigenic peptide, suppress autoimmune diabetes. J Exp Med. 199(11): 1467-1477.

Thimme R, Appay V, Koschella M, Panther E, Roth E, Hislop AD, Rickinson AB, Roland-Jones SL, Blum HE, & Pircher H. (2005). Increased expression of the NK cell receptor KLRG1 by virus-specific CD8 T-cells during persistent antigen stimulation. J Virol. 79(18): 12112-12116.

Thomas L. Cellular and Humoral Aspects of the Hypersensitive States (ed. Lawrence HS). Hoeber-Harper, New York, 1959. 529-532.

Thompson RH, Gillett MD, Cheville JC, Lohse CM, Dong H, Webster WS, Krejci KG, Lobo JR, Sengupta S, Chen L, Zincke H, Blute ML, Strome SE, Leibovich BC, & Kwon ED. (2004). Costimulatory B7-H1 in renal cell carcinoma patients: Indicator of tumor aggressiveness and potential therapeutic target. Proc Natl Acad Sci. 101(49): 17174-17149.

Thompson RH, Webster WS, Cheville JC, Lohse CM, Dong H, Leibovich BC, Kuntz SM, Sengupta S, Kwon ED, & Blute ML. (2005). B7-H1 glycoprotein blockade: a novel strategy to enhance immunotherapy in patients with renal cell carcinoma. Urology. 66(5 Suppl): 10-14.

Thornton AM, Donovan EE, Piccirillo CA, & Shevach EM. (2004). Cutting edge: IL-2 is critically required for the in vitro activation of CD4+CD25+ T-cell suppressor function. J Immunol. 172(11): 6519-6523.

Thornton AM & Shevach EM. (1998). CD4+CD25+ immunoregulatory T-cells suppress polyclonal T-cell activation in vitro by inhibiting interleukin 2 production. J Exp Med. 188(2): 287-296.

Thornton AM & Shevach EM. (2000). Suppressor effector function of CD4+CD25+ immunoregulatory T-cells is antigen nonspecific. J Immunol. 164(1): 183-190.

Tiemessen MM, Jagger AL, Evans HG, van Herwijnen MJC, John S, & Taams LS. (2007). CD4+CD25+Foxp3+ regulatory T-cells induce alternative activation of human monocytes/macrophages. Proc Natl Acad Sci. 104(49): 19446-19451.

Tran DQ, Ramsey H, & Shevach EM. (2007). Induction of FOXP3 expression in naive human CD4+FOXP3 T-cells by T-cell receptor stimulation is transforming growth factor-beta dependent but does not confer a regulatory phenotype. Blood. 110(8): 2983-2990.

Travis MA, Reizis B, Melton AC, Masteller E, Tang Q, Proctor JM, Wang Y, Bernstein X, Huang X, Reichardt LF, Bluestone JA, & Sheppard D. (2007). Loss of integrin alpha(v)beta8 on dendritic cells causes autoimmunity and colitis in mice. Nature. 449(7160): 361-365.

Tsuji T, Matsuzaki J, Caballero OL, Jungbluth AA, Ritter G, Odunsi K, Old LJ, & Gnjatic S. (2012). Heat shock protein 90-mediated peptide-selective presentation of cytosolic tumor antigen for direct recognition of tumors by CD4+ T-cells. J Immunol. 188(8): 3851-3858.

Turk MJ, Guevara-Patino JA, Rizzuto GA, Engelhorn ME, Sakaguchi S, & Houghton AN. (2004). Concomitant tumor immunity to a poorly immunogenic melanoma is prevented by regulatory T-cells. J Exp Med. 200(6): 771-782.

van der Burg SH, Piersma SJ, de Jong A, van der Hulst JM, Kwappenberg KMC, van den Hende M, Welters MJP, Van Rood JJ, Fleuren GJ, Melief CJM, Kenter GG, & Offringa R. (2007). Association of cervical cancer with the presence of CD4+ regulatory T-cells specific for human papillomavirus antigens. Proc Natl Acad Sci. 104(29): 12087-12092.

van der Stoep N, Quinten E, Alblas G, Plancke A, van Eggermond MCJA, Holling TM, & van den Elsen PJ. (2007). Constitutive and IFNgamma-induced activation of MHC2TA promoter type III in human melanoma cell lines is governed by separate regulatory elements within the PIII upstream regulatory region. Mol Immunol. 44(8): 2036-2046.

Van Parijs L & Abbas AK. (1998). Homeostasis and self-tolerance in the immune system: turning lymphocytes off. Science. 280(5361): 243-248.

Vence L, Palucka AK, Fay JW, Ito T, Liu YJ, Banchereau J, & Ueno H. (2007). Circulating tumor antigen-specific regulatory T-cells in patients with metastatic melanoma. Proc Natl Acad Sci. 104(52): 20884-20889.

Vignali DAA, Collison LW, & Workman CJ. (2008). How regulatory T-cells work. Nat Rev Immunol. 8(7): 523-532.

Voehringer D, Koschella M, & Pircher H. (2002). Lack of proliferative capacity of human effector and memory T-cells expressing killer cell lectin like receptor G1 (KLRG1). Blood. 100(10): 3698-3702.

von Boehmer H. (2005). Mechanisms of suppression by suppressor T-cells. Nat Immunol. 6(4): 338-344.

Wang HY, Lee DA, Peng G, Guo Z, Li Y, Kiniwa Y, Shevach EM, & Wang RF. (2004). Tumor-specific human CD4+ regulatory T-cells and their ligands: implications for immunotherapy. Immunity. 20(1): 107-118.

Wang HY, Peng G, Guo Z, Shevach EM, & Wang RF. (2005). Recognition of a new ARTC1 peptide ligand uniquely expressed in tumor cells by antigen-specific CD4+ regulatory T-cells. J Immunol. 174(5): 2661-2670.

Wang J, Ioan-Facsinay A, van der Voort EIH, Huizinga TWJ, & Toes REM. (2007). Transient expression of FOXP3 in human activated nonregulatory CD4+ T-cells. Eur. J. Immunol. 37(1): 129-138.

Wang L, Pino-Lagos K, de Vries VC, Guleria I, Sayegh MH, & Noelle RJ. (2008). Programmed death 1 ligand signaling regulates the generation of adaptive Foxp3+CD4+ regulatory T-cells. Proc Natl Acad Sci. 105(27): 9331-9336.

Watanabe N, Gavrieli M, Sedy JR, Yang J, Fallarino F, Loftin SK, Hurchi MA, Zimmerman N, Sim J, Zang X, Murphy TL, Russell JH, Allison JP, & Murphy KM. (2003). BTLA is a lymphocyte inhibitory receptor with similarities to CTLA-4 and PD-1. Nat Immunol. 4(7): 670-679.

Weiner HL. (2001). Induction and mechanism of action of transforming growth factor-beta-secreting Th3 regulatory cells. Immunol Rev. 182: 207-214.

Wherry EJ, Ha SJ, Kaech SM, Haining WN, Sarkar S, Kalia V, Subramaniam S, Blattman JN, Barber DL, & Ahmed R. (2007). Molecular signature of CD8+ T-cell exhaustion during chronic viral infection. Immunity. 27(4): 670-684.

Wherry EJ, Teichgraber V, Becker TC, Masopust D, Kaech SM, Antia R, von Andrian UH, & Ahmed R. (2003). Lineage relationship and protective immunity of memory CD8 T-cell subsets. Nat Immunol. 4(3): 225-234.

Wildin RS, Ramsdell F, Peake J, Faravelli F, Casanova JL, Buist N, Levy-Lahad E, Mazzella M, Goulet O, Perroni L, Bricarelli FD, Byrne G, McEuen M, Proll S, Appleby M, & Brunkow ME. (2001). X-linked neonatal diabetes mellitus, enteropathy and endocrinopathy syndrome is the human equivalent of mouse scurfy. Nat Genet. 27(1): 18-20.

Woo EY, Chu CS, Goletz TJ, Schlienger K, Yeh H, Coukos G, Rubin SC, Kaiser LR, & June CH. (2001). Regulatory CD4(+)CD25(+) T-cells in tumors from patients with early-stage non-small cell lung cancer and late-stage ovarian cancer. Cancer Res. 61(12): 4766-4772.

Woo SR, Turnis ME, Goldberg MV, Bankoti J, Selby M, Nirschl CJ, Bettini ML, Gravano DM, Vogel P, Liu CL, Tangsombatvisit S, Grosso JF, Netto G, Smeltzer MP, Chaux A, Utz PJ, Workman CJ, Pardoll DM, Korman AJ, Drake CG, & Vignali DAA. (2012). Immune inhibitory molecules LAG-3 and PD-1 synergistically regulate T-cell function to promote tumoral immune escape. Cancer Res. 72(4): 917-927.

Workman CJ, Cauley LS, Kim IJ, Blackman MA, Woodland DL, & Vignali DA. (2004). Lymphocyte activation gene-3 (CD223) regulates the size of the expanding T-cell population following antigen activation in vivo. J Immunol. 172(9): 5450-5455.

Workman CJ, Rice DS, Dugger KJ, Kurschner C, & Vignali DA. (2002). Phenotypic analysis of the murine CD4-related glycoprotein, CD223 (LAG-3). Eur J Immunol. 32(8): 2255-2263.

Workman CJ & Vignali DAA. (2005). Negative regulation of T-cell homeostasis by lymphocyte activation gene-3 (CD223). J Immunol. 174(2): 688-695.

Wu M, Fang H, & Hwang ST. (2001). Cutting edge: CCR4 mediates antigen-primed T-cell binding to activated dendritic cells. J Immunol. 167(9): 4791-4795.

Xie Y, Akpinarli A, Maris C, Hipkiss EL, Lane M, Kown EKM, Muranski P, Restifo NP, & Antoy PA. (2010). Naïve tumor-specific CD4+ T-cells differentiated in vivo eradicate established melanoma. J Exp Med. 164(2): 916-925.

Xystrakis E, Boswell SE, & Hawrylowicz CM. (2006). T regulatory cells and the control of allergic disease. Expert Opinion on Biological Therapy. 6(2): 121-133.

Yamazaki S, Dudziak D, Heidkamp GF, Fiorese C, Bonito AJ, Inaba K, Nussenzweig MC, & Steinman RM. (2008). CD8+ CD205+ splenic dendritic cells are specialized to induce Foxp3+ regulatory T-cells. J Immunol. 181(10): 6923-6933.

Yee C, Thompson JA, Byrd D, Riddell SR, Roche P, Celis E, & Greenberg PD. (2002). Adoptive T-cell therapy using antigen-specific CD8+ T-cell clones for the treatment of patients with metastatic melanoma: in vivo persistence, migration, and antitumor effect of transfected T-cells. Proc Natl Acad Sci. 99(25): 16168-16173.

Yu P, Gregg RK, Bell JJ, Ellis JS, Divekar R, Lee HH, Jain R, Waldner H, Hardaway JC, Collins M, Kuchroo VK, & Zahouani H. (2005). Specific T regulatory cells display broad suppressive functions against experimental allergic encephalomyelitis upon activation with cognate antigen. J Immunol. 174(11): 6772-6780.

Zaloudik J, Moore M, Ghosh AK, Mechl Z, & Rejthar A. (1988). DNA content and MHC class II antigen expression in malignant melanoma: clinical course. J Clin Pathol. 41(10): 1078-1084.

Zarour HM, Maillere B, Brusic V, Coval K, Williams E, Pouvelle-Moratille S, Castelli F, Land S, Bennouna J, Logan T, & Kirkwood JM. (2002). NY-ESO-1 119-143 is a promiscuous major histocompatability complex class II T-helper epitope recognized by Th1- and Th2-type tumor-reactive CD4+ T-cells. Cancer Res. 62(1): 213-218.

Zeng G, Wang X, Robbins PF, Rosenberg SA, & Wang RF. (2001). CD4(+) T-cell recognition of MHC class II-restricted epitopes from NY-ESO-1 presented by a prevalent HLA DP4 allele: association with NY-ESO-1 antibody production. Proc Natl Acad Sci. 98(7): 3964-3969.

Zhang L, Gajewski TF, & Kline J. (2009). PD-1/PD-L1 interactions inhibit antitumor immune responses in a murine acute myeloid leukemia model. Blood. 114(8): 1545-1552.

Zhou G, Drake CG, & Levitsky HI. (2006). Amplification of tumor-specific regulatory T-cells following therapeutic cancer vaccines. Blood. 107(2): 628-636.

Zhou G & Levitsky HI. (2007). Natural regulatory T-cells and de novo-induced regulatory T-cells contribute independently to tumor-specific tolerance. J Immunol. 178(4): 2155-2162.

Zhou G & Levistsky HI. (unpublished data).

Zhou Q, Bucher C, Munger ME, Highfill SL, Tolar J, Munn DH, Levine BL, Riddle M, June CH, Vallera DA, Weigel BJ, & Blazar BR. (2009a). Depletion of endogenous tumor-associated regulatory T-cells improves the efficacy of adoptive cytotoxic T-cell immunotheraphy in murine acute leukemia. Blood. 114(18): 3793-3802.

Zhou Q, Munger E, Highfill S, Tolar J, Weigel BJ, Riddle M, Sharpe AH, Vallera DA, Azuma M, Levine BL, June CH, Murphy WH, Munn DH, & Blazar BR. (2010). Program death-1 signalling and regulatory T-cells collaborate to resist the function of adoptively transferred cytotoxic T lymphocytes in advanced acute myeloid leukemia. Blood. 116(14): 2484-2493.

Zhou X, Bailey-Bucktrout SL, Jeker LT, Penaranda C, Martinez-Llordella M, Ashby M, Nakayama M, Rosenthal W, & Bluestone JA. (2009b). Instability of the transcription factor Foxp3 leads to the generation of pathogenic memory T-cells *in vivo*. Nat Immunology. 10(9): 1000-1007.

Zhu C, Anderson AC, Schubart A, Xiong H, Imitola J, Khoury SJ, Zheng XX, Strom TB, & Kuchroo VK. (2005). The Tim-3 ligand galectin-9 negatively regulates T helper type 1 immunity. Nat Immunol. 6(12): 1245-1252.

Zippelius A, Batard P, Rubio-Godoy R, Bioley G, Lienard D, Lejeune F, Rimoldi D, Guillaume P, Meidenbauer N, Mackensen A, Rufer N, Lubenow N, Speiser D, Cerottini JC, Romero P, & Pittet MJ. (2004). Effector function of human tumor-specific CD8 T-cells in melanoma lesions: a state of local functional tolerance. Cancer Res. 64(8): 2865-2873.

Zou W. (2005). Immunosuppressive networks in the tumour environment and their therapeutic relevance. Nat Rev Cancer. 5(4): 263-274.

Zou W. (2006). Regulatory T-cells, tumour immunity and immunotherapy. Nat Rev Immunol. 6(4): 295-307.

MATTHEW MORGAN MOAKE

667 Stirling St. • Baltimore, MD 21202 • moake@jhmi.edu • 443.745.9089

EDUCATION

2004-Present
Johns Hopkins University School of Medicine, Baltimore, MD
Candidate for Doctorate of Medicine, Anticipated May 2014

Johns Hopkins University School of Medicine, Baltimore, MD
Candidate for Doctorate of Philosophy, Cellular & Molecular Medicine, Anticipated May 2014
Dissertation: "Direct Recognition of Tumors by Regulatory T-Cells with Suppression of Immune Rejection."

2000-2004
Cornell University, Ithaca, NY
Bachelor of Science in Biology w/ Molecular & Cell Concentration
Summa cum Laude, 4.01 GPA

RESEARCH

2005 – Present
Department of Oncology, JHU School of Medicine
Tumor Immunology Research – Dr. Hyam Levitsky
Project: Evaluating the ability of regulatory T-cells to directly recognize antigens presented by tumor cells with resultant downstream implications on tumor rejection, immune suppression, and antigen specificity.

2004
Department of Virology, **JHU School of Medicine**
Molecular Virology Research - Dr. Gary Hayward
Project: Evaluating the effects of KSHV gene expression on key cell cycle genes and their role in cellular carcinogenesis.

2001-2004
Department of Food Microbiology, Cornell University NYSAES
Food Microbiology Research – Dr. Randy Worobo
Project: Identifying, isolating, & characterizing novel secondary bacterial metabolites and anticancer agent using basic microbiologic and cell culture screening techniques.

2003
Department of Biological Chemistry, Cornell University Research Program on Biodiversity
Field Ecology Research – Dr. Eloy Rodriguez

Project: Field analysis of mercury pollution within the Rio Fresco river basin near Gorotire, Brazil.

2002
Laboratory of Human Carcinogenesis, NCI/NIH
Cancer Research - Dr. Curtis Harris
Project: Microarray analysis of p53 and NOS2 KO murine tissue gene expression. Analysis of the p53-mediated induction of apoptosis via reactive oxygen species.

2001
Section on Immune Biology of Retroviral Infection, NCI/NIH
HIV Vaccine Research - Dr. Marjorie Robert-Guroff
Project: Analyzing the antibody-based mucosal immune response of immunized macaques.

PUBLICATIONS

Qin L, Smith BD, Tsai HL, Yaghi NK, Neela PH, Moake MM, Fu J, Prince GT, Goswami M, Rosner GL, Levitsky HI, & Hourigan CS. (2013). Induction of high titer IgG antibodies against multiple leukemia-associated antigens in CML patients with clinical responses to K562/GVAX immunotherapy. Blood Cancer J. 3(e145): 1-11.

Mathe E, Nguyen GH, Funamizu M, He P, Moake MM, Croce CM, & Hussain SP. (2012). Inflammation regulates microRNA expression in cooperation with p53 and nitric oxide. Int J Cancer. 131(3): 760-765.

Liu G, Moake MM, Har-el Y, Long CM, Chan KWY, Cardona A, Jamil M, Walczak P, Gilad AA, Sgouros G, van Zijl PCM, Bulte JWM, & McMahon MT. (2012). In vivo multicolor molecular MR imaging using diamagnetic chemical exchange saturation transfer liposomes. Magnetic Resonance in Medicine. 67(4): 1106-1113.

Hu H, Moake MM, & Worobo RW. (2005) Genetic characterization of antimicrobial peptides. In: Food Biotechnology: Second Edition, Revised and Expanded. Shetty K, Paliyath G, Pometto A, & Levin RE, Eds. Marcel Dekker, Inc.: New York. 1439-1477.

Moake MM, Padilla-Zakour OI, & Worobo RW. (2006). Comprehensive review of patulin control methods in foods. Comprehensive Reviews in Food Science & Food Safety. 4(1): 8-21.

Basaran N, Quintero-Ramos A, Moake MM, Churey JJ, & Worobo RW. (2004). Influence of apple cultivars on inactivation of different strains of *Escherichia coli* O157:H7 in apple cider by UV irradiation. Appl Environ Microbiol. 70(10): 6061-6065.

Hussain SP, Amstad P, Kaneko I, Robles A, He P, Ichimiya M, Araki Y, Hofseth LJ, Moake MM, Forrester KS, & Harris CC. (2004). p53-induced upregulation of MnSOD

and GPx but not catalase increases oxidative stress and apoptosis. Cancer Res. 64(7): 2350-2356.

Zhao J, Pinczewski J, Gomez-Roman VR, Venzon D, Kalyanaraman VS, Markham PD, Aldrich K, Moake MM, Montefiori DC, Lou Y, Pavlakis GN, & Robert-Guroff M. (2003). Improved protection of rhesus macaques against intrarectal SIV_{mac251} challenge by a replication competent Ad5hr-SIV*env/rev* and Ad5hr-SIV*gag* recombinant priming/gp120 boosting regimen. J Virology. 77(15): 8354-8365.

Martin NI, Hu H, Moake MM, Churey JJ, Whittal R, Worobo RW, & Vederas JC. (2003). Isolation, structural characterization, and properties of mattacin (polymyxin M), a cyclic peptide antibiotic produced by *Paenabacillus kobensis* M. J Biol Chem. 278(15): 13124-13132.

POSTERS, PRESENTATIONS, & ABSTRACTS

Moake MM, Zhou G, & Levitsky HI. Specificity of tumor antigen-specific regulatory T-cell suppression. Poster & Abstract at the 2011 Cancer Research Institute Annual International Cancer Immunotherapy Symposium. New York, NY. (October 4, 2011).

Liu G, Har-el Y, Moake MM, Long CM, Walczak P, Gilad AA, Zhang J, Cardona A, DeLiso MA, Jamil M, Sgouros G, Bulte JWM, van Zijl PCM, & McMahon MT. Multi-color in vivo MR imaging of lymph nodes using DIACEST liposomes. Poster & Abstract at the 2010 World Molecular Imaging Congress. Kyoto, Japan. (September 10, 2010).

Liu G, Har-el Y, Moake MM, Long CM, Walczak P, Gilad AA, Zhang J, Cardona A, DeLiso MA, Jamil M, Sgouros G, Bulte JWM, van Zijl PCM, & McMahon MT. Multi-color in vivo MR imaging of lymph nodes using DIACEST liposomes. Presentation by Liu G & Abstract at the 18th International Society of Magnetic Resonance in Medicine. Stockholm, Sweden. (May 5, 2010).

Long CM, Moake MM, Levitsky HI, & Bulte JW. Use of magnetovaccination and MRI for investigating cancer vaccine dynamics. Presentation by Long CM & Abstract at the Radiologic Society of North America Annual Meeting (Molecular Imaging Session). Chicago, IL. (Nov 2009).

Moake MM & Levitsky HI. Immunomodulatory effects of the chromatin remodeling drugs 5-aza-2'-deoxycytidine and MS 275. Poster & Abstract at the 2005 JHUSOM MD/PhD Retreat. Hershey, PA. (November 2005).

Hu H, Moake MM, Churey JJ, Martin NI, Vederas JC, & Worobo RW. Biochemical and genetic characterization of mattacin (polymyxin M). Poster & Abstract at the ASM 2003 General Meeting. Washington, D.C. (May 2003).

Moake MM, Hussain P, Stain F, Hofseth L, He P, & Harris CC. Oxidative stress and the p53 response pathway. Poster & Abstract at the NIH Summer 2002 Poster Day. Bethesda, MD. (August 2002).

Moake MM, Aldrich K, & Robert-Guroff M. The mucosal immune response of macaques immunized with an Ad5hr-SIV recombinant/gp120 prime/boost regimen: antibodies in secretory fluid. Poster & Abstract at the NIH Summer 2001 Poster Day. Bethesda, MD. (August 2001).

AWARDS & ACHIEVEMENTS

Robert L Lindsay Meritorious Service Award, 2012
Cancer Research Institute STaRT Graduate Training Fellowship, 2009-2012
Cornell University Graduate, *Summa cum Laude*, 2004
Cornell University Merrill Presidential Scholar, 2004
Cornell University Ho-Nun-De-Kah Paul Schreurs Memorial Award, 2004
Cornell University Ertel-Diament Pre-Medical Award, 2004
Goldwater Scholarship, 2002-2004
Cornell University Tradition Fellow, 2000-2004
Cornell University CALS Charitable Trust Grant for Undergraduate Research, 2002
Cornell University Hatch Multistate Grant for Undergraduate Research, 2002
Cornell University Morley Grant for Undergraduate Research, 2002
NIH Undergraduate Scholarship Program (UGSP), 2000-2002

ACTIVITIES & SERVICE

2007-present
Maryland Juniors Volleyball Club
Head and/or assistant volleyball coach for a total of 8 junior girls club volleyball teams ages 12-18. Activities included running practices several times per week (November – June), coaching all day tournaments approximately twice monthly, and running day-long training clinics.

2007-Present
Chesapeake Regional Volleyball Association (CHRVA)
CHRVA is the local governing body for the United States Volleyball Association, which oversees adult and juniors volleyball nationwide. I have been involved with both the adult and juniors programs in a number of different roles, including coaching juniors (above), organizing adult tournaments, officiating, training juniors officials, and guiding regional policy changes.

2009–2010
Baltimore Board of Women's Sports (BBOWS) Volleyball Official
Officiated middle and high school volleyball for local boys and girls teams approximately twice weekly between August and November.

2007–2010
JHU School of Medicine Histology Teaching Assistant
Prepared lectures, assisted with microscope- and computer-based laboratories, and graded student presentations and exams during the first year medical/graduate student histology course each fall.

2004–2009
Johns Hopkins Hospital IPC Big Buddy Program
Served as a mentor to a patient of the JHH Intensive Primary Care (IPC) Clinic, which cares for children with HIV, with activities approximately two Sundays per month.

2004–2007
Chesapeake Habitat for Humanity (HFH)
General volunteer for construction and demolition projects for the local chapter of HFH approximately two Saturdays per month.

2004-2006
Baltimore Rescue Mission
Medical volunteer at a local homeless shelter approximately two evenings per month.

2000-2004
Cornell University Habitat for Humanity (HFH)
A campus based chapter of HFH, which partnered with affiliates from local New York counties to organize and oversee student construction activities, fundraisers, community outreach events, and spring break volunteer trips. My roles included that of President (2002-2003), Work Projects' Chair (2001-2002), Board Member (2000-2001, 2003-2004), and general volunteer (2000-2004).

PROFESSIONAL AFFILIATIONS

American Medical Student Association
American Medical Association